DEVELOPMENT OF AN ELECTRONIC SIZE AND

COLOUR GRADER FOR TOMATOES

BY

JOERG WALTER von BECKMANN

B.Sc. Mount Allison University, 1971

M.Sc. University of British Columbia, 1972

A THESIS SUBMITTED IN PARTIAL FULFILMENT

OF THE REQUIREMENTS FOR THE DEGREE OF

DOCTOR OF PHILOSOPHY

IN THE

Department of Plant Science

(Bio-Resource Engineering)

We accept this thesis as conforming to

the required standard

Department of Bio-Resource Engineering

The University of British Columbia
2075 Wesbrook Place
Vancouver, Canada
V6T 1W5

Date April 29, 1976.

ABSTRACT

The greenhouse tomato industry in British Columbia requires that tomatoes be colour graded into four categories, and size graded, based on diameter, into four categories. Automatic colour graders for only two category classifications have been developed, while a size grader based on weight is commercially available. To meet industry demands, automatic size and colour grading of greenhouse tomatoes for the fresh market is necessary. The development of an automatic size and colour grader, which fulfills industry grading requirements is needed to reduce production costs and to accelerate the implementation of complete mechanization in tomato handling.

This thesis outlines the design, fabrication and testing of a grading machine capable of simultaneously size and colour grading tomatoes into fourteen different size and colour categories at a rate of five tomatoes per second. The number of categories may be increased or decreased to meet individual needs. Tomatoes are randomly fed onto a conveyor with one inch (2.5 cm) minimum spacing and passed single file under a fibre optic illuminating and sensing head. Size and colour of individual tomatoes are measured electronically and the information stored in a memory until each tomato reaches an appropriate eject location, where the tomato is pneumatically ejected into a storage bin. The memory and eject mechanisms are synchronized with the conveyor belt so

that changes in belt speed do not affect grading. The
grading rate is strictly a function of mechanical handling
operations, and is limited by the ability of the pneumatic
eject system to supply enough air to remove tomatoes from
the conveyor in the allotted time.

Colour grading is based on the ratio of light re-
flected from the tomato surface in two narrow bands of the
visible spectrum. Size grading is based on a diameter
measurement of the tomato, as it passes under the sensing
head, with a grading resolution of approximately 3/64 inch
(0.12 cm). Misclassification of oversized or undersized
tomatoes in a given size category was less than 10%.

TABLE OF CONTENTS

LIST OF TABLES

LIST OF FIGURES

ACKNOWLEDGEMENTS

The author wishes to sincerely thank Dr. N. R. Bulley (Department of Bio-Resource Engineering, University of British Columbia), the Director of this research project, for his guidance and criticism over the past four years. His encouragement when things were not going as expected and his enthusiasm when they were, are greatly appreciated.

The efforts of my Committee Chairman, Dr. V. C. Runeckles in co-ordinating this research with the Department of Bio-Resource Engineering, and the time spent by the members of the committee, Dr. P.A. Jolliffe, Dr. C.A. Hornby, Dr. G.W. Eaton and especially Dr. E.O. Nyborg, in reviewing the thesis, are acknowledged.

Special thanks to Mrs. E. Stewart for the many typings of the manuscript, and for her patience.

Sincerest gratitude is extended to Western Greenhouse Co-operative, Burnaby, B.C. who supplied all the tomatoes for the research at no cost. Without their co-operation the research would have been difficult to carry out.

The research was financed by the National Research Council of Canada.

INTRODUCTION

Approximately 4.2 million pounds (1.9 million kg)*
of greenhouse tomatoes were produced in the British Columbia
Lower Mainland in 1975. About 87% of the annual production
occurs from April to late August, with a peak production of
280,000 lb (126,000 kg) per week. Most Lower Mainland
tomatoes are marketed by the Western Greenhouse Co-operative
in Burnaby, B.C.

Tomatoes are graded according to both size and
colour as well as for general quality according to Federal
and Co-operative Standards**. At present, the major grading
operation is the responsibility of the individual grower. The
graded produce is packed in 20 lb (9 kg) boxes and delivered
to the co-op warehouse where a small percentage of the boxes
is inspected and graded.

The inspection of a few boxes which are below
standard can down-grade an entire shipment which in many
cases is inequitable to the grower. Similarly, many boxes
can contain below average produce but be graded as prime
quality resulting from random sampling inspection. Since
federal standards lack tolerances for a single size measure-
ment, and colour grading is subjective, it is probable that
each grower grading tomatoes based on the present standards,

---

*   Data courtesy of Western Greenhouse Co-operative,
      Burnaby, B.C.
** The Standards for tomato grading are found in Appendix A.

will deliver varying grades of tomatoes according to individual interpretation.

The need for one set of size and colour standards for all growers and the grading of every tomato according to these standards is evident. If only those tomatoes which do not meet the standards are down-graded, then every grower will be paid fairly for his product delivered.

Ideally, to minimize handling and to avoid unnecessary expense to each grower in hiring a seasonal grading staff, produce should be delivered to the warehouse ungraded, and graded there according to a uniform standard. Larger growers could size and colour grade their own produce if it was beneficial to them. The maintenance of standards can be accomplished by use of an automatic size and colour grader, which has been calibrated and verified by federal graders.

This report deals with the development of an automatic electronic size and colour grader for tomatoes. The automatic grader, in order to be acceptable must be able to categorize tomatoes into four colour categories and four size categories.

The process of automatically grading tomatoes by size and colour involves the following steps:

a) Load tomatoes onto a conveyor.

b) Arrange tomatoes in single file (singulate).

c) Transport to a sensing and grading area.

d) Categorize individual tomatoes into specific size and colour categories.

e) Store category information until tomato reaches its size and colour category eject station.

f) Transport tomato to appropriate eject station downstream from sensing area.

g) Eject the tomato from the conveyor into appropriate storage bin or onto a cross-conveyor.

The research reported here involves the design of an electronic and mechanical system to include steps c) through g) as described above.

Many loading and conveying systems which singulate fruit are available, and it was not the objective of this research to develop a new conveying system for tomatoes.

The aim of the research was the development of a high speed electronic grading system which would simultaneously size and colour grade tomatoes in one operation, thus involving only a single handling process. The development of an eject system was not of major importance in this study although preliminary tests of a pneumatic system are described.

LITERATURE REVIEW

The evaluation of fruit ripeness has included
methods such as the measure of reflected light intensity from
the fruit surface (1,4,5,8,9,10,11,13,14,15,16,17,24,25,28,
29,33,35)*, the measure of transmitted light intensity through
the fruit, or optical density (2,3,5,10,11,18,21,22,23,25,26,
27,30,31,36,37), firmness testing using instruments such as
the Magness-Taylor Fruit Pressure Tester and an Instron
Universal Tester (11,15,24,25) and vibrational techniques
(25,32).

The most popular methods for "on-line" grading of
fruit are those involving colour evaluation either by reflec-
tance or transmittance. One reason for the use of colour as
a grading criterion is best summarized by Bittner et al. (4),
"The overall quality of fruit is a function of many factors,
but appearance is the main factor on which the consumer makes
the decision".

Firmness testing or vibrational techniques require
that the fruit be stationary and physically handled which
usually requires more time than a colour measurement. The
colour measurement may be obtained while the fruit is in
motion. Firmness tests on tomatoes have shown good correla-
tions with visual colour evaluation and reflected light
measurements at specific wavelengths in the visible spectrum,
as described by Hood et al. (15). Colour alone therefore, is

* Numbers in parentheses refer to appended references.

a reasonable measure of fruit firmness in tomatoes.

There appears to be no universal agreement as to which of the two light measuring techniques, transmittance or reflectance is most suitable for fruit grading.

The transmittance technique involves the illumination of one side of the fruit and the sensing of light transmitted through the fruit, usually on the other side. The surface colour of the fruit, such as the colour of an apple peel, contributes little to the optical density of the fruit. Transmittance, therefore, is a measure of internal fruit colour and not external colour. This technique is generally used in grading fruit for processing. The disadvantage of a transmittance measurement is that the fruit must be placed into a cup or onto an aperature, and a good light seal is required around the illuminated area. Modelling clay has been used as a light sealant (3). For fruit such as blueberries, which are relatively uniform in size, the sealant is not necessary (21,22,23); however, the supporting cup must conform well to the fruit shape. Integrating spheres have been placed around the fruit (3), or a light receptor is placed in direct contact with the fruit (36), which further complicates handling of the fruit at high sorting rates.

For fresh-market fruit, reflectance would appear to be most suitable as a ripeness measurement, since the external appearance, or reflected colour, is what the consumer sees. Reflectance lends itself better to high speed grading systems

than transmittance. Fruit does not have to be placed in special cups, only separated by some distance from the next fruit. A light seal is not required, since the fruit is illuminated and the reflected light received from the same side. The distance that the fruit is located from the light source or sensor is not as critical since neither is placed in direct contact with the fruit. The fruit can flow continuously past the sensing element on a simple conveyor system. Fruit size uniformity is not a necessity since special cups are not required to carry the fruit. The size variation is an important consideration when dealing with tomatoes. Sizes range from under two inches (5 cm) to 3 1/2 inches (9 cm) in diameter.

The reflected light intensity from a fruit surface over the visible spectrum alone does not correlate with the colour of the fruit. However, the intensities at specific wavelengths, or narrow wavelength bands does correlate with the surface colour (4,5,8,11,15,28). The question arises as to which wavelength or combination of wavelengths of reflected light produces the best correlation with fruit colour. Furthermore, how should the measured light intensity, or intensities, be handled in order to produce a colour index? Should a single measurement be used, or should two or more electronic signals be added, subtracted, divided, etc.?

As early as 1953, Powers et al. (29) discussed three criteria which could be used for sorting lemons based

on the intensity of light reflected from their surfaces.
The first is a measure of a single intensity of a narrow
wavelength band in the visible spectrum. The single reflec-
tance measurement is subject to sensitivity variations in
the measuring instrument as well as changes in object distance
from the sensor and size of fruit. The second criterion is
the measure of the ratio of two reflected light intensities
at different narrow wavelength bands in the visible spectrum.
The effects of instrument sensitivity, distance and size are
cancelled out using this technique. Greater sensitivity to
small variations in colour may be obtained using a percen-
tage change in reflectance at two narrow bands in the visible
spectrum. This is the third criterion discussed. The
method involves the measure of the difference between the
reflected light at two wavelengths divided by the intensity
at one of the wavelengths. The latter criterion was the one
used for the lemon grader.

It is clear from the work of Powers et al. (29)
that at least two reflected light intensities are required,
combined arithmetically by either division, or subtraction
and division to produce a signal proportional to colour and
independent of extraneous interferences. The findings have
been ignored by many researchers, and "new" colour graders
have been developed as late as 1969 and 1974 (1,9,33) which
use only a single intensity measurement. It is of no sur-
prise that Burkhardt et al. (9) encountered sorting problems

when the fruit varied in size. The correlation of three intensities to fruit maturity by Bittner et al. (5) by the division of one by the product of the other two showed no significant advantage over the simple ratio of two intensities.

As to the choice of two wavelengths to be combined in a ratio, no two wavelengths are ideal for all fruit. The wavelength ratios of 670 nm/730 nm (5), 540 nm/630 nm (11), 520 nm/670 nm (14), and 525 nm/670 nm (15) have all been used to sort tomatoes. The above wavelength ratios have been used primarily to separate tomatoes into two colour categories, red and green, except for the first, which was correlated over four colour categories.

Apparently, the ideal wavelength ratio to be used in a grader depends on the number of colour categories to be separated. Two colour category separations would require a different wavelength ratio than four colour category separations.

Since the development of the lemon grader by Powers et al. (29) in 1953, little progress has been made in the field of electronic colour grading of fruits and vegetables using reflectance as the grading criterion. They described a machine consisting of a conveyor which oriented lemons with their major axis perpendicular to the direction of travel. At the end of the conveyor, the lemons were dropped through an illuminated compartment, where the reflected light was

received by photodetectors. The photodetector signals were used to activate deflecting vanes which categorized the lemons into one of five colour grades. The few improvements which have been made since then are the result of the advancement of electronic technology since the early 1950's. Instead of photo-multiplier tubes, semiconductors are now in use. Switching circuits are no longer comprised of vacuum tubes but of transistors and integrated circuits. Some of the subtle details of colour grading systems have been ignored in the literature, such as proper timing sequences, data processing when more than two colour categories are involved, and simplification of triggering and memory components that is required.

Singulating and conveying of fruit is of importance in any grading system. Both operations are specific for the fruit being handled. The orientation system used by Powers et al. (29) would be unsuitable for anything but lemons, and the eject mechanism, or deflecting vanes could not be used for tomatoes. The single filer described by Brantley et al. (6), which was designed for sweet potatoes and cucumbers, may have some potential application for tomatoes.

The orientation device described by Burkhardt et al. (9) for dried prunes would probably not work for tomatoes. The single filer and a transport conveyor described by Greenwood et al. (13) consisted of two parallel vee belts, similar to that of Brantley et al. (6), but was designed for

tomatoes. Tomatoes were ejected using mechanical plungers and pneumatic assistance to lift the tomatoes from the two belts. Heron et al. (14) suggested the use of a flat conveyor belt for tomatoes with no singulation of fruit, which is an excellent ideal, however, the proportion of speculation to test results is not clear in the published work. Mason et al. (20) describe a vibrational technique for orienting fruit in a packing tray which could possibly assist in the orientation of tomatoes on a conveyor belt.

Electronic size grading of fruits and vegetables is virtually unknown. Mechanical methods of size grading involving the rolling of fruit over holes of various sizes does not appear promising for tomatoes. The multiple belt, adjustable vee size grader for sweet potatoes and cucumbers described by Brantly et al. (6) and Goodman et al. (12) could be used for tomatoes. The disadvantage of such a grading system is that the size grading is strongly weighted in favour of over-size grading, i.e. the minimum diameter for the fruit becomes the measurement criterion rather than the maximum diameter. Maximum diameter is used as the tomato size standard (Appendix A). A weight grader has been developed by FMC Corporation, U.S.A., and has been commercially available for some time. The weight grader requires that fruit be singulated into individual weighing cups, which are then mechanically compared to preset spring-loaded mechanisms, and the fruit dropped onto a cross-conveyor when the weight of the fruit exceeds that of the

spring force. Grading by weight is not the standard for tomatoes. The use of an image sensing array, similar to a television camera, has been recently suggested as a device for measuring lengths and areas of agricultural products (7). The device may be more suited to a research instrument than a commercial grader.

A combined size and colour grader for tomatoes has not yet been developed. The combination of a size grader and a colour grader involves more than just the operation of a size grader and/or colour grader in tandem. A colour grader, for four colours of tomatoes, in conjunction with the Brantley et al. (6) size grader for five sizes, for example, would require either one colour grader and four size graders, or one size grader and five colour graders to perform the complete grading operation. Clearly, there is a need for a size/colour grader which using a single conveyor system simultaneously size and colour categorizes and ejects the fruit from the conveyor into the appropriate packing bin or onto a cross-conveyor.

The need for automatic grading of fruits and vege-tables is well documented (19,32). The increasing cost and shortage of labour alone has necessitated the development of automatic harvesting, grading and packing equipment for agricultural produce (34). The future for automatic grading equipment lies in the increased sophistication towards multiple operations and simplification to minimize product handling and damage.

S E C T I O N   I

COLOUR GRADER

C H A P T E R   1

PHYSICAL PROPERTIES OF TOMATES AS RELATED

TO COLOUR GRADING.

INTRODUCTION

Based on the work of Powers et al. (29) and others, it was decided that a ratio of reflectances at two narrow wavelength bands of the visible spectrum would be a suitable criterion for colour evaluation. A study was conducted to determine the wavelength ratio which would provide the best separation among the four colour categories -- firm ripe, semi-ripe, turning and green -- based on the reflected intensities at each wavelength band.

MATERIALS AND METHODS

Twenty tomatoes* (variety Vendor) were chosen for the study, and grouped into four colour categories of five tomatoes each: firm ripe, semi-ripe, turning and green, as described by the Canada Department of Agriculture Standards (Appendix A). No attempt was made to separate mature green from immature green tomatoes. The green tomato group probably included a mixture of mature and immature tomatoes.

A spectrophotometer (Unicam Ultraviolet Spectrophotometer, Model SP800B) was calibrated to 100% reflectance (zero absorbance) for the range 350 nm to 800 nm using a magnesium oxide standard. Since plexiglass petri dishes were to be used to hold the tomatoes during the reflectance tests, the magnesium oxide standard was then placed behind a plexiglass petri dish. The reflectance dropped to approximately 85% across the 350 nm to 800 nm range. The spectrophotometer was recalibrated to 100% reflectance with the plexiglass dish in front of the standard.

A tomato section was cut from each tomato to fill the petri dish (60 mm dia X 20 mm deep) and the tomato skin was flattened against the viewed side of the petri dish. The dish was covered and placed in the sample holder.

Several samples were scanned at a fast (approximately 2 minutes for total spectrum) and then at a slow

---

*   All tomatoes used in this research were obtained from Western Greenhouse Growers Co-operative, Burnaby, B.C.

(approximately 8 minutes for the total spectrum) rate, and no difference was noted between the two traces. Consequently, all subsequent scans were carried out at the fast speed.

The absorbance (A) was measured at 10 nm intervals from 380 nm to 800 nm for each of the twenty spectrograms and converted to percent reflectance using the relationship:

$$R(\%) = 10^{-A} \times 100\% \quad * \qquad [1-1]$$

Reflectance ratios were calculated by dividing the percent reflectances of 903 different wavelength pairs beginning with 380 nm/390 nm, 380 nm/400 nm.....to 790 nm/800 nm for each tomato. The mean reflectance ratio of the five tomatoes in each colour category was calaculated for each permutation. The differences of mean reflectance ratios between adjacent colour categories, i.e. firm ripe-semi-ripe; semi-ripe-turning; and turning-green were calculated for each permutation. The three differences of mean reflectance ratios between adjacent colour categories were summed to produce a maximum reflectance ratio difference for each wavelength ratio, as suggested by Goddard et al. (11). To illustrate, if the difference between mean reflectance ratios of the firm ripe and semi-ripe tomatoes at the 600 nm/660 nm wavelength ratio was 0.34, and the difference between semi-ripe and turning was 0.63, and the difference between turning and green was 0.5, then the maximum difference between the means at the 600 nm/660 nm wavelength ratio would be 1.51.

* See Unicam Spectrophotomer Model SP800B Manual.

The larger the difference between the means of adjacent colour categories, the larger will be the sum of the three means, and the greater the separation between colour categories, according to Goddard et al. (11).

RESULTS AND DISCUSSION

The "top 50" maximum total differences between means
of adjacent colour categories and their associated wavelength
ratios are listed in Table 1.1 in descending order beginning
with the greatest difference. The results agree with those
of Goddard et al. (11), who found that the 550 nm/680 nm and
540 nm/680 nm wavelength ratios yielded "a reasonably accurate
separation for the good tomatoes (red) and green tomatoes
categories from the other grade categories".

Careful examination of each of the adjacent colour
category mean reflectance ratio differences indicates that
the 550 nm/680 nm wavelength ratio does not include the
greatest difference between firm ripe and semi-ripe, nor
between semi-ripe and turning. The large difference between
turning and green at this ratio is the predominant factor in
the total (maximum) difference. The 550 nm/680 nm ratio is
probably acceptable for the separation of green from turning
tomatoes, but it is not the best ratio for separating the
semi-ripe from firm ripe or semi-ripe from turning.

The wavelength ratio which best separates all four
colour categories equally would show approximately the same
differences between the means of each category, assuming the
standard deviations about the mean to be small, and equal.

The "top 5" wavelength ratios for each of the three
colour comparisons are listed in Table 1.2, in descending
order according to the priority of maximum difference between

TABLE 1.1 "TOP 50" WAVELENGTH RATIOS BASED ON MAXIMUM TOTAL
DIFFERENCES BETWEEN MEANS OF THE REFLECTANCE RATIOS
FOR FOUR COLOUR CATEGORIES.

No.	Ratio	Total Difference	Semi -Firm	Turning -Semi	Green -Turning
1	550/680	3.776	0.212	1.426	2.139
2	540/680	3.690	0.196	1.340	2.154
3	560/680	3.686	0.206	1.448	2.033
4	530/680	3.501	0.160	1.128	2.213
5	570/680	3.458	0.220	1.421	1.817
6	550/670	3.422	0.207	1.301	1.914
7	540/670	3.343	0.191	1.221	1.931
8	560/670	3.340	0.201	1.322	1.817
9	530/670	3.173	0.156	1.031	1.986
10	570/670	3.129	0.215	1.294	1.620
11	580/680	3.078	0.286	1.306	1.486
12	520/680	2.974	0.138	0.908	1.928
13	590/680	2.798	0.352	1.154	1.292
14	580/670	2.778	0.278	1.180	1.320
15	520/670	2.697	0.134	0.831	1.732
16	600/680	2.588	0.390	0.980	1.218
17	590/670	2.512	0.341	1.028	1.144
18	550/660	2.388	0.190	1.061	1.137
19	540/660	2.333	0.176	0.995	1.163
20	560/660	2.329	0.184	1.078	1.067
21	600/670	2.301	0.373	0.853	1.075
22	530/660	2.218	0.143	0.841	1.234
23	570/660	2.175	0.197	1.052	0.927
24	610/680	2.157	0.350	0.778	1.030
25	510/680	2.139	0.127	0.682	1.330
26	510/670	1.939	0.124	0.622	1.192
27	580/660	1.913	0.256	0.944	0.713
28	520/660	1.885	0.124	0.676	1.086
29	610/670	1.885	0.326	0.656	0.904
30	550/690	1.863	0.173	0.941	0.749
31	620/680	1.841	0.295	0.647	0.899
32	540/690	1.820	0.160	0.882	0.778
33	560/690	1.816	0.168	0.956	0.692
34	550/650	1.750	0.178	0.881	0.692
35	530/690	1.733	0.130	0.744	0.858
36	540/650	1.710	0.164	0.825	0.721
37	560/650	1.706	0.172	0.897	0.638
38	590/660	1.701	0.313	0.799	0.589
39	570/690	1.691	0.178	0.931	0.581
40	530/650	1.628	0.134	0.699	0.796
41	630/680	1.594	0.196	0.568	0.830
42	570/650	1.585	0.183	0.870	0.531
43	620/670	1.582	0.266	0.529	0.786
44	550/640	1.568	0.172	0.809	0.587
45	500/680	1.560	0.118	0.540	0.902
46	540/640	1.532	0.158	0.757	0.616
47	560/640	1.528	0.166	0.823	0.539
48	600/660	1.508	0.341	0.631	0.536
49	580/690	1.475	0.233	0.832	0.410
50	520/690	1.472	0.113	0.597	0.762

TABLE 1.2   "TOP 5" WAVELENGTH RATIOS FOR EACH OF THREE
COLOUR COMPARISONS ACCORDING TO PRIORITY
OF MAXIMUM DIFFERENCE BETWEEN ADJACENT
COLOUR CATEGORIES.

λ_a/λ_b	Semi-Firm	Turning-Semi	Green-Turning
PRIORITY: Semi-Ripe -- Firm Ripe			
600/680	.390	.980	1.218
600/670	.373	.853	1.075
590/680	.352	1.154	1.292
610/680	.350	.778	1.030
590/670	.341	1.028	1.144
PRIORITY: Turning -- Semi-Ripe			
560/680	.206	1.448	2.033
550/680	.212	1.426	2.139
570/680	.220	1.421	1.817
540/680	.196	1.340	2.154
560/670	.201	1.322	1.817
PRIORITY: Green -- Turning			
530/680	.160	1.128	2.213
540/680	.196	1.340	2.154
550/680	.212	1.426	2.139
560/680	.206	1.448	2.033
530/670	.156	1.031	1.986

the means of firm ripe-semi-ripe; semi-ripe-turning; and turning-green The data indicates that the maximum separation of firm ripe and semi-ripe is obtained with the 600 nm/680 nm ratio; for semi-ripe to turning, 560 nm/680nm and for turning to green, 530 nm/680 nm.

Although the large differences between the means of two colour categories imply good separation, the standard deviation in each group may be so large that no significant difference between the means exists.

The Students' t-test was used to compare the means of adjacent colour categories for the 50 wavelength ratios listed in Table 1.1. The "top 5" wavelength ratios for each of the three colour comparisions are listed in Table 1.3, in descending order according to the priority of maximum t values for firm ripe vs. semi-ripe; semi-ripe vs. turning, and turning vs. green. Comparisons of the sequence of wavelength ratios in Table 1.2 to those in Table 1.3 shows that selection of an optimum wavelength ratio based on the differences between means will be different from the selection based on Students' t-test. The difference points in the direction of the ideal wavelength ratio for the separation of the groups, but Students' t-test is probably a more reliable indicator.

The question still remains, "Which single wave-length ratio will equally separate all four colour categories?" Based on the values of t in Table 1.3 and their associated confidence levels, it appears that any wavelength ratio from

TABLE 1.3   "TOP 5" WAVELENGTH RATIOS FOR EACH OF THREE
              COLOUR COMPARISONS ACCORDING TO PRIORITY OF
              MAXIMUM STUDENTS t VALUES FOR ADJACENT COLOUR
              CATEGORIES.

λ_a/λ_b	Firm-Semi	Semi-Turning	Turning-Green
PRIORITY: Firm-Ripe -- Semi-Ripe			
600/660	4.648**	6.751***	8.542***
610/680	4.366**	5.797***	7.084***
620/680	4.234**	5.407***	7.246***
600/680	4.094**	6.313***	7.314***
610/670	3.971**	5.896***	9.074***
PRIORITY: Semi-Ripe -- Turning			
560/640	2.932*	9.147***	7.123***
550/640	3.088*	9.146***	7.867***
540/640	3.262*	9.027***	8.320***
570/690	2.905*	9.009***	5.627***
560/690	2.895*	8.786***	6.189***
PRIORITY: Turning -- Green			
520/670	2.876*	6.973***	13.938***
510/670	3.198*	6.599***	13.514***
530/670	2.790*	7.346***	12.844***
520/660	3.187*	7.068***	12.143***
510/680	3.295*	6.815***	11.964***

*** Significant at 0.1% level
** Significant at 1% level
* Significant at 5% level

one of the three priority groups would separate semi-ripe
from turning, and turning from green. However, only the
wavelength ratios in the firm ripe vs. semi-ripe priority
group separate firm ripe from semi-ripe at the 99% confidence
level -- the wavelength ratios in the other two groups
separate at only the 95% confidence level. A choice of any
one wavelength ratio in the 600 nm/660 nm to 610nm/670 nm
group should result in good separation among the four
colour categories, but the best wavelength ratio would be
600 nm/660 nm, since it shows the greatest values of t for
both firm ripe vs. semi-ripe and semi-ripe vs. turning, and
the second largest value of t for turning vs. green.

C H A P T E R   2.

THEORY RELATED TO THE DEVELOPMENT

OF A COLOUR GRADER.

INITIAL CONSIDERATIONS

Ideally, to maximize the use of the reflectance ratio technique, the same area on the tomato surface should be viewed by both sensing elements. This minimizes variations due to colour differences over the tomato surface. A measure of the ratio of the reflected light at two wavelengths cancels any effect of reflected light intensity variation (as a result of varying tomato sizes) if the same area is viewed by the two sensors. Initial tests were conducted with a combination of incandescent and fluorescent light sources and two sensing elements all mounted in a metal housing. Both geometrical and thermal problems were encountered. The measured reflectance ratio was found to vary with tomato size using this housing, indicating that different areas of the tomato were being sensed.

A trifurcated fibre optic assembly, Figure 2.1, was considered. One furcation would be used to direct the light source onto the tomato surface, and the other two to direct equal portions of the reflected light to each of the photo-detectors.

The light emitting and receiving end of the fibre optic bundle was chosen so that it would emit light through a rectangle 1 in (2.5 cm) X 0.063 in (0.16 cm) with its lengths being perpendicular to the movement of the tomato under the fibre bundle. A random fibre arrangement was chosen to ensure uniform lighting of the tomato surface as well as uniform

26

FIGURE 2.1 TRIFURCATED FIBRE OPTIC ASSEMBLY

LIGHT SOURCE

N/3 FIBRES

N/3 FIBRES

½ OF REFLECTED LIGHT

½ OF REFLECTED LIGHT

N/3 FIBRES

N FIBRES

BOTTOM VIEW

0.063"

1.000"
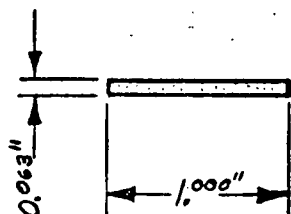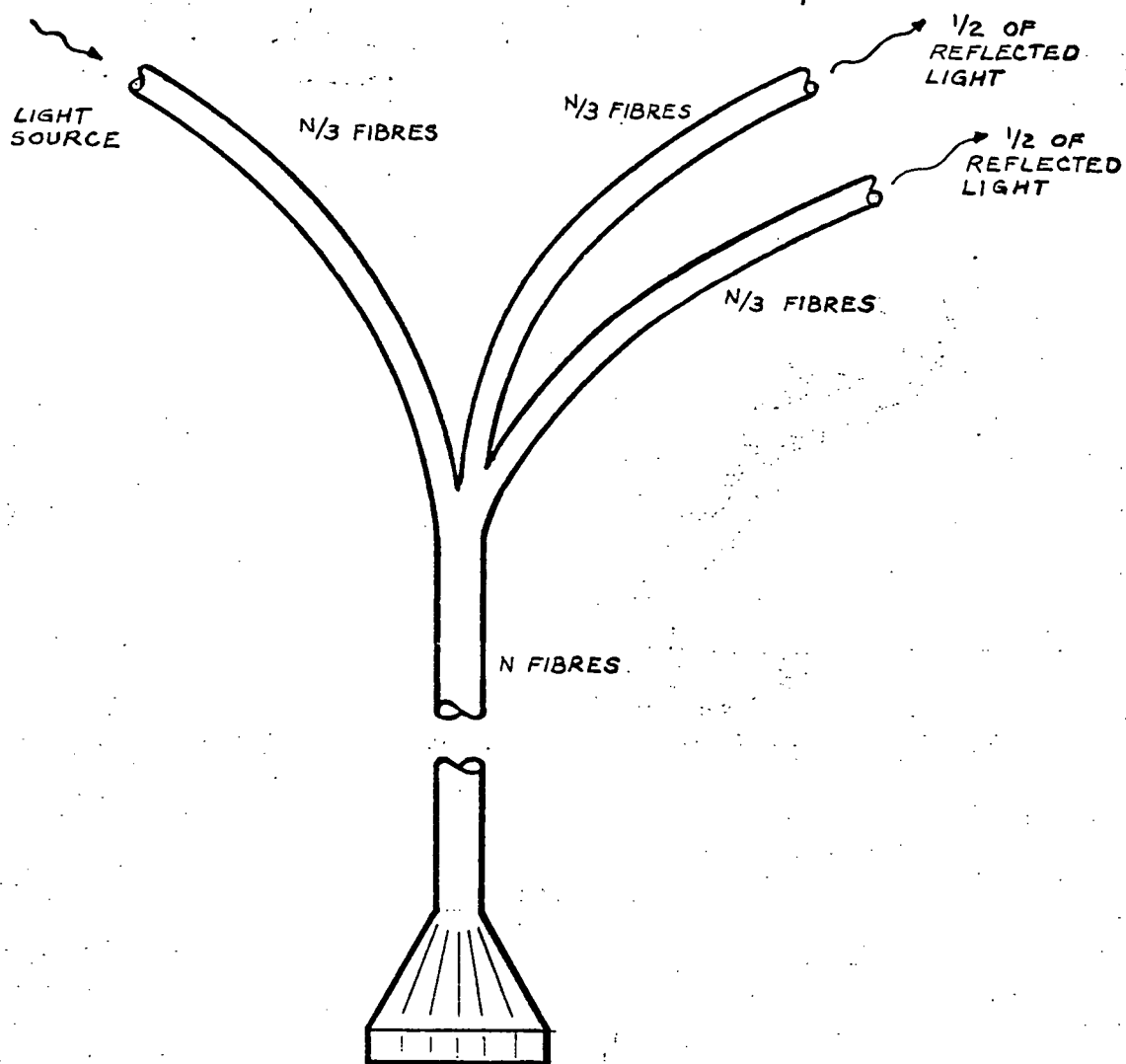
FIBRE MOLD NO. X-723
MFD. BY DOLAN-JENNER INC.
MASSACHUSETTS

light reception. The minimum tomato surface area illumina-
ted and viewed would be an inch (2.5 cm) wide strip over the
length of the tomato as it passed under the fibre bundle.

A phototransistor was chosen as the photodetector
over other devices such as photo diodes, photo multiplier
tubes, and photo cells, since it is designed primarily for
analog applications (as opposed to digital for the photo
diode), has a high light sensitivity, a wide operating vol-
tage range and would be suitable for use in conjunction with
integrated circuits.

A typical spectral response curve for a photo-
transistor is shown in Figure 2.2. Most silicon phototran-
sistors and photo diodes exhibit the same response.

A high intensity tungsten lamp ($3500^{O}K$ colour
temperature) was considered for use as a light source, since
it provides a spectral output rate of change that is relatively
uniform over the visible range. The spectral energy distribu-
tion of a tungsten lamp at $3500^{O}K$ filament temperature is
shown in Figure 2.3. Lower operating temperatures (e.g.
$3300^{O}K$) have little effect on the shape of the spectral
energy distribution. A fluorescent lamp was deemed undesir-
able due to the sharp spikes in its spectral distribution at
specific wavelengths.

Based on the findings in Chapter 1, the ideal optic
filters would require peak wavelengths of 600 nm and 660 nm
respectively. Optic filters vary in their relative peak

FIGURE 2.2 RELATIVE RESPONSE OF A
TYPICAL PHOTOTRANSISTOR

TYPE FPT120A.
AFTER FAIRCHILD
HANDBOOK OF OPTO-
ELECTRONICS.
FEB. 1973 p. 6-16
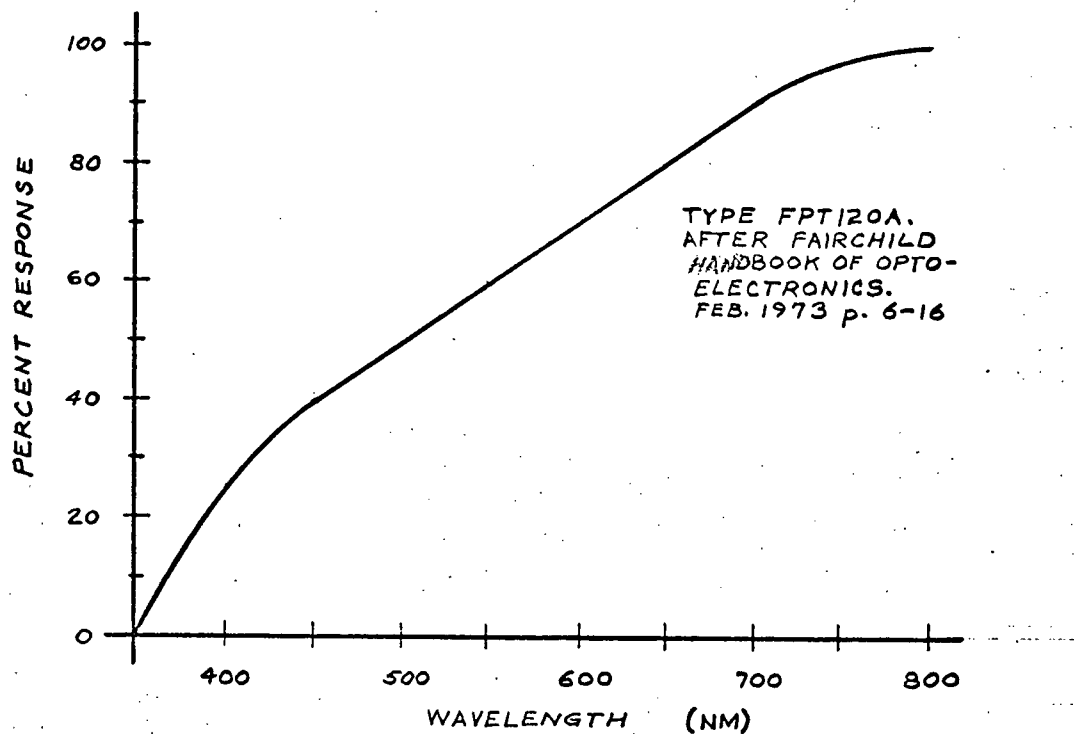
FIGURE 2.3 TUNGSTEN FILAMENT LAMP
SPECTRAL DISTRIBUTION

3500°K

AFTER ILLUMINATING
ENGINEERING SOCIETY
LIGHTING FUNDAMENTALS
COURSE.
1971 p. 3-1
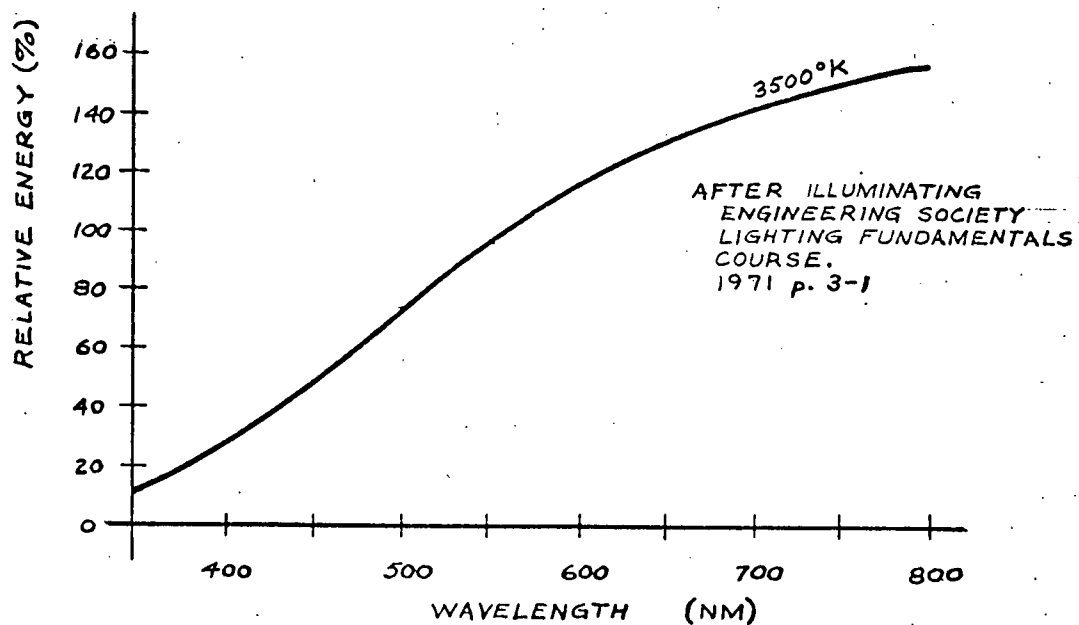
transmissions and have finite band widths encompassing more than a discrete wavelength. The range of transmitted wavelengths for a particular filter is usually expressed in terms of a half bandwidth. The choice of half bandwidths for the above filters is governed primarily by the data in Table 1.3. The data shows that deviation from either the 600 nm or 660 nm peak wavelength by 10 nm generally decreases the separation between colour categories. If possible, therefore, the filters should have narrow bandwidths.

Integration of the energy being transmitted over the band width of the optic filter must be taken into account when designing the optic system. What is the effect on the final reflectance ratio if the band width of one or both filters or their relative peak transmsissions are changed? What effect will the use of a light source other than a standard tungsten lamp have on the final ratio obtained? An analysis of the entire light source, sample, light detector system will provide answers to these and other questions.

ANALYSIS OF LIGHT SOURCE, SAMPLE, DETECTOR

An analysis was carried out to study the effects of light source-sample-detector geometry on the measurement of reflectance. The effects of using various optic filters, and light sources were also investigated.

A schematic of the source-sample-detector system is shown in Figure 2.4. Each optic filter was conveniently located between the output of the fibre optic bundle and the photodetector.

Since the final ratio to be obtained from the photo-transistors will be the ratio of either two voltages or currents, the ratio will be a dimensionless quantity, which will simplify the system analysis through the use of relative rather than absolute quantities.

The components of the analysis are as follows:

λ_1 = peak wavelength of the short wavelength optic filter.

λ_2 = peak wavelength of the long wavelength optic filter.

$\lambda_1 - a$ = short wavelength filter transmission lower limit (at approximately 0.1% peak transmission).

$\lambda_1 + a$ = short wavelength filter transmission upper limit (at approximately 0.1% peak transmissions).

$\lambda_2 - b$ = long wavelength filter transmission lower limit (at approximately 0.1% peak transmission).

$\lambda_2 + b$ = long wavelength filter transmission upper limit (at approximately 0.1% peak transmission).

A = relative energy of the light source, at a given λ between 380 and 800 nm.

B = relative reflectance of a tomato, at a given λ between 380 and 800 nm.

FIGURE 2.4   SCHEMATIC OF SOURCE-SAMPLE-DETECTOR SYSTEM
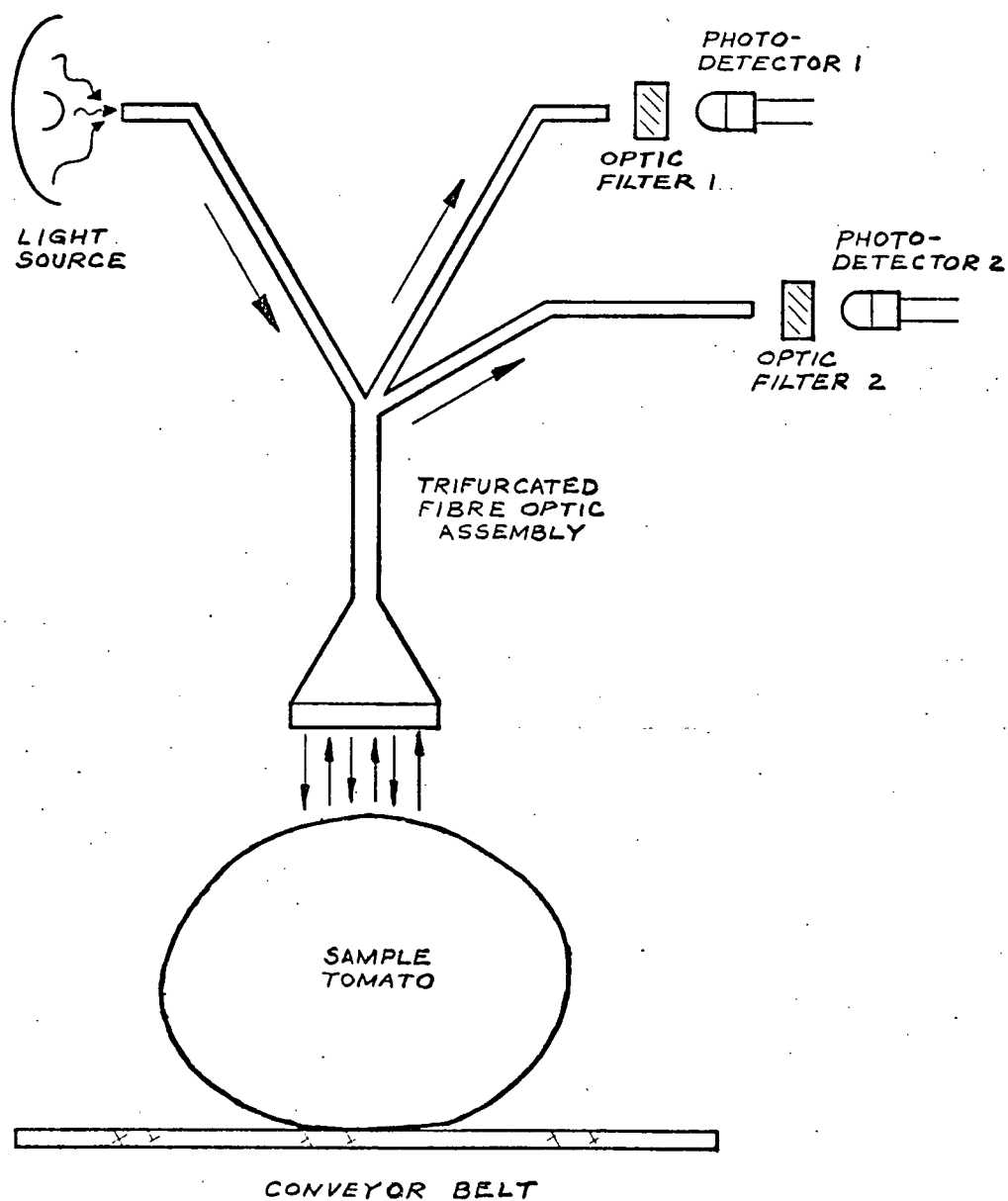
C_1 = relative transmission of the short wavelength optic filter, at a given λ between 380 and 800 nm.

C_2 = relative transmission of the long wavelength optic filter, at a given λ between 380 and 800 nm.

D = relative response of the photodetector, at λ between 380 and 800 nm.

E_1 = output of the photodetector receiving the short wavelengths of light integrated between $(\lambda_1 - a)$ and $(\lambda_1 + a)$.

E_2 = output of the photodetector receiving the long wavelengths of light integrated between $(\lambda_2 - b)$ and $(\lambda_2 + b)$.

In this analysis, the reflectance ratio E_1/E_2 is the ratio of output currents of the photodetectors, each current being proportional to the energy impinging on the semi-conductor surfaces. This energy is a function of factors such as the output of the light source, the reflectance of the tomato, and the transmissions of the filters. Taking these factors in to account yields the following relationship:

$$\frac{E_1}{E_2} = \frac{\int_{(\lambda_1 - a)}^{(\lambda_1 + a)} [A(\lambda) \cdot B(\lambda) \cdot C_1(\lambda) \cdot D(\lambda)]d\lambda}{\int_{(\lambda_2 - b)}^{(\lambda_2 + b)} [A(\lambda) \cdot B(\lambda) \cdot C_2(\lambda) \cdot D(\lambda)]d\lambda} \qquad [2-1]$$

Approximations for the Integrals

$A(\lambda)$, $B(\lambda)$, $C(\lambda)$ and $D(\lambda)$ are complex functions whose definition as equations is not necessary for the purpose of this analysis. Approximations for the integrals may be obtained by summation of incremental areas under the representative curves of the functions from $(\lambda_1 - a)$ to $(\lambda_1 + a)$ and from $(\lambda_2 - b)$ to $(\lambda_2 + b)$. The incremental distance, $\Delta\lambda = 10$ nm was chosen for each area measurement.

Data for the spectral energy distribution of the light source and for the response of the photodetector was collected from 380 nm to 800 nm in 10 nm steps, from the curves in Figures 2.2 and 2.3. The data from the 20 spectrograms was also collected over the same range in 10 nm steps. The spectrograms for a typical firm ripe and green tomato are shown in Figure 2.5.

For the analysis, the curve representing the optic band pass filter was to be flexible in peak transmission and band width, and due to the complexity of the Gaussian function which normally represents the transmission characteristics of this type of filter, it was decided that an isosceles triangle would serve as a reasonable approximation for the transmission curves. The relative transmission over the band width (where band width = 2 half band width for the triangle) was calculated from the equal sides of the triangle, after peak transmission, peak wavelength, and half band width were chosen for analysis.
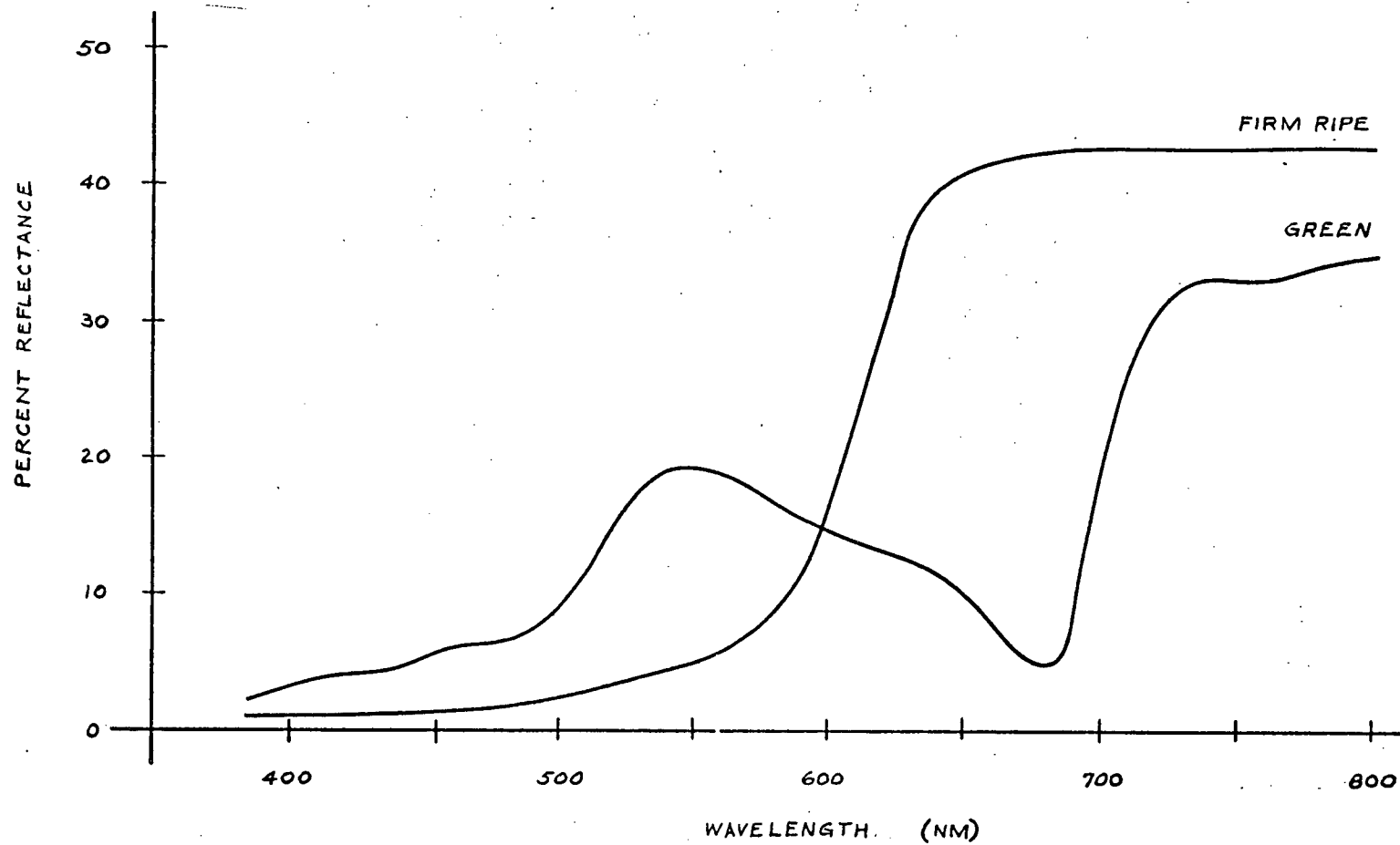
FIGURE 2.5 SPECTROGRAM OF A TYPICAL
FIRM RIPE AND GREEN TOMATO

Using the summation of areas, the integrals could
be approximated and the ratio E_1/E_2 calculated using the
relationship:

$$\frac{E_1}{E_2} = \frac{\sum\limits_{i=0,10,20....}^{m} A\,\Delta\,\lambda_p\ B\,\Delta\,\lambda_p\ C_1\,\Delta\,\lambda_p\ D\,\Delta\,\lambda_p}{\sum\limits_{j=0,10,20....}^{n} A\,\Delta\,\lambda_q\ B\,\Delta\,\lambda_q\ C_2\,\Delta\,\lambda_q\ D\,\Delta\,\lambda_q} \qquad [2\text{-}2]$$

where $p = \lambda_1 - a + i$

           $q = \lambda_2 - b + j$

           m = 2 X half band width of the short wavelength
           filter

           n = 2 X half band width of the long wavelength
           filter.

Various optic filters, half band widths, illumina-
ting lamp spectral curves, etc. were tested in equation [2-2]
and the ratio E_1/E_2 calculated for each of the 20 tomatoes
(Chapter 1).

For any set of input conditions, the largest of
the 20 ratios $G = E_1/E_2$ (corresponding to the greenest tomato)
was adjusted to a value of 10, and subsequently the remaining
19 ratios were normalized by multiplying each by the normali-
zing factor:

$$F = 10/G. \qquad [2\text{-}3]$$

RESULTS OF ANALYSIS

The effects of varying peak transmission and half band width of the optic filters on the measured reflectance ratio were studied to enable a filter selection to be made which suited the requirements for maximum statistical separation among colour categories. The wavelength ratio of prime concern was 600 nm/660 nm -- previously suggested as the optimum ratio.

The effect of using different light sources was studied by reversing the spectral output curve of the 3500K$^{\circ}$ tungsten lamp to produce a hypothetical lamp whose irradiance at 350 nm was that of the normal tungsten at 800 nm; the irradiance at 360 nm was that of the normal tungsten lamp at 790 nm etc.

Effects of Peak Transmission

The 600 nm/660 nm mean reflectance ratios, obtained when filters of equal half band widths of 20 nm and 40 nm and various combinations of peak transmissions from 20% to 60% were used in the analysis, are shown in Table 2.1. Values of t resulting from a t-test on the means of adjacent colour categories are listed in Table 2.2.

Effects of Filter Half Band Width

The 600 nm/660 nm mean reflectance ratios, obtained when combinations of 20 nm/20 nm to 40 nm/40 nm half band widths, and 20% and 40% peak transmissions were used for the 600 nm and 660 nm filters respectively, are

TABLE 2.1   NORMALIZED REFLECTANCE RATIOS OF 600nm/660nm,
             FOR COMBINATIONS OF EQUAL HALF BAND WIDTH
             FILTERS AND VARIOUS % TRANSMISSIONS: VALUES
             OBTAINED BY INTEGRATING OVER THE BAND WIDTHS.

Half Band Width of 600 nm Filter	=	20 nm
Half Band Width of 660 nm Filter	=	20 nm
Transmission of 600 nm Filter	=	20% to 60%
Transmission of 660 nm Filter	=	20% to 60%

	Firm Ripe	Semi-Ripe	Turning	Green
Mean*	2.35	3.95	7.14	9.65
S.D.**	0.13	0.80	0.67	0.27

Half Band Width for 600 nm Filter	=	40 nm
Half Band Width for 660 nm Filter	=	40 nm
Transmission of 600 nm Filter	=	20% to 60%
Transmission of 660 nm Filter	=	20% to 60%

	Firm Ripe	Semi-Ripe	Turning	Green
Mean*	1.83	2.97	6.11	9.61
S.D.**	0.10	0.67	0.80	0.51

*   Mean = Average of 5 tomatoes.

**   S.D. = Standard Deviation.

TABLE 2.2   STUDENTS t VALUES FOR COMPARISON
OF MEAN REFLECTANCE RATIOS OF FOUR
COLOUR CATEGORIES BASED ON DATA IN
TABLE 2.1

Half Band Width of 600 nm Filter	=	20 nm
Half Band Width of 660 nm Filter	=	20 nm
Transmission of 600 nm Filter	=	20% to 60%
Transmission of 660 nm Filter	=	20% to 60%

Firm Ripe vs. Semi-Ripe	Semi-Ripe vs. Turning	Turning vs. Green
4.387**	6.806***	7.730***

Half Band Width for 600 nm Filter	=	40 nm
Half Band Width for 660 nm Filter	=	40 nm
Transmission of 600 nm Filter	=	20% to 60%
Transmission of 660 nm Filter	=	20% to 60%

Firm Ripe vs. Semi-Ripe	Semi-Ripe vs. Turning	Turning vs. Green
3.807**	6.711***	8.216***

*** Significant at 0.1% level

** Significant at 1% level

shown in Table 2.3.

Table 2.4 lists the values of t resulting from the comparison of means of adjacent colour categories shown in Table 2.3.

Light Source Effects

Reversing the spectral output curve of the tungsten lamp, and testing this new hypothetical lamp in the analysis showed no significant change in the statistical separation between adjacent colour categories.

TABLE 2.3   NORMALIZED REFLECTANCE RATIOS OF 600 nm/660 nm,
             FOR COMBINATIONS OF VARIOUS HALF BAND WIDTHS AND
             TWO % TRANSMISSIONS: VALUES OBTAINED BY INTE-
             GRATING OVER THE BAND WIDTHS.

Half Band Width (nm) for		Percent Transmission for		Firm Ripe	Semi-Ripe	Turning	Green
600nm	660nm	600nm	660nm	Mean* / S.D.**	Mean / S.D.	Mean / S.D.	Mean / S.D.
20	20	20	40	2.35	3.95	7.14	9.65
				0.13	0.80	0.67	0.27
30	20	20	40	2.42	3.94	7.13	9.66
				0.13	0.78	0.68	0.27
40	20	20	40	2.52	3.94	7.11	9.66
				0.12	0.75	0.69	0.26
20	30	20	40	2.42	4.05	7.27	9.69
				0.14	0.81	0.67	0.27
30	30	20	40	2.46	3.99	7.19	9.67
				0.13	0.78	0.68	0.27
40	30	20	40	1.77	2.89	5.98	9.56
				0.10	0.66	0.80	0.54
20	40	20	40	2.52	4.20	7.44	9.75
				0.14	0.82	0.65	0.25
30	40	20	40	2.30	3.79	7.12	9.58
				0.12	0.73	0.76	0.39
40	40	20	40	1.85	2.97	6.11	9.61
				0.10	0.67	0.80	0.51

*   Mean = Average of 5 tomatoes

**   S.D. = Standard Deviation.

TABLE 2.4   STUDENTS t VALUES FOR COMPARISON OF MEAN
                   REFLECTANCE RATIOS OF FOUR COLOUR CATE-
                   GORIES BASED ON DATA IN TABLE 2.3.

Half Band Width (nm) for		Percent Transmission for		Firm-Ripe vs. Semi-Ripe	Semi-Ripe vs. Turning	Turning vs. Green
600nm	660nm	600nm	660nm			
20	20	20	40	4.387**	6.806***	7.730***
30	20	20	40	4.293**	6.885***	7.706***
40	20	20	40	4.177**	6.951***	7.727***
20	30	20	40	4.444**	6.866***	7.551***
30	30	20	40	4.326**	6.915***	7.563***
40	30	20	40	3.767**	6.674***	8.302***
20	40	20	40	4.511**	6.926***	7.386***
30	40	20	40	4.465**	7.075***	6.457***
40	40	20	40	3.807**	6.711***	8.261***

*** Significant at 0.1% level

** Significant at 1% level

DISCUSSION

The mean reflectance ratios listed in Table 2.1 indicate that there is no effect on the 600 nm/660 nm reflectance ratio if the half band widths of the filters are held constant and the peak transmissions altered. If the half band widths of the 600 nm and 660 nm filters are increased from 20 nm to 40 nm each, the means for each colour category are decreased. The decrease is not significant for any colour category at the 1% confidence level. Widening the band width of the filters results in integration remote from 600 nm and 660 nm where separation of firm ripe and semi-ripe tomatoes is greatest. The decreased separation between these two categories is reflected by the lower value of t as shown in Table 2.2.

Typical peak transmissions of 20% for the 600 nm filter and 40% for the 660 nm filter were chosen for the rest of the 600 nm/660 nm ratio analysis. Table 2.3 shows that combinations of half band widths from 20 nm/20 nm to 40 nm/40 nm produces a gradual decrease in the mean reflectance ratios of each colour category.

The corresponding values of t for the comparison of the means of adjacent colour categories of Table 2.3 are listed in Table 2.4. The value of t for the firm ripe vs. semi-ripe decreases consistently with the increasing bandwidth of the 600 nm filter. Widening the 660 nm half bandwidth shows a slight increase in t values except when in

combination with the 600 nm - 40 nm filter. The 600 nm -
20 nm filter combined with the 660 nm - 40 nm filter indicates
the best separation between firm ripe and semi-ripe. The
values of t for semi-ripe vs. turning and turning vs. green
do not seem to change with half band width variations, but
remain relatively constant.

The changes in half band width from 20 nm to 40 nm
for either filter do not significantly affect the separa-
tion of firm ripe vs. semi-ripe, semi-ripe vs. turning, and
turning vs. green. Examination of effects beyond 40 nm half
band widths was unnecessary since a 40 nm half band width
describes an inexpensive band pass (as opposed to narrow band
pass or very narrow band pass) filter.

In summary, the half band width of the interference
filter chosen for the colour separation is less critical than
the choice of peak wavelength. The peak transmission of the
filter does not affect the separation between colour cate-
gories. The type of light source used is not critical,
provided that the peak wavelengths of the filters also exist
in the light source to a detectable degree. Inexpensive
narrow band pass interference filters having half band widths
of 20 nm are common, and the choice of one at 600 nm and one
at 660 nm should be acceptable.

The comparison of t values in Table 2.2 and Table
1.3 indicates that analysis using equation [2-2] does not
alter the statistical separation of the mean reflectance

ratios examined.   Therefore the complete analysis is not

necessary to establish this separation and the reflectance

ratio at two wavelengths may be used as described in

Chapter 1.

The analysis of the system is necessary, however,

to obtain the following information.   The normalizing factor

F [2-3] is the gain ratio of the two photodetector amplifiers.

A scale of 10 was used for the analysis, but any convenient

scale, N, will produce similar results.   Now,

$$F \; = \; N/G \hspace{4cm} [2\text{-}4]$$

where   G = maximum value of E_1/E_2, calculated
                   from [2-2] for the greenest tomato.

The two photodetector amplifiers must be adjusted

so that their gain ratio (short wavelength photodetector

gain/long wavelength photodetector gain) is equal to F.

Reflectance ratios for all tomatoes will then be maintained

within the limits $0 \leq E_1/E_2 \leq N$.

C H A P T E R   3

DESIGN APPROACH

INTRODUCTION

It has been established that the ratio of reflected light at two narrow wavelength bands in the visible spectrum will be the criterion for colour grading in the present design. Specific components such as photodetectors and optic filters must now be selected. Having made the selection, a signal processing unit must be designed to carry out the task of dividing the two photodetector signals to produce the reflectance ratio, to categorize the tomato based on the reflectance ratio, and to transfer the signal to an appropriate eject mechanism. The mechanism is activated when the tomato and eject mechanism are in juxtaposition. The signal processor will be divided into two sections -- the analog processor, and the digital processor. The analog processor handles the information up to the point where categorization occurs. Signal handling then proceeds through the digital processor.

Fruit and vegetable conveying systems are available commercially and it was not the aim of this research to invent a new conveying system for tomatoes. Since many conveyors are flat belts, it was decided that all efforts should be concentrated towards designing a tomato grader which would be compatible with existing conveying systems. This would allow the purchase of "off the shelf" conveyors, as well as easy adaptation of the grader for organizations which already had such conveyors in use.

The fruit ejection mechanism was not a stock item, and its design will be described. Many possibilities were considered for moving the tomatoes off the belt, but a high pressure pneumatic system was found the most suitable.

A test conveyor, 6 feet in length, was built using a flat, matte black belt, 6 inches wide. A black belt was chosen, since it provided a low reflectance at the two critical wavelengths relative to the tomatoes transported on it. This provided a constant low reflectance background. The belt was chain driven by a variable speed motor, allowing testing at various conveyor speeds.

In many cases, the "ideal" components required for the system design were not commercially or readily available. Consequently, reasonable substitutions have been incorporated where necessary.

INITIAL COMPONENT SELECTION

Light Source

A Dolan-Jenner Model No. 150, variable intensity light source comprising a standard DNE projection lamp (3350°K colour temperature) with dichroic reflector was used.

Photodetectors

Two FPT 120A* phototransistors were chosen primarily for their high sensitivity.

The spectral response curve of the FPT 120A was previously shown in Figure 2.2.

Optic Filters

At the beginning of the research, both the 600 nm and 660 nm interference filters were not available. It was decided that the 600 nm filter might be substituted by a 550 nm filter which was available. The specifications for the two filters are listed below:

Peak wavelength	550 nm	660 nm
Half bandwidth	20 nm	20 nm
Peak Transmission	20%	40%

Referring to Table 1.1, the 550 nm/660 nm wavelength ratio ranks eighteenth in the list, based on the maximum total difference between means of adjacent colour categories. The statistical separation between adjacent colour categories using the 550 nm/660 nm wavelength ratio

---

* Manufactured by Fairchild Semiconductor Corp., Mountain View, California.

was studied using the analysis described in Chapter 2, to
ensure that this ratio could be used as a reasonable sub-
stitute for the ideal 600 nm/660 nm ratio. The spectral
distribution of the DNE bulb, the optic filter data, the FPT
120A response curve, and the spectrographic data of the
previously tested 20 tomatoes was programmed into equation
[2-2] to generate predicted values of E_1/E_2. The resulting
means and standard deviations for the four colour categories,
and the t-values of adjacent colour categories are listed in
Table 3.1. The data in Table 3.1 suggests that good separa-
tion between semi-ripe and turning, and turning and green
may be expected. The separation between firm ripe and semi-
ripe will be relatively poor, using the 550 nm/660 nm filter
combination; however, the rest of the system design should
not be adversely affected. The 550 nm filter was therefore
used as a substitute for the 600 nm filter.

Analog and Digital Families

Figure 3.1 shows a standard phototransistor
amplifying circuit where the output voltage, V_o, is a function
of incident radiant energy on the photo-sensitive semi-
conductor area. Two amplifiers measuring the energy trans-
mitted through the optic filters produce two voltages which
are functions of the light reflected from the tomato surface.
Division of the two voltages to produce the desired reflec-
tance ratio is readily accomplished through the use of a
standard Operational Amplifier (Op Amp) circuit. Since the

TABLE 3.1   NORMALIZED REFLECTANCE RATIO MEANS,
                 STANDARD DEVIATIONS, AND STUDENTS t
                 VALUES FOR FOUR COLOUR CATEGORIES
                 USING A 550 nm/660 nm WAVELENGTH
                 RATIO: VALUES OBTAINED BY INTE-
                 GRATING OVER THE BAND WIDTHS.

	Filter	
	550 nm	660 nm
Half Band Width	20 nm	20 nm
Peak Transmission	20 %	40%

	Firm-Ripe	Semi-Ripe	Turning	Green
Mean	0.458	1.193	5.329	9.646
S.D.	0.051	0.583	0.961	0.388

	t - Values
Firm-Ripe vs. Semi-Ripe	2.805*
Semi-Ripe vs. Turning	8.227***
Turning vs. Green	9.313***

*** Significant at 0.1% level

*   Significant at 5%   level

FIGURE 3.1 STANDARD NPN PHOTOTRANSISTOR
AMPLIFIER USING AN FPT120A
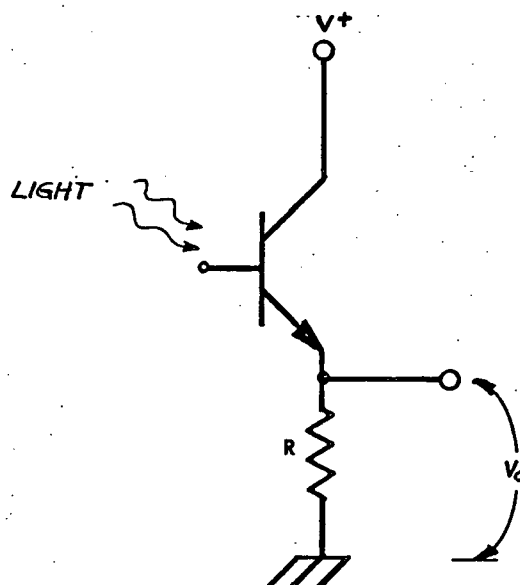
dividing circuit is an integral part of the system, it was decided that analog signal processing should be done using the Op Amps. Modern Op Amps are available as integrated circuits, which generally operate on a split $\pm$ 15 volt power supply.

The choice of digital families that could be used was broad. The high speed switching capability of the popular TTL (Transistor-Transistor Logic) circuits was believed to be more of a hindrance than an asset for this type of instrument. The devices are very susceptible to noise, requiring much electrical shielding. The low +5 volt supply voltage of the TTL circuits rendered it even less compatible with the Op Amps.

The newly developed and rapidly expanding family of CMOS (Complementary Symmetry-Metal Oxide Semiconductor) was found to be very suitable for this design. The CMOS family has many advantages over TTL circuits. The CMOS devices will operate on a +15 volt power supply making them highly compatible with the Op Amps. Their quiescent power dissipation is typically 10^{-6} that of TTL circuits, and switching of small analog signals is achieved with bilateral switches unknown to the TTL family. The noise immunity of the CMOS devices is much higher than TTL logic devices. The lower switching speed of 5 megahertz (MHz) as opposed to 30 MHz for TTLs was not a hindrance, since sorting operations will typically be below $10H_z$. For these reasons, the CMOS family was chosen for the digital processing section of the colour grader.

ELECTRONIC COLOUR GRADING SYSTEM:

OVERVIEW

A block diagram of the electronic signal processor of the colour grader is shown in Figure 3.2. There are two sections to the signal processor -- the analog processor and the digital processor. The analog processor senses the presence of the tomato through the summation of the photo-detector output signals and continuously calculates the reflectance ratio as the tomato passes under the sensing head. The peak reflectance ratio is used to categorize the tomato into one of four colour categories. The category information is entered into the digital processor at the time the tomato leaves the sensing area, and the data moves through a memory as the tomato travels downstream from the sensing head. When the categorized tomato is in line with its eject station, a signal appears at the output of the memory which is used to operate an electromechanical eject mechanism.

A light beam chopper disk and photodetector are attached to the axle of one of the conveyor pulleys, and the chopped electrical signal is used to synchronize the movement of the data in the memory with the movement of the conveyor belt. The memory is comprised of three shift registers, one for each of the three colour categories: firm ripe, semi-ripe and turning. The green tomatoes were allowed to fall off the end of the conveyor. Each shift register has a different storage capacity, depending on the lineal distance
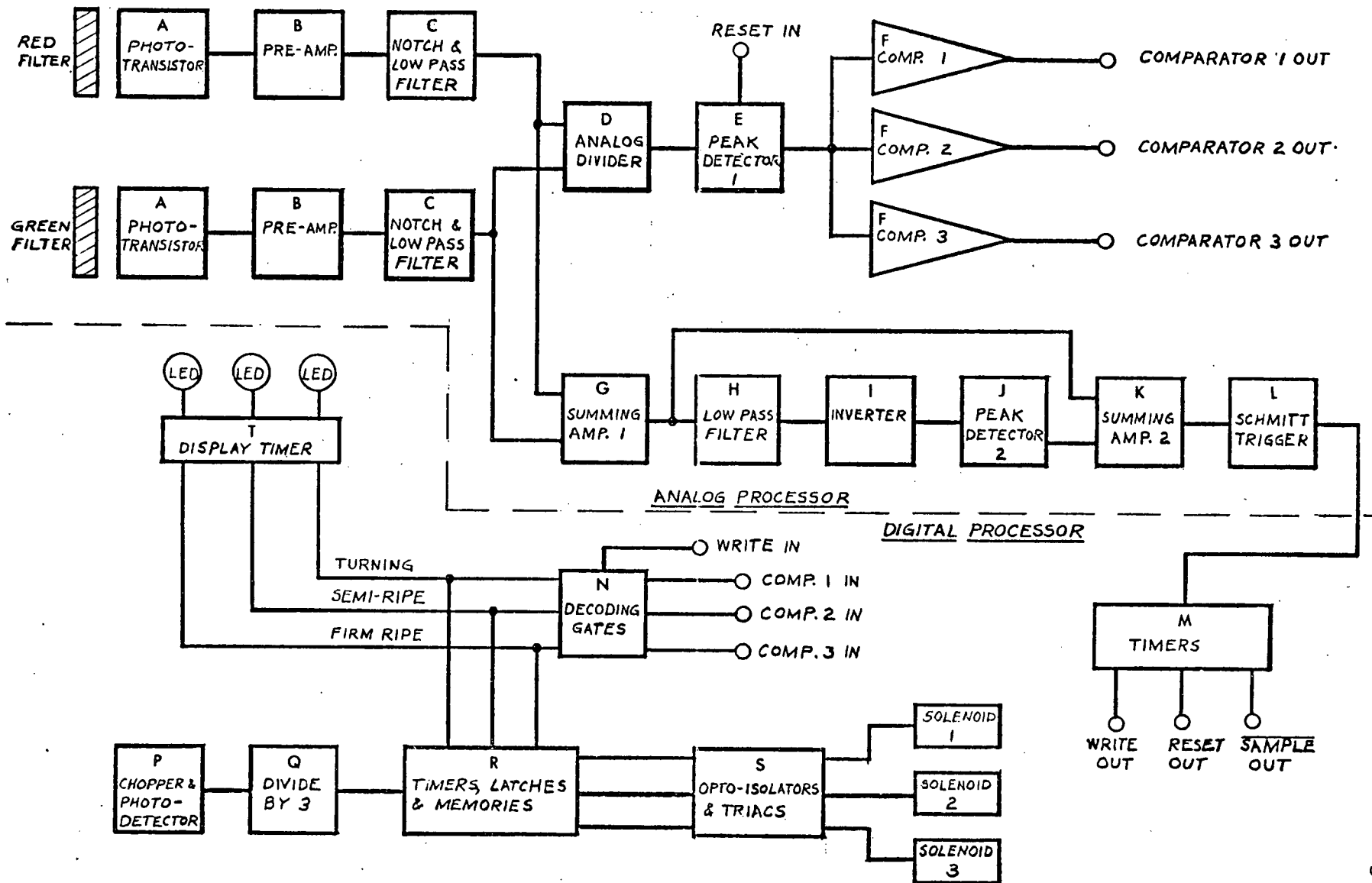
FIGURE 3.2 COLOUR GRADER BLOCK DIAGRAM

54

downstream from the sensing head that a particular eject station is located. A categorized tomato and its eject station will always coincide at ejection time regardless of conveyor belt speed, due to the memory-conveyor belt synchronization.

The solenoids incorporated in the pneumatic eject system were standard 110v AC types, and it was necessary to isolate these devices from the low voltage signal processing circuit by means of an opto-isolator interface.

Each of the blocks in Figure 3.2 will be discussed in more detail, with respect to function, design and necessity. Where possible, the analog and digital processors will be dealt with separately.

ANALOG SIGNAL PROCESSOR

Divider Circuit (Box D, Figure 3.2)

The circuit chosen to divide the two photodetector voltages is shown in Figure 3.3. It consists of an MC1495* and two type 741** Op Amps. The second 741 Op Amp is used as a summing amplifier, whereas the MC1495 and first 741 are used for the division operation. The characteristics of the circuit are as follows:

(a) $0 < V_x \leq + 10$ volts.

(b) -10 volts $\leq V_z \leq + 10$ volts.

(c) $V_{o1} = -10\ V_z/V_x$

where V_z = output voltage from the "green" photo-transistor

V_x = output voltage from the "red" photo-transistor

Initial testing of this circuit showed that the saturation voltage (V_{o1} = constant, for any V_x, V_z) was -12.5 volts. The output voltage range of the divider is therefore zero to -12.5 volts if V_x and V_z are positive. Since the CMOS devices operate from zero to +15 volts, it was found advantageous to add +12.5 volts to the divider output using a summing amplifier to change the output range of +12.5 to zero volts. The new equation for the circuit is:

---

*   MC prefix indicates component manufactured by Motorola Semi-conductor, Inc., Phoenix, Arizona.
**   Type 741 Op Amps are manufactured by Motorola Semi-conductor, Inc. (MC1741); Fairchild Semi-conductor Corp. (μA741), Mountain View, California; RCA Corp. (CA3741) Somerville, New Jersey; and others.
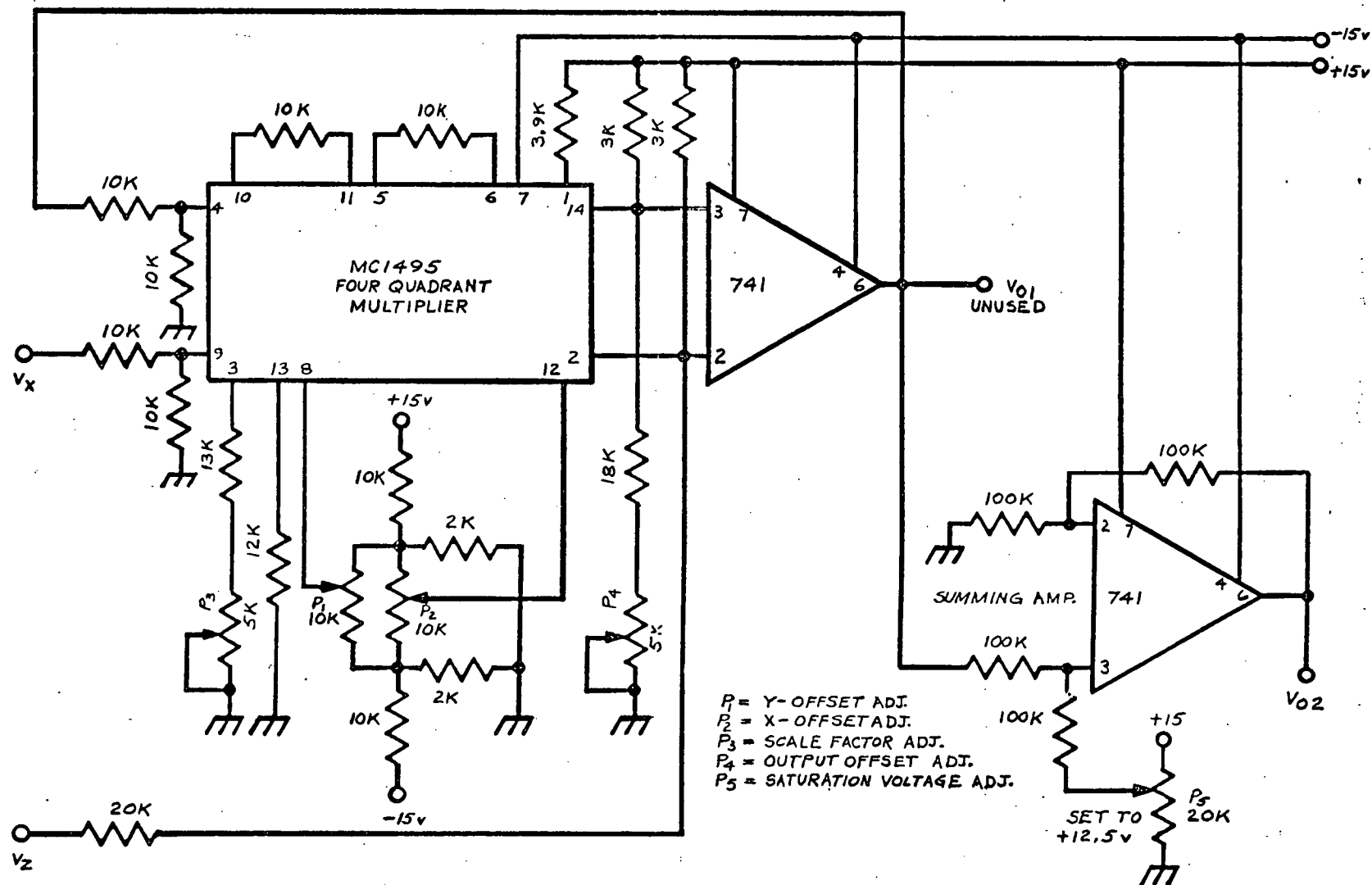
FIGURE 3.3   ANALOG DIVIDER CIRCUIT

57

$$V_{o2} = 12.5 - 10\, V_z/V_x \qquad [3-1]$$

From [3-1] it may be shown that for the range

$0 \le V_{o2} \le 12.5$, the input range to the divider must be

$0 \le V_z/V_x \le 1.25$. Therefore, in equation [2-4], N = 1.25.
It may be shown using the analysis in Chapter 2, that a given
ratio F = 1.60 will maintain V_z/V_x within the above limits.
Consequently the gain of the "green" amplifier should be
1.60 X gain of the "red" amplifier. Using equation [3-1],
the predicted mean output voltages for the four colour cate-
gories based on the twenty tomatoes (Chapter 1) were calcu-
lated, and are listed in Table 3.2.

The potentiometers, P_1 through P_4, in Figure 3.3,
are adjusted initially so that the circuit operates within
the specified limits and is balanced*. Potentiometer P_5 is
adjusted to approximately -12.5 volts so that V_{o2} is zero
when $V_z > 1.25\ V_x$.

---

* See Motorola Linear Integrated Circuits Data Book, 1972,
  (second edition) p. 7-387 for calibration procedure.

TABLE 3.2   PREDICTED MEAN OUTPUT VOLTAGES FOR FOUR COLOUR
CATEGORIES BASED ON EQUATION [3-1] AND THE
TWENTY TOMATOES (Chapter 1).

Colour	V_{o2} (volts)
Firm Ripe	11.93
Semi-Ripe	11.00
Turning	5.82
Green	0.41

Phototransistor and Preamplifier Circuits (Box A,B,Figure 3.2)

The high impedance output of the phototransistor amplifier shown in Figure 3.1 was followed by a low-gain, non-inverting type 741 Op Amp which provided a low impedance output. The 741 Op Amp also provides a fine offset adjustment to establish the black conveyor belt as a zero voltage reference. The schematics for the "red" and "green" amplifiers are shown in Figure 3.4.

(a) The output voltage of the red amplifier may not exceed + 10 volts (input restriction on V_x of the divider). A large, firm ripe tomato was placed under the light sensing head, 1/2 in (1.3 cm) from the fibre optic bundle*, and a quantum measurement of 0.25 $\mu E/m^2$ sec (micro Einsteins/ meter^2 sec) was obtained through the 660 nm filter at 75% of the light intensity scale of the illuminator. This reflected quantum level is equivalent to 1.5×10^{-3} mw/cm^2 (milliwatts/cm^2). Specification sheets for the FPT 120A do not yield information below 5×10^{-3} mw/cm^2; consequently the phototransistor collector current at +15 volts supply was measured at various quantum levels, and a linear regression performed on the data. The resulting equation was:

$$I_{CE} = 54.2 \ Q^{1.392} \qquad\qquad [3-2]$$

* This will produce the maximum voltage expected for the red amplifier.

FIGURE 3.4   RED AND GREEN PHOTOTRANSISTOR AMPLIFIERS

RED AMPLIFIER
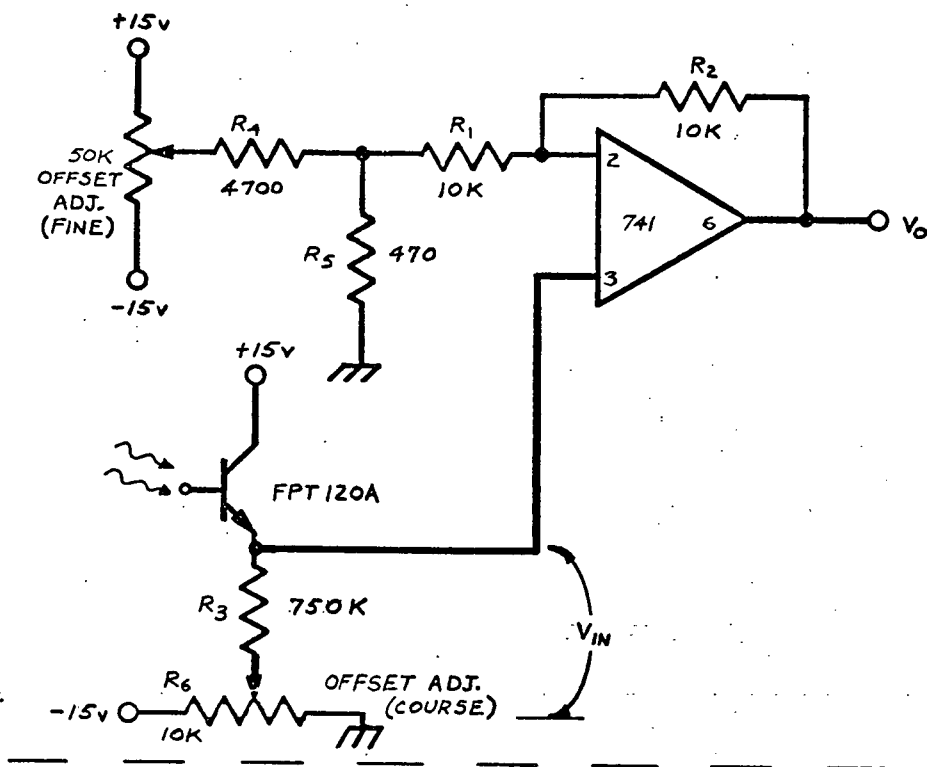
GREEN AMPLIFIER
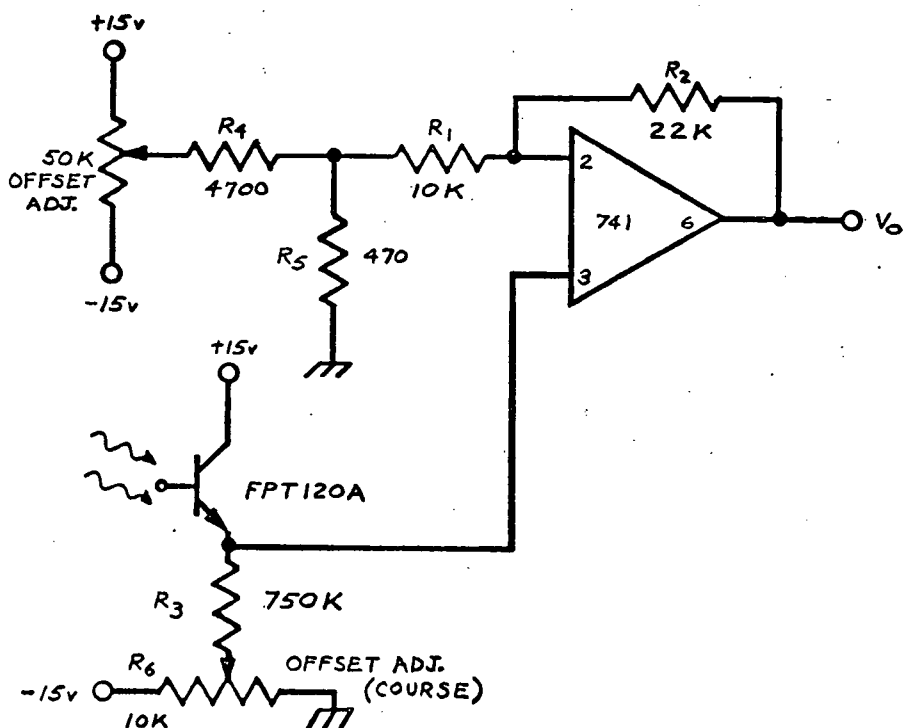
where I_{CE} = collector current in μA (micro amps)

Q   = quanta, in $\mu E/m^2$ sec.

Equation [3-2] yields I_{CE} = 7.9 μA for the firm ripe

tomato.

The black conveyor belt reflectance was also

measured through the 660 nm filter, and found to be

0.06 $\mu E/m^2$ sec. The current generated due to the back-

ground using equation [3-2] yields I'_{CE} = 1.1 μA.

Neglecting the fine offset adjustment, the equation

governing the output of each of the non-inverting

amplifier circuits is:

$$V_o = (\frac{R_2}{R_1} + 1) V_{in} \qquad [3-3]$$

where

V_o = output voltage (referenced to ground)

V_{in} = input voltage (referenced to ground)

$(\frac{R_2}{R_1} + 1)$= A_v = closed loop gain.

If R_1 = R_2 = 10KΩ, then A_v = 2, and if the maximum

value of V_o = 10 volts, then V_{in} = 5 volts for the

large firm ripe tomato.

If R_6 is sufficiently small so as not to contribute

significantly to R_3, then the current through the photo-

transistor and the resistor, R_3, is the same. When the

photo input results from the black belt only,

$$\frac{V_{in} - V_c}{R_3} = 1.1 \ \mu A \qquad\qquad [3-4]$$

where

V_{in} = 0 (zero volts for background)

V_c = course offset adjustment voltage

therefore,

$$V_c = -1.1 \ R_3 \qquad\qquad [3-5]$$

When the photo input is from the firm ripe tomato, again the current through the phototransistor and R_3 is the same. Substituting [3-5], and the firm ripe tomato photo current yields:

$$\frac{V_{in} - (-1.1 \ R_3)}{R_3} = 7.9 \ \mu A$$

since,

V_{in} = 5 volts,

therefore,

R_3 = 735 KΩ, or a suitable value would be

$$R_3 = 750 \ K\Omega \qquad\qquad [3-6]$$

Substituting [3-6] in [3-5] yields

V_c = -0.825 volts.

A value of R_6 = 10 KΩ would be suitable for the course offset adjustment.

The fine offset adjustment range is governed by the equation:

$$V_{offset} = \pm V_{supply} \, (R_5/R_4) \qquad [3\text{-}7]$$

If,

$$R_4 = 4.7 \text{ K}\Omega, \text{ and}$$

$$R_5 = 470 \ \Omega$$

$$V_{offset} = \pm 1.5 \text{ volts}$$

(b)   Since the gain ratio F is equal to 1.60 as described in the divider circuit, the gain of the green amplifier must be 1.60 times the gain of the red amplifier, or $A_v = 3.20$, i.e.

$$\frac{R_2}{R_1} + 1 = 3.2$$

or $R_2 = 2.2 \ R_1 \qquad [3\text{-}8]$

Let R_1 and R_3 for the green amplifier equal R_1 and R_3 for the red amplifier, i.e.

$$R_1 = 10 \text{ K}\Omega, \text{ and}$$

$$R_3 = 750 \text{ K}\Omega$$

then from [3-8],

$$R_2 = 22 \text{ K}\Omega.$$

The background reflectance was measured through the 550 nm filter and found to be 0.05 $\mu E/m^2$ sec. From equation [3-2], the current generated in the green phototransistor is:

$$I''_{CE} = 0.84 \ \mu A.$$

As in [3-4],

$$\frac{V_{in} - V_c}{R_3} = 0.84 \ \mu A. \qquad [3-9]$$

Substituting

$$V_{in} = 0$$

$$R_3 = 750 \ K\Omega$$

then, $\quad V_c = -0.63 \ volts$

The fine offset adjustment range was selected equal to that of the red amplifier.

Notch Filter and Low Pass Filter (Box C, Figure 3.2)

The phototransistor amplifiers are very sensitive to light intensity variations, such as those created by the 60 Hz sine wave driving the light source.

The two voltage peaks, one positive and one negative per cycle in the 60 Hz sine wave produce an undesirable 120 Hz noise signal at each phototransistor output. A twin-T notch filter using LM302* voltage followers was chosen to sharply cut the signal at 120 Hz. A low pass active filter with a 24 Hz cut-off frequency, using a 741 Op Amp was placed behind the notch filter to minimize other low frequency noise, such as 60 Hz.

The notch filter passes all frequencies except a very narrow band of frequencies around a center frequency f_o, which in this case is 120 Hz. The low pass filter passes all low frequencies up to the cut-off frequency, f_c, where the signal amplitude is cut by 3dB and attenuation continues through the higher frequencies, at a rate of 9dB/octave.

The need for both filters may be illustrated as follows. Since most of the noise was 120 Hz, the most effective filtering was desired for that frequency. The "notch depth" or maximum attenuation of the 120 Hz notch filter was measured and found to be -45dB. A low pass filter having a 9dB/octave slope, in order to be as effective

---

* LM prefix refers to components manufactured by National Semi-conductor Corp., Santa Clara, California.

as the notch filter at 120 Hz, would require a cut-off
frequency of 4 Hz. This limitation would interfere with
sorting operations which were expected to be above 4
tomatoes/second. Sorting rates above approximately 20
tomatoes/second were not expected, therefore a low pass
filter with a cut-off of 24 Hz was chosen (standard compon-
ents may be used) to be placed in series with the notch
filter.

Figure 3.5 is a schematic of one of two identical
filter circuits used in the colour grader, one circuit
following the red phototransistor amplifier, and the other
following the green phototransistor amplifier (Figure 3.4).
The equations governing the component selection for the
notch filter are as follows:

$$f_o = \frac{1}{2\pi R_1 C_2} \qquad\qquad\qquad [3\text{-}10]$$

$$R_2 = R_1/2 \qquad\qquad\qquad [3\text{-}11]$$

$$C_1 = 2C_2 \qquad\qquad\qquad [3\text{-}12]$$

For maximum efficiency, component matching is
critical -- resistors should be 0.1% tolerance; capacitors
1% tolerance. Components with these tolerances were not
readily available so 1% resistors and 2% capacitors were
used, requiring a variable band width adjustment through the
use of the 100 KΩ potentiometer and the LM302 voltage follower
in the feed back loop to the junction of C_1 and R_2.

TWIN-T NOTCH
FILTER

V_{IN}

133K 1%
R_1

133K 1%
R_1

0.01μF
2%

C_1

0.01μF
2%

133K
1%

R_2

133K
1%

0.01μF 2%

0.01μF 2%

C_2

C_2

LM302   6

3

6 LM302

100K

(2) 0.047μF

C_3

2

741   6

V_0

3

100K

R_3

100K

R_4

LOW PASS
FILTER

C_4 0.047μF
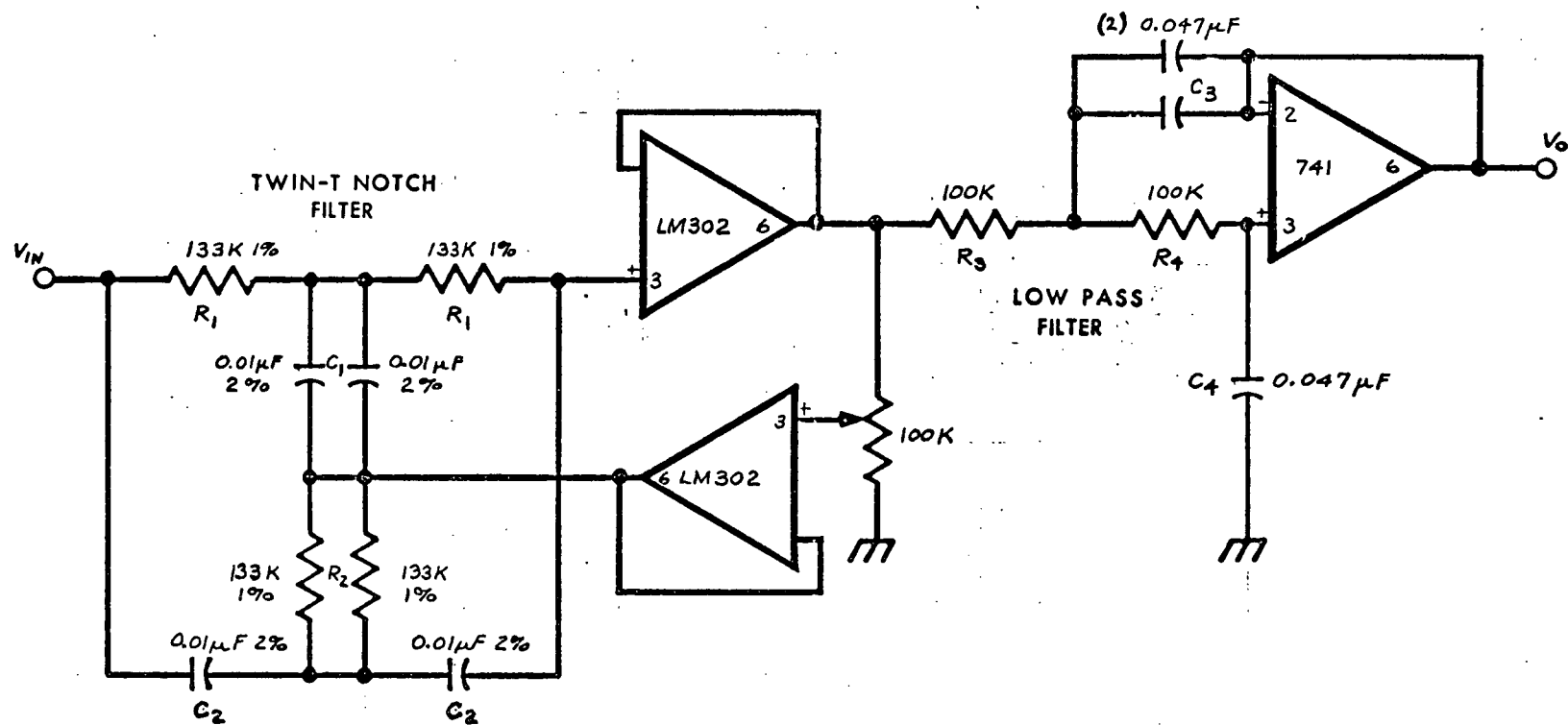
FIGURE 3.5   NOTCH AND LOW PASS FILTERS

Selection of components was made using equations [3-10] through [3-12] as follows:

Let C_2 = 0.01 μF,

now $R_1 = \dfrac{1}{2\pi f_o C_2}$

R_1 = 133 KΩ

R_2 = 66.5 KΩ (two 133 KΩ resistors in parallel)

C_1 = 0.02 μF (two 0.01 μF capacitors in parallel).

The equations governing component selection for the low pass filter are:

$$C_3 = \frac{R_3 + R_4}{2 \sqrt{2}\, \pi\, f_c\, R_3\, R_4} \qquad\qquad [3\text{-}13]$$

$$C_4 = \frac{1}{\sqrt{2}\, \pi\, f_c\, (R_3 + R_4)} \qquad\qquad [3\text{-}14]$$

If $R_3 = R_4$, then [3-13] becomes

$$C_3 = \frac{1}{\sqrt{2}\, \pi\, f_c\, R_3} \qquad\qquad [3\text{-}15]$$

Let R_3 = 100 KΩ, and f_c = 24 Hz, then

C_3 = 0.094 μF, and

$C_4 = \dfrac{1}{2C_3}$ = 0.047 μF.

Tolerances for R_3, R_4, C_3 and C_4 are not critical, since a cut-off frequency slightly above or below 24 Hz resulting from component mismatch is inconsequential.

The unity gains of the active filters do not

alter signal amplitude, except at frequencies above 24 Hz, where attenuation occurs at a rate of 9dB/octave, as desired.

71

Peak Detector 1 (Box E, Figure 3.2)

PEAK DETECTOR 1 is an analog storage circuit,
which stores the most positive signal appearing at the input.
The stored voltage appears at the output of the circuit. A
schematic of the peak detector circuit is shown in Figure 3.6.

The function of the 741 Op Amp and diodes is to
allow capicator C_1 to charge to the input voltage, but not
to discharge. The high input impedance ($10^{12}\Omega$) of the LM302
voltage follower, drains very little current from the capaci-
tor C_1 resulting in a constant voltage appearing at the out-
put after the peak is stored; with minimal drift of the
stored voltage over time. Resetting the peak detector to
zero is accomplished by a positive (HIGH) pulse at the control
input of the CD4066 bilateral switch. The bilateral switch
is identical to a small signal relay, but since it is a semi-
conductor, it has no moving contacts and cannot wear out. The
reset pulse at the control input causes the bilateral switch
to close, allowing C_1 to discharge to a zero potential through
R_1. The output voltage V_o will remain at zero volts until the
reset pulse goes LOW and a new signal appears at the peak
detector input.

Figure 3.7a shows typical divider output (PEAK
DETECTOR 1 input) signals for uniformly coloured firm ripe
and semi-ripe tomatoes of equal size, as the tomato passes
under the sensing head. Due to edge effects of the spherical
tomato, the divider output signal is bell shaped. If the
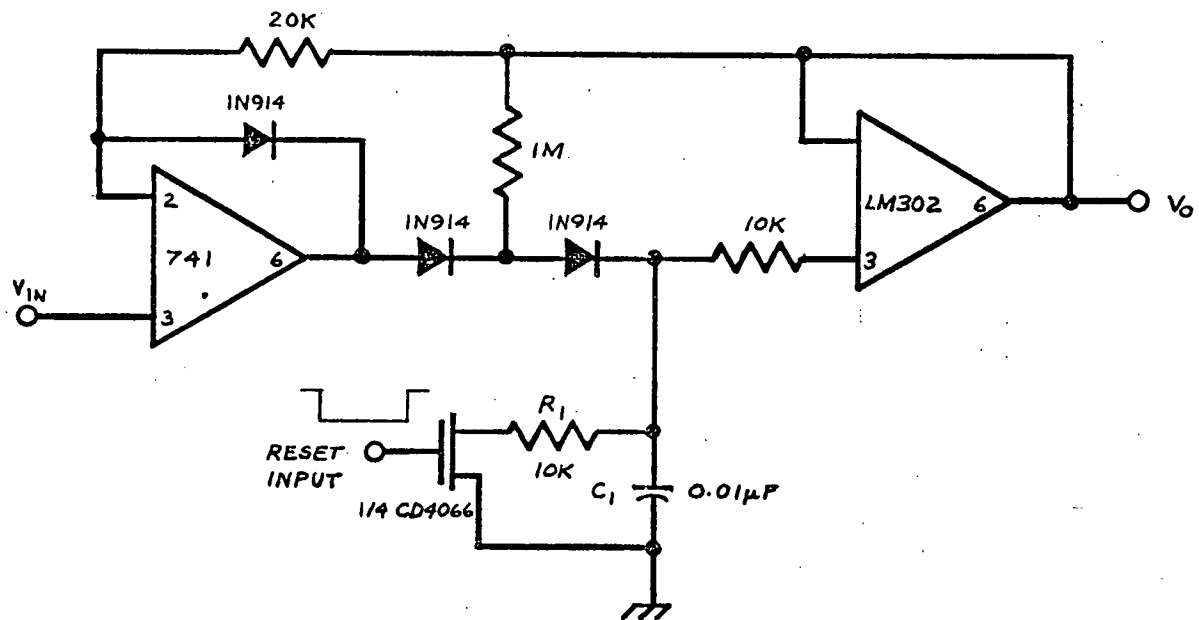
FIGURE 3.6 PEAK DETECTOR 1

FIGURE 3.7 OUTPUT VOLTAGES FOR TYPICAL
FIRM RIPE, AND SEMI - RIPE TOMATOES
(a) DIVIDER OUTPUT FOR UNIFORMLY RIPE
TOMATO
(b) DIVIDER OUTPUT FOR NON - UNIFORMLY
RIPE TOMATO
(c) PEAK DETECTOR OUTPUT FOR (a)
AND (b)

VOLTS

(a)

(b)

(c)

V_{PEAK}

V_{PEAK}

FIRM RIPE

SEMI - RIPE

TIME
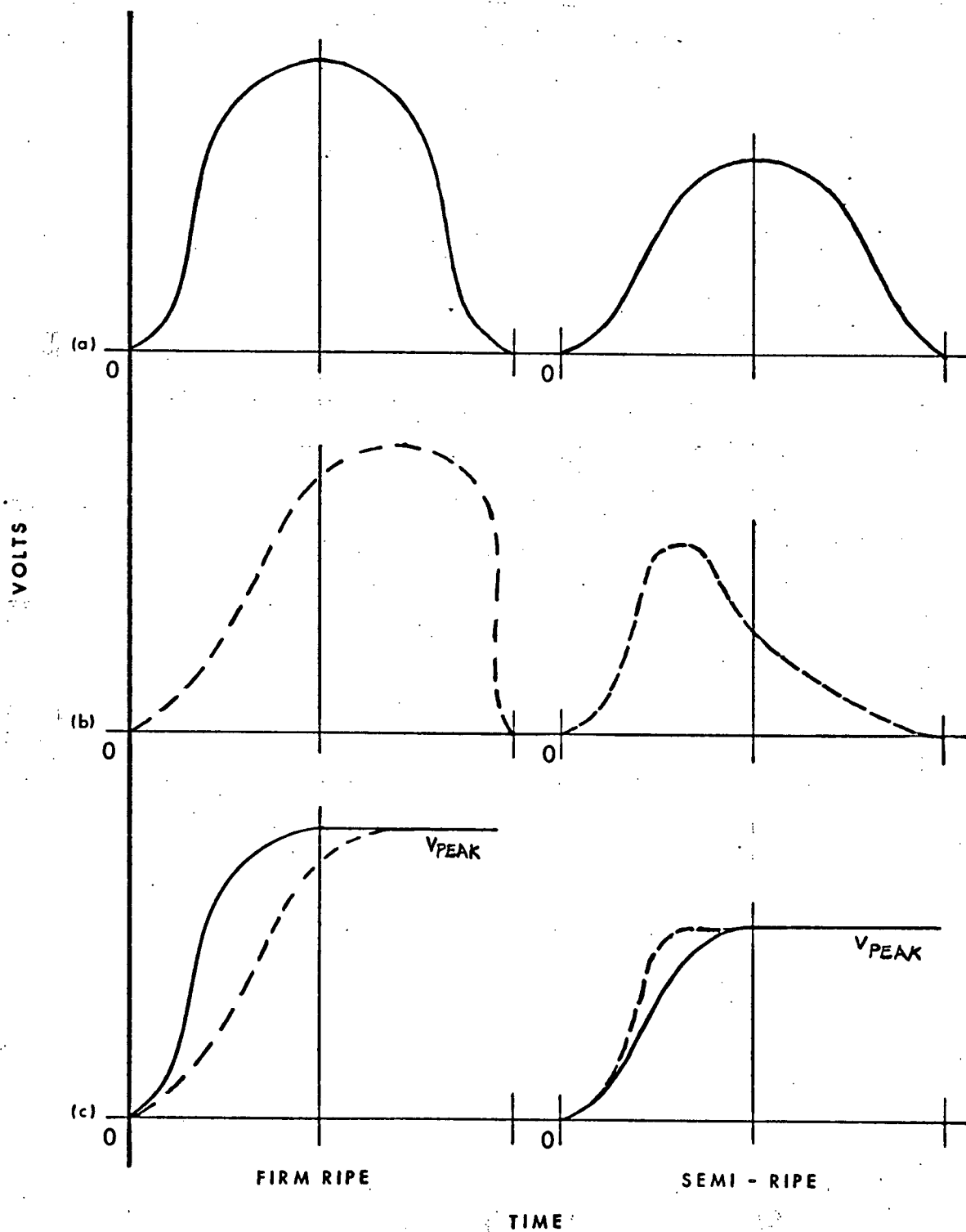
voltage was measured midway between the leading and trailing edges of the signal, the voltage read would be the peak voltage -- the maximum redness -- without the need for a peak detector circuit. Unfortunately, tomatoes are not always uniform in ripeness, i.e. one area may be redder than another.

Typical divider output signals for non-uniform firm ripe and semi-ripe tomatoes are shown in Figure 3.7b. Now the mid-point between leading and trailing edges does not indicate maximum redness. Figure 3.7c shows the peak detector output signal for either uniformly ripe or non-uniformly ripe tomatoes. For both types of tomatoes, the maximum redness, V_{PEAK}, will be measured and stored.

Comparators 1, 2 and 3 (Box F, Figure 3.2)

The schematic of the comparator circuit used is shown in Figure 3.8. The output of PEAK DETECTOR 1 is continuously and simultaneously present at the input of the three comparators, COMPARATOR 1, 2 and 3. Referring to Figure 3.8 when the input voltage, V_{IN}, i.e. PEAK DETECTOR 1 output voltage, exceeds the set voltage V_{SET} of a comparator, the voltage output, V_O, of that comparator drops from +14 to zero volts, due to the high open loop gain of the 741 amplifier (typically 200,000). The comparator essentially goes from the positive saturated state to the negative saturated state. The IN914 diode at the output of each comparator clamps V_O between zero and +14 volts, otherwise V_O would range from +14 volts to -14 volts. The two IN914's across the input of each comparator are input protection diodes.

V_{SET} is a threshold voltage for a comparator. Since four colour categories are to be separated, three different comparators and V_{SET} adjustments are required. Two adjustments, $V_{SET\ 2}$ and $V_{SET\ 3}$ are available on the front panel of the colour sorter cabinet, for setting the cutoff voltages separating turning from semi-ripe, and semi-ripe from firm ripe. The green cutoff voltage, $V_{SET\ 1}$, is adjusted internally on the circuit board, since this voltage requires only an initial set up.

The output of each comparator is either HIGH (state 1) or LOW (state 0).

FIGURE 3.8   COMPARATOR CIRCUIT
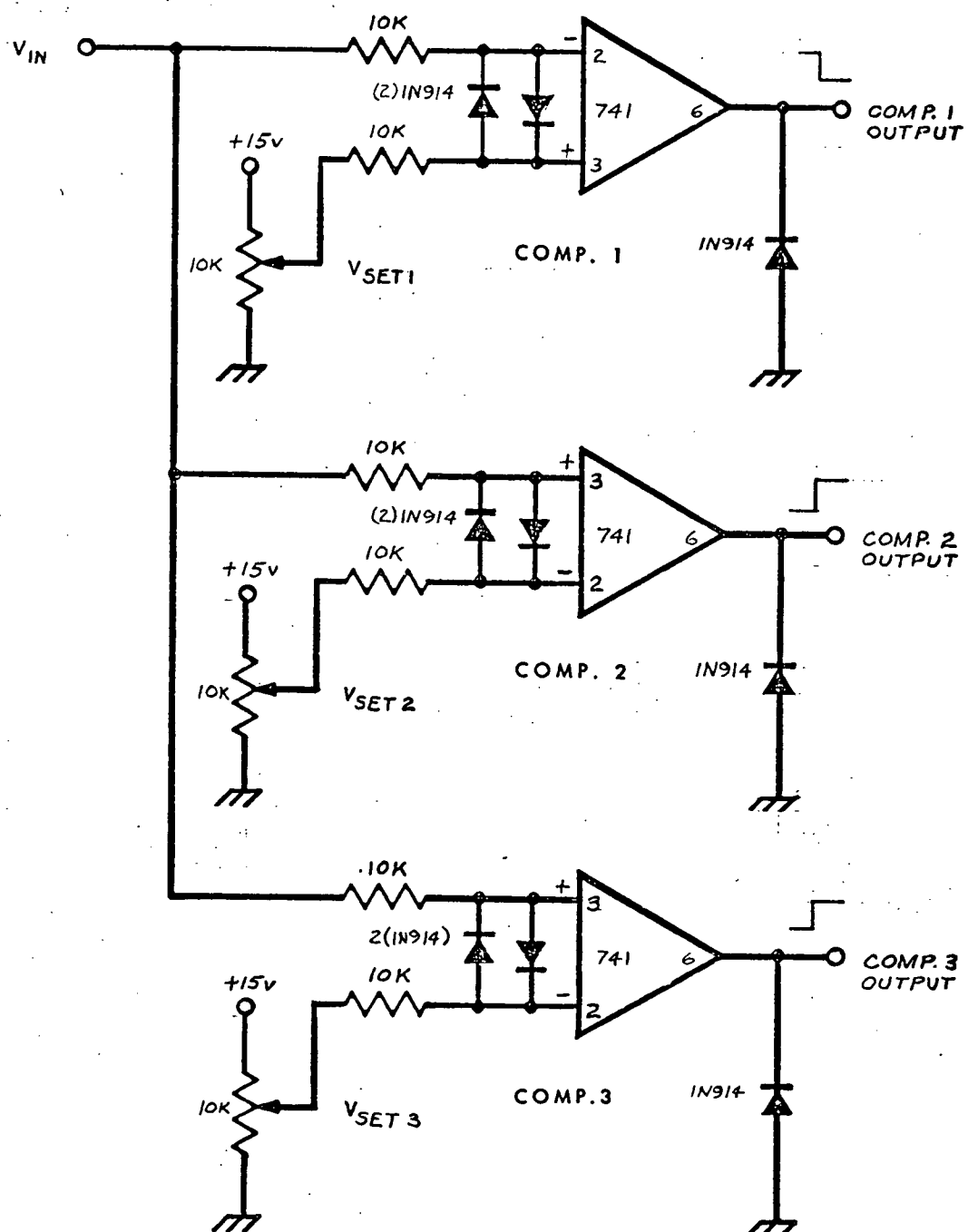
The output states of the three comparators and the colour categories they represent are shown in Table 3.3.

The outputs of the comparators are digital waveforms compatible with CMOS devices, and these outputs are connected to the digital processor, as shown in Figure 3.2.

TABLE 3.3   OUTPUT STATES OF COMPARATORS
                        1, 2, and 3, FOR FOUR COLOUR
                        CATEGORIES

Colour Category	OUTPUT STATE		
	COMP. 1	COMP. 2	COMP. 3
Green	1	0	0
Turning	0	0	0
Semi-Ripe	0	1	0
Firm Ripe	0	1	1

Summing Amplifier 1 (Box G, Figure 3.2)

Rather than use a separate light activated, or
mechanically activated trigger, which senses the presence of
a tomato under the sensing head, it was decided that the two
signals at the divider input could be summed to produce a
uniform output signal, regardless of the colour of the tomato.
The divider output cannot be used effectively as a trigger,
since the signal amplitude varies with colour. The sum of
the red and green signals, however, is relatively constant
for red and green tomatoes, since a red tomato produces a
large red signal and a small green signal, and a green tomato
produces a large green signal and a small red signal.

The major drawback in a summing amplifier such as
this is that small drifts at the input are additive, resulting
in large drifts at the output. The drift at the inputs may
be due to small light intensity variations or changes in
ambient temperature.

The trigger voltage should ideally be zero when no
tomato is present, i.e. when the sensing head sees only the
light reflected from the black conveyor belt. To offset the
small amount of reflected light from the belt, a background
zero voltage adjustment was included in the circuit.

A schematic diagram of the non-inverting 741 SUMMING
AMPLIFIER 1 is shown in Figure 3.9. The output voltage V_o
in the sum of $V_{IN\ 1}$ and $V_{IN\ 2}$, provided that the offset is
adjusted to zero. The offset adjustment is adjusted for

FIGURE 3.9 SUMMING AMPLIFIER 1

80

FIGURE 3.9 SUMMING AMPLIFIER 1
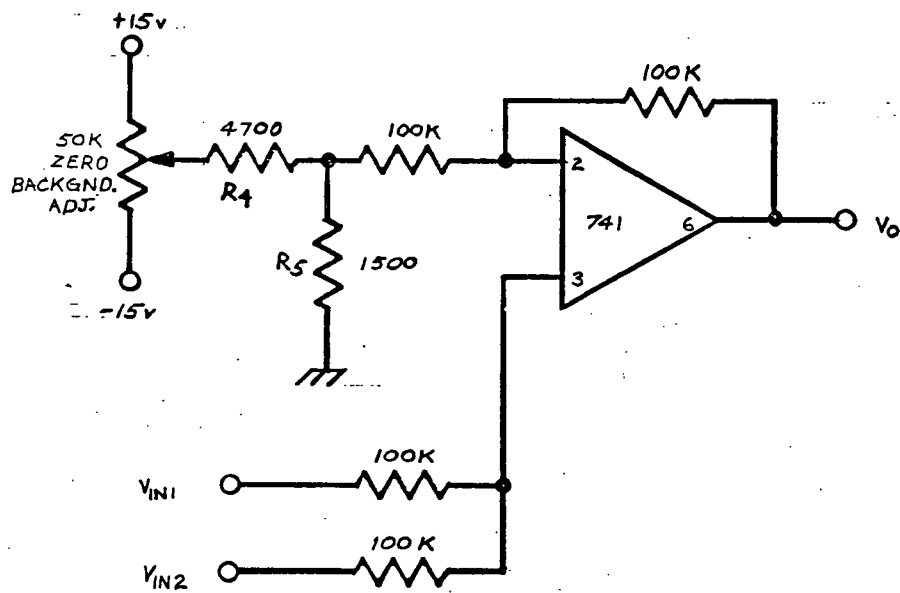
zero output at a given light intensity with the sensing head viewing the black conveyor belt. The offset range is approximately ± 4.8 volts as described in equation [3-7]. Drift in the zero adjustment due to slow input variations will adversely affect the trigger signal.

Belt Background Monitor (Box H,I,J,K, Figure 3.2)

The function of the belt background monitor is to
monitor minor drift in the initial zero adjustment of SUMMING
AMPLIFIER 1 (Box G, Figure 3.2) and to continuously compen-
sate for any drift.

The circuit is comprised of a low pass active
filter, an analog inverter, PEAK DETECTOR 2, and SUMMING
AMPLIFIER 2, using 741 Op Amps. The schematic of the belt
background monitor circuit is shown in Figure 3.10.

The low pass filter, with a 10 Hz cutoff frequency,
was required to suppress any high frequency noise present at
the SUMMING AMPLIFIER 1 output. Noise at the input of the
peak detector can result in an erroneous background correc-
tion. Component selection was made using equations [3-13]
and [3-14].

The output of the low pass filter is of the same
polarity as the output of SUMMING AMPLIFIER 1. The inverting
amplifier, having unit gain, changes the polarity of the
SUMMING AMPLIFIER 1 signal. This signal is fed into PEAK
DETECTOR 2 which stores the most positive signal at its
input, i.e. the most negative output voltage of SUMMING
AMPLIFIER 1.

SUMMING AMPLIFIER 2 sums the output of PEAK DETECTOR
2 and the output of SUMMING AMPLIFIER 1 to produce an output
voltage, V_o. V_o is the same as V_{IN} with background drift
compensation.
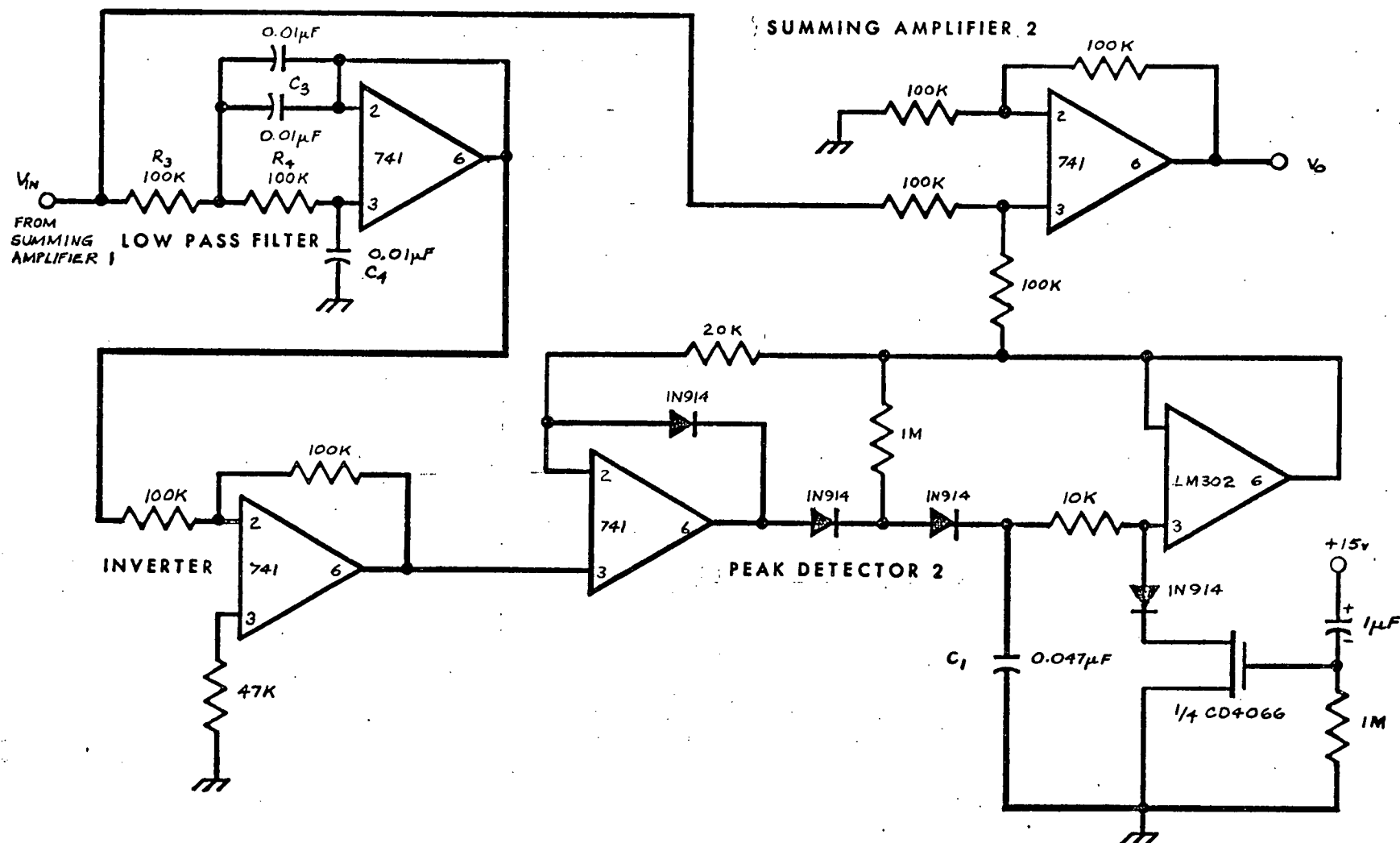
FIGURE 3.10 BELT BACKGROUND MONITOR

To illustrate, suppose that the output of SUMMING AMPLIFIER 1 has drifted to 0.5 volts, while the sensing head is viewing the black conveyor belt. The output of PEAK DETECTOR 2 will be -0.5 volts, and the sum of the two voltages V_o, will be zero volts. When a tomato passes under the sensing head, the output of SUMMING AMPLIFIER 1 rises rapidly from 0.5 to 5 volts, for example, and at the same time the inverting amplifier output drops from -0.5 to -5 volts. But the output of PEAK DETECTOR 2 remains at -0.5 volts, the most positive input voltage; consequently V_o of SUMMING AMPLIFIER 2 changes from (-0.5 + 0.5) = 0 volts to (-0.5 + 5.0) = 4.5 volts. The output of SUMMING AMPLIFIER 2 is thus always referenced to zero volts, and does not change with slight variations in belt background reflectance.

The divider output signal as mentioned previously varies in amplitude according to the colour of the tomato, and was therefore not used as a trigger since many green tomatoes would not produce a signal great enough to be detected above background. SUMMING AMPLIFIER 1 and 2 overcome the problem of signal amplitude variation with colour, but the summing amplifier outputs are functions of light intensity, i.e. tomato size. Very small tomatoes may not be as readily detected as large ones.

Schmitt Trigger Circuit (Box L, Figure 3.2)

The function of the Schmitt trigger circuit, shown in Figure 3.11 is to change the bell-shaped signal at the output of SUMMING AMPLIFIER 2 into a square pulse where the leading edge is used as an "on" trigger for the analog signal processor and the trailing edge is used as an "off" trigger. When no tomato is present, PEAK DETECTOR 1 is in a reset position, with the output of the Schmitt trigger HIGH, since its inverting input is normally at zero volts or LOW.

The two threshold voltages of the Schmitt trigger were chosen as low as practical such that V_{th} = 1 volt, and V'_{th} = 0.5 volts. The output of the Schmitt trigger will go LOW when V_{IN} > 1 volt, and will return HIGH when V_{IN} < 0.5 volts. This will allow up to 0.5 volts of noise to appear at the Schmitt trigger input as a result of rapid background fluctuations, due to dirt on the conveyor or unevenness in its reflectance, before the sorting operation is affected.

The HIGH level of the Schmitt trigger is about +14 volts, which is compatible with the CMOS logic circuits. The LOW level of the Schmitt trigger is usually -14 volts, which is 13.5 volts below the lowest acceptable input voltage to the CMOS devices. The output of the Schmitt trigger is clamped with a IN914 diode to ground, resulting in an output swing from -0.7 volts to +14 volts. This clamping technique was found more favourable than placing a diode in the feed-back loope of the Op Amp, which is another clamping procedure.

FIGURE 3.11   SCHMITT TRIGGER CIRCUIT
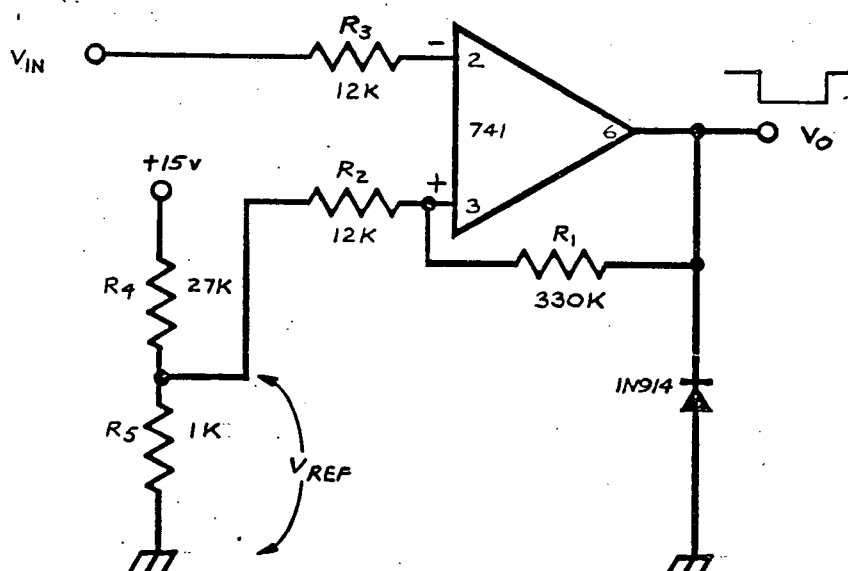
Referring to Figure 3.11, the threshold voltages are defined as follows:

$$V_{th} = \frac{R_2 \, (V_o - V_{ref})}{R_1 + R_2} + V_{ref} \qquad [3\text{-}16]$$

$$V'_{th} = \frac{R_2 \, (V'_o - V_{ref})}{R_1 + R_2} + V_{ref} \qquad [3\text{-}17]$$

where V_{th} = first threshold voltage

V'_{th} = second threshold voltage

V_o = output voltage when solving for V_{th}

V'_o = output voltage when solving for V'_{th}

R_1, R_2 = resistance values in the circuit.

Since V_{th} = 1 volt, and V'_{th} = 0.5 volts, V_{ref}, R_1 and R_2 must be determined. In general, equation [3-16] yields:

$$V_{ref} = \frac{V_{th} \, (R_1 + R_2) - R_2 \, V_o}{R_1} \qquad [3\text{-}18]$$

substituting V_{th} = 1 and V_o = +14 in [3-18] and solving for R_1, gives:

$$R_1 = \frac{13 \, R_2}{1 - V_{ref}} \qquad [3\text{-}19]$$

substituting V'_{th} = 0.5 and V'_o = -0.7 in [3-17] and solving for R_2 gives:

$$R_2 = \frac{R_1 \, (2 \, V_{ref} - 1)}{2.4} \qquad [3\text{-}20]$$

substituting [3-20] in [3-19] yields:

$$V_{ref} = 0.54 \text{ volts} \qquad [3\text{-}21]$$

substituting [3-21] in [3-20] yields:

$$R_2 = 0.035 \, R_1 \qquad\qquad [3-22]$$

Now, let R_1 = 330 KΩ

then R_2 = 12 KΩ

$R_3 = R_1 /\!/ R_2$* = 12 KΩ for minimum offset error

input bias current.

V_{ref} is obtained by the use of the voltage

divider, R_4 and R_5.

If R_4 is connected to the +15 volt supply and R_5 to ground,

then for V_{ref} = 0.54 volts,

$$R_4 = 26.8 \, R_5. \qquad\qquad [3-23]$$

Choosing suitable values of R_4 and R_5 gives:

R_4 = 27 KΩ

R_5 = 1 KΩ.

It is evident that signal drift at the input to
the Schmitt trigger must be corrected by a circuit such as
the belt background monitor since a constant input above
0.5 volts due to drift would not allow the Schmitt trigger
to turn off.

The output of the Schmitt trigger circuit is a
digital waveform compatible with the CMOS logic devices, and
this signal will be transferred to the digital processor.
Although V_o drops to -0.7 volts and CMOS devices are rated
to -0.5 volts, the "overdrive" may be reduced by adding a

---

* Net parallel resistance

current limiting resistor between the Schmitt trigger and the CMOS device input. Any resistor between 1.5 KΩ and 10 KΩ is suitable.

DIGITAL SIGNAL PROCESSOR

Timing Circuit (Box M, Figure 3.2)

The function of the timing circuit, Figure 3.12,

which is activated by the Schmitt trigger pulse, is to unlock

PEAK DETECTOR 1 from its reset state and to transfer colour

category information to the digital processor. When a tomato

enters the viewing area of the sensing head, the leading edge

of the Schmitt trigger pulse unlocks PEAK DETECTOR 1, and

colour categorization begins. When the tomato leaves the

viewing area of the sensing head, the trailing edge of the

Schmitt trigger pulse triggers the timing circuit to produce

a 210 µs WRITE pulse, which allows the information at the

comparator outputs to be decoded and stored in the memory.

The trailing edge of the WRITE pulse resets PEAK DETECTOR 1.

The timing circuit is comprised of four NOR gates

(1-CD4001)* two of which operate as a monostable multivibrator.

The 1.5 KΩ resistor at the input to the first NOR gate is a

current protection resistor, limiting the input gate current

to 10 ma, maximum. The protection was added to prevent damage

to the gate in the event that the Schmitt trigger voltage

dropped to -15 volts, due to diode failure in the Schmitt

trigger circuit.

The 10 KΩ delay resistor (Figure 3.12) at input

---

* CD prefix refers to CMOS devices manufactured by RCA Corp.,
Somerville, New Jersey.
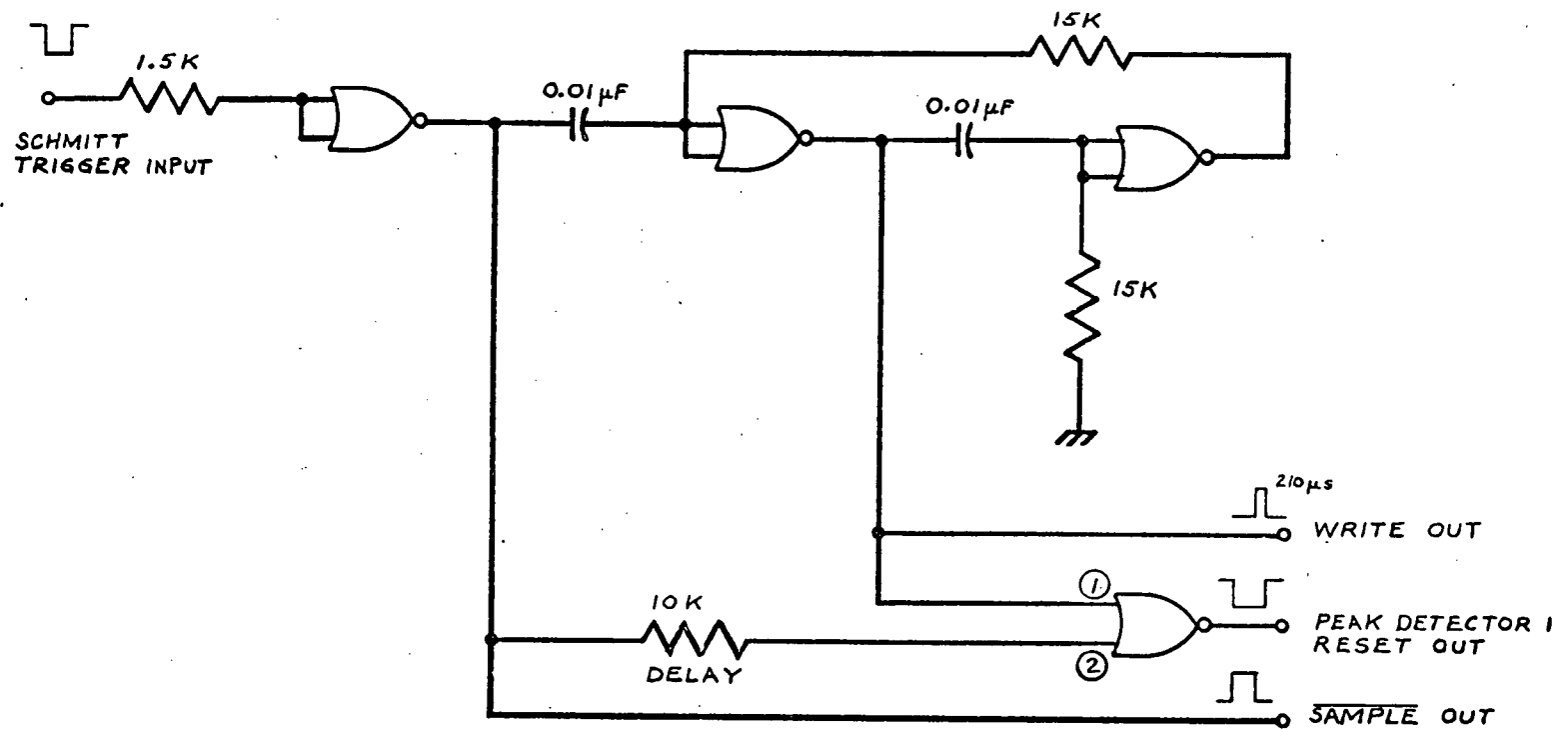
FIGURE 3.12 TIMING CIRCUIT

#2* of the final NOR gate is used to compensate for the signal delay which occurs at input #1 due to the extra gate in that input line. Without delay compensation, two pulses will appear at the RESET output, one of which is in error.

The RESET output pulse width is equal to the sum of the Schmitt trigger pulse and the WRITE signal pulse widths. The RESET output is connected to the control input of the CD4066 bilateral switch, Figure 3.6.

The $\overline{\text{SAMPLE}}$ output is the complement of the Schmitt trigger pulse and will be discussed later in Section II.

---

* # refers to circled points in figure.

Decoding Gates (Box N, Figure 3.2)

The outputs of the three comparators (COMP. 1,
COMP. 2 and COMP. 3) change continuously as the output of
PEAK DETECTOR 1 rises to its maximum value for a particular
tomato. Once the peak voltage has been reached and is stored,
the three comparator outputs remain relatively constant, and
the colour category information is ready to be transferred
to the shift register memories, which are synchronized to
the movement of the belt.

Since it was decided that the green tomatoes were
to travel to the end of the conveyor belt, only three shift
register memories were required -- one for firm ripe, one for
semi-ripe and one for turning tomatoes. The memory input
information is decoded from the output states of COMP. 2 and
COMP. 3, via the three NOR gates, NOR 1, NOR 2, and NOR 3,
Figure 3.13. Turning tomatoes are categorized when the input
voltage of the comparators is less than $V_{SET\ 2}$ for COMP. 2,
Figure 3.8. Note that green tomatoes also produce voltages
less than $V_{SET\ 2}$. Separation of these two colour categories
is controlled by the output of COMP. 1, which is LOW for all
except green tomatoes, permitting information to be written
into the memories through NOR 4, Figure 3.13. For example,
if a green tomato is being sensed, the output of COMP. 1 is
HIGH, resulting in a LOW output at NOR 4 even when the WRITE
signal appears at the other input to NOR 4. No information
is transferred to the memory through NAND gates, NAND 1,

FIGURE 3.13 DECODING GATES
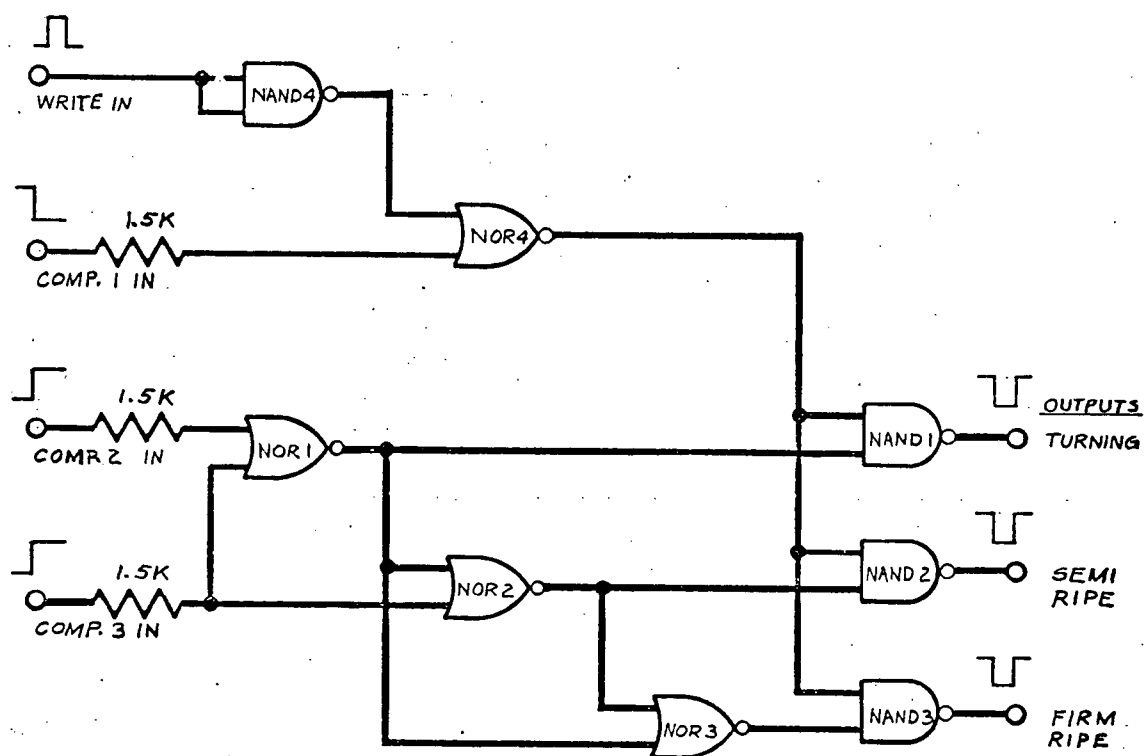
NAND 2, and NAND 3, and the green tomato travels to the end of the conveyor as though it was never sensed. For all other tomato categories, the output of COMP. 1 is LOW, thus allowing the WRITE pulse to appear at the output of NOR 4, and the information from the NOR 1, NOR 2, and NOR 3 outputs to be transferred to the outputs of NAND 1, NAND 2, and NAND 3, for the duration of the WRITE pulse. In theory, all three NAND gates will normally be HIGH, and only one will go LOW for the WRITE pulse duration. In practice it is possible for more than one output to be low for a fraction of the WRITE pulse width due to minute drift in PEAK DETECTOR 1 which will result in double categorization of one tomato. A circuit, the data latches, will be described later which accepts only the first category signal received.

The 1.5 KΩ resistors at the inputs to the NOR gates are current protection resistors.

Light Chopper and Photodetector (Box P, Figure 3.2)

The light chopper disk is a thin, metal, circular disk with small holes, regularly spaced, near the circumference. For the size of conveyor belt pulley used, the hole spacing and disk diameter was chosen so that the center-to-center distance between the small holes was equal to approximately 1/2 inch (1.3 cm) of conveyor belt.

The disk was mounted on the axle of one of the conveyor pulleys, and a light source placed on one side of the disk and a photodetector on the other side, so that the light and detector were aligned with the hole centers of the disk. As the disk rotates, the light beam is transmitted through the disk to the photodetector as the holes pass, and the light is blocked by the area between the holes. The photodetector output, as the belt moves, is a digital signal with one cycle for each 1/2 inch (1.3 cm) of belt movement. The frequency of this digital signal will be determined by the conveyor belt speed, but each clock cycle will remain constant with respect to the length of conveyor belt moving past a fixed point.

The photodetector chosen was a CA3062 light sensitive operational amplifier, and the schematic of the circuit used in shown in Figure 3.14. Other photodetectors, such as a photo diode or phototransistor could have been used, but the CA3062 can be wired easily as a Schmitt trigger, which, due to its hysteresis characteristic makes the photodetector

FIGURE 3.14   LIGHT CHOPPER PHOTODETECTOR
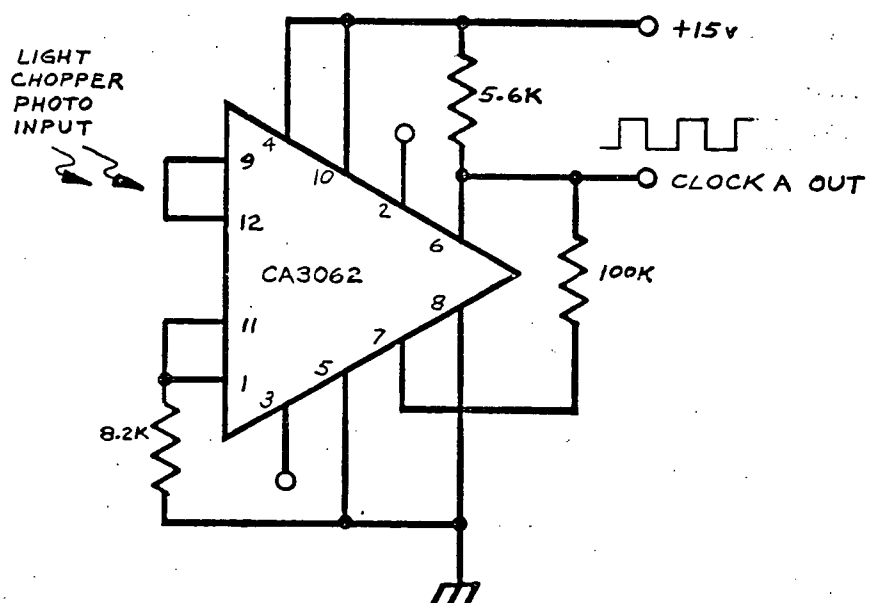
circuit very stable. The digital output signal of the
CA3062 will be referred to as CLOCK A.

Divide-by-3 Circuit (Box Q, Figure 3.2)

The function of the divide-by-3 circuit is to divide the CLOCK A frequency by 3, so that each cycle at the output now represents 1 1/2 in (3.8 cm) of conveyor belt.

It was initially planned that the CLOCK A signal be used to shift the memory information one shift location (bit) every clock cycle. This would require a bit to be available in a memory (e.g. a firm ripe memory) for every 1/2 in (1.3 cm) downstream that the eject station is located. The last eject station was located 24 in (61 cm) downstream from the sensing head, thus requiring a 48 bit shift capability. At the time of the circuit design, common shift registers had 4 or 8 bit storage capability, and for the three memories needed, about 14 integrated circuits would have been required.

It was believed that fewer bits could be used if memory information was spaced 1 1/2 in (3.8 cm) apart rather than 1/2 in (1.3 cm).

This means that any two tomatoes must be a minimum of 1 1/2 in (3.8 cm) apart on the belt from center to center, i.e. greater than 3/4 in (1.9 cm) in diameter. This factor is not limiting, since small tomatoes are generally double that size. The number of shift register bits can thus be reduced by a third.

The divide-by-3 circuit schematic is shown in Figure 3.15. The circuit is comprised of CD4011 NAND gates and a CD4018 pre-settable divide-by-"N" counter. Two NAND

FIGURE 3.15   DIVIDE-BY-3 CIRCUIT   100

CLOCK A
OUTPUT

CLOCK A
INPUT

CD4018
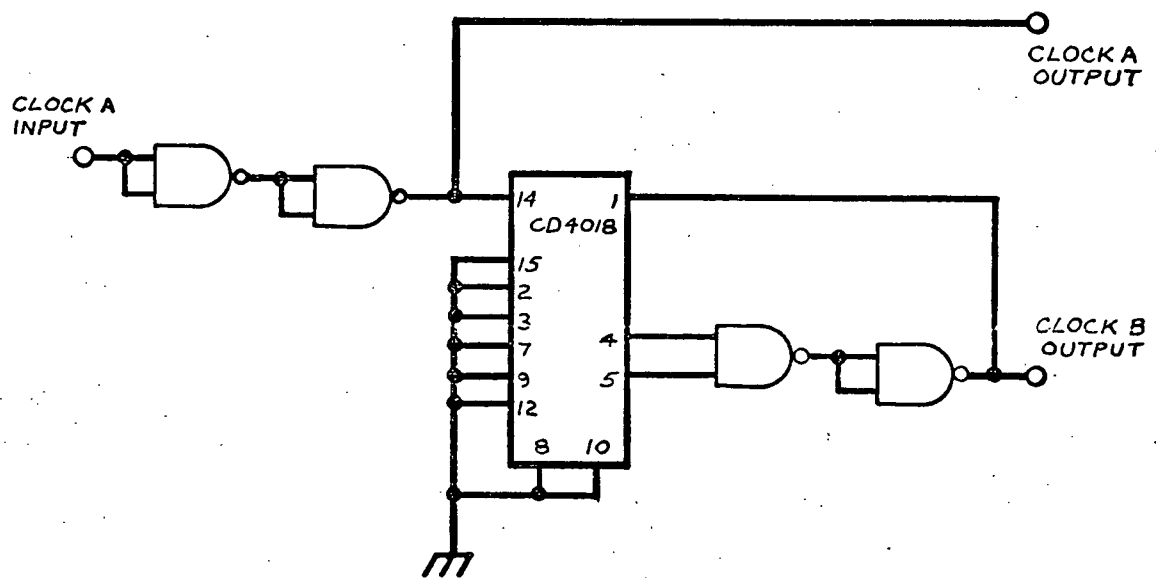
CLOCK B
OUTPUT

gates are employed as pulse shapers at the input to the counter, since the CLOCK A rise and fall time is around 10 µs, which is close to the maximum allowable rise and fall time of the CD4018 clock input. The two NAND gates "speed up" the clock pulse transistion from HIGH to LOW, and LOW to HIGH.

Two of the outputs of the CD4018 are connected to the inputs of a CD4011 NAND gate, the output of which is inverted and fed back to the "data" input of the CD4018. This is a standard circuit configuration for a divide-by-3 function using the CD4018.

The CLOCK A frequency divided-by-3 will be referred to as CLOCK B. The CLOCK A output will be used later in Section II.

Data Latches, Timers and Memory Circuits (Box R, Figure 3.2)

Data cannot be entered into the shift register memories at anytime, nor can the data be retrieved at anytime. Certain conditions must be met before data can successfully and consistently be stored.

(a) The data (a HIGH or LOW state) must be present at the input to the shift register at least 700 ns (nanoseconds) before the clock input goes high.

(b) The storage of the data occurs as the clock signal changes state from either a HIGH to LOW, or LOW to HIGH depending on the shift register used, so the input data must not change state during clock transition.

(c) Once the clock input has reached either a HIGH or LOW level, no more data can be entered into the shift register until the next cycle of the clock starts.

The function of the data latches, Figure 3.16, (one latch for each shift register memory) is to act as a temporary storage location for the colour category data until the data can be transferred into the shift register. Maximum storage time in the latch will be one cycle of CLOCK B. As soon as a pulse occurs at the output of one of the decoding gates (Figure 3.13), its corresponding latch changes from a normally HIGH to a LOW output.

FIGURE 3.16   LATCHING CIRCUIT
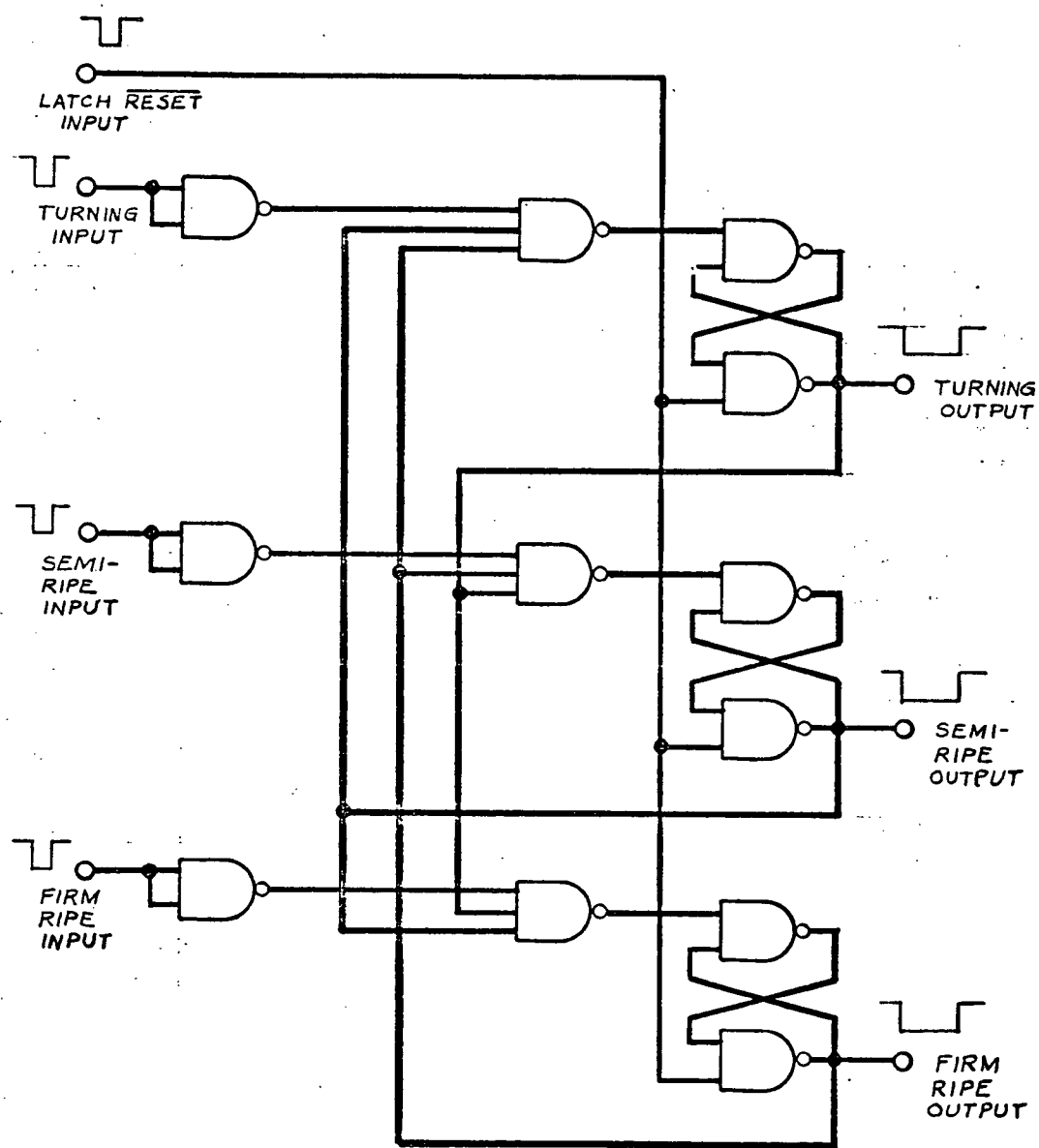
The change in state of one latch instantly blocks, or gates out signals arriving at the other two latches, because of the CD4023 3-input NAND gates. Only after the set latch is reset to its normally HIGH output state can any more information be accepted and transferred. All three latches are simultaneously reset.

The two timers (Figure 3.17) associated with the data latches are used to produce a "set up" time and a reset pulse. The set-up time was chosen as a modest 14 μs, and the reset pulse width as 6μs.

At every negative going (from HIGH to LOW) CLOCK B pulse that occurs at the input of the set-up timer, a 14 μs positive pulse is produced. As the trailing edge of the 14 μs pulse changes from HIGH to LOW, the RESET timer is triggered to produce a 6 μs positive RESET pulse. Since the SET UP timer is triggered on the negative going edge of CLOCK B, and the transfer of data into the shift register (CD4015) occurs on the positive edge of the clock pulse, it was necessary to invert CLOCK B ($\overline{\text{CLOCK B}}$) for the shift registers using two CD4011 gates. Similarly, resetting of the data latches requires a negative going pulse, so the RESET pulse was also inverted ($\overline{\text{RESET}}$) using two CD4011 gates. The two gates used for each inversion were wired in parallel in order to increase their current drive capabilities.

Both the data input (DATA IN) and latch output (LATCH OUT) are normally HIGH, as shown in Figure 3.18. The

FIGURE 3.17   DATA LATCH TIMERS
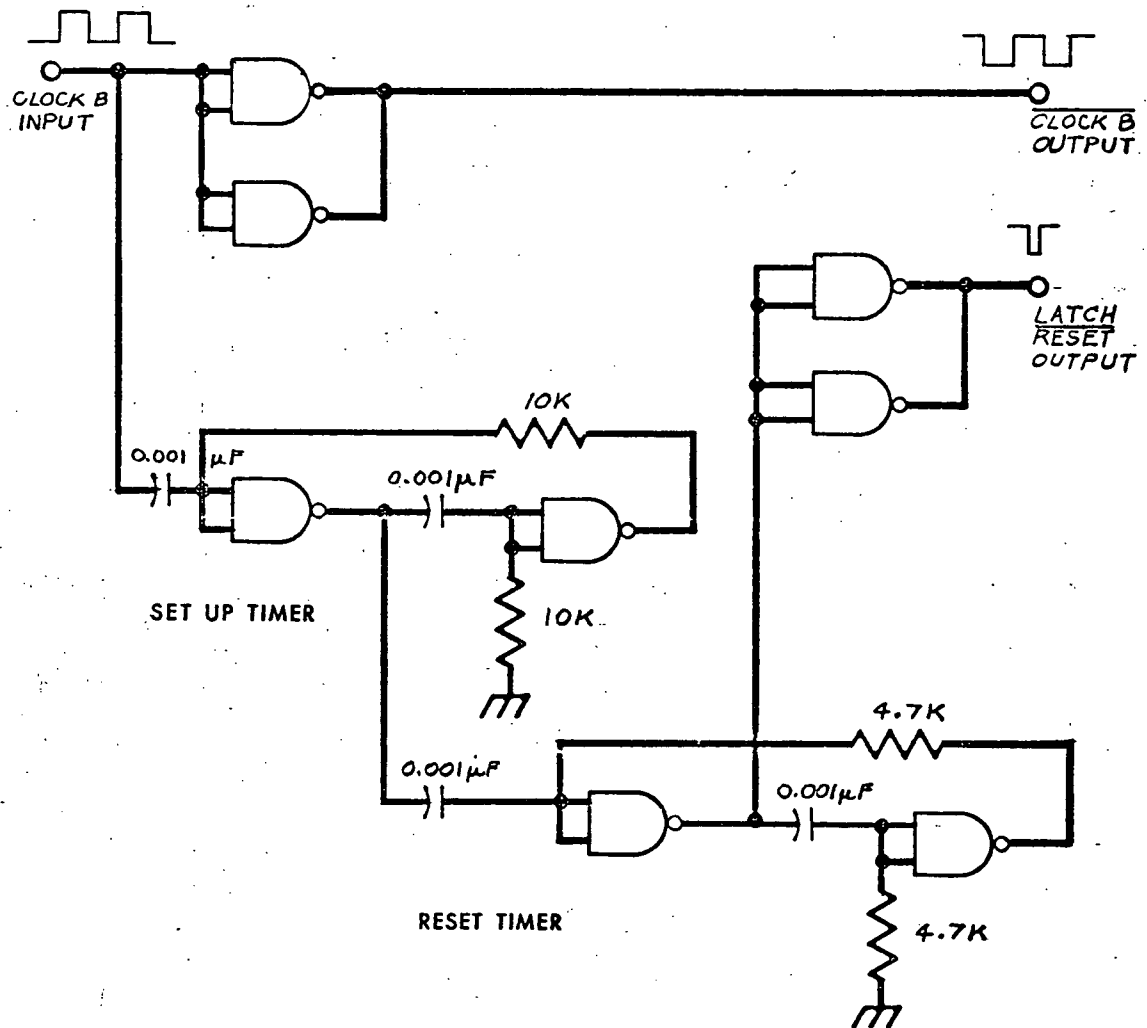
FIGURE 3.18   DATA LATCH WAVEFORMS
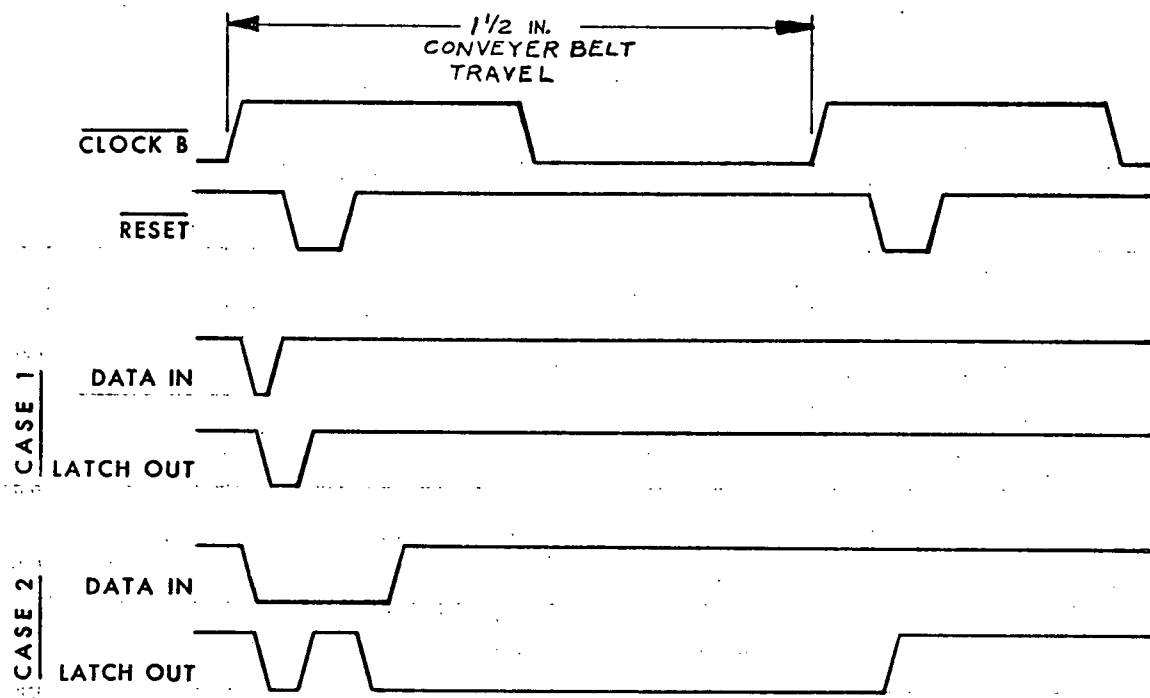
shift register memory, therefore, sees a constant HIGH input, and stores a "1" every time $\overline{\text{CLOCK B}}$ changes from a LOW to a HIGH state. When the data input goes LOW (indicating that a tomato has been categorized) a "0" must be transferred into the shift register as soon as the next $\overline{\text{CLOCK B}}$ LOW to HIGH transition occurs. The most difficult situation, i.e. worst case which must be considered, occurs during the SET UP time:

Case 1: WRITE pulse width less than the sum of SET UP and RESET times.

Suppose that $\overline{\text{CLOCK B}}$ has already changed from a LOW to a HIGH state, and the data latch output is still HIGH, as shown in Figure 3.18. The data latch input is set LOW before the latch $\overline{\text{RESET}}$ pulse arrives. The duration of the latch input LOW pulse is always equal to the length of the WRITE pulse. If the WRITE pulse is very short, the latch output will be set LOW until the $\overline{\text{RESET}}$ pulse occurs, at which time the latch output returns HIGH. At the next positive $\overline{\text{CLOCK B}}$ transition, the latch output is HIGH, as normal, and the data has been lost.

Case 2: WRITE pulse width greater than the sum of SET UP and RESET times.

The difference between Case 2 and Case 1 is that in Case 2 the WRITE pulse width (the data latch input) is greater than the sum of the SET UP and RESET times (Figure 3.18). Now, when the RESET pulse appears, the data latch output changes from LOW to HIGH for the duration of the $\overline{\text{RESET}}$ pulse, and

returns to a LOW state since the data latch input is still
LOW. The latch output will remain LOW until the next $\overline{RESET}$
pulse. The LOW signal will be transferred into the shift
register on the next positive transition of $\overline{CLOCK\ B}$, after
which the $\overline{RESET}$ pulse resets the latch.

The three memory circuits used for turning, semi-
ripe and firm ripe classifications are shown in Figure 3.19.
The firm ripe memory is comprised of one CD4015 dual 4 bit
shift register, with the two 4 bit shift registers wired in
series to follow an 8 bit shift. The semi-ripe memory is com-
prised of one and a half CD4015's (12 bits) and the turning
memory of two CD4015's (16 bits). A shift of one bit "down
the memory" is equivalent to one clock cycle, or 1 1/2 in (3.8 cm)
of conveyor belt movement. The firm ripe memory is therefore
capable of shifting information 12 in (30 cm) downstream from
the sensing head, where the information was first stored in
the memory. Similarly, the semi-ripe memory stores informa-
tion for 18 in (46 cm) downstream from the sensing head, and
the turning memory for 24 in (61 cm). Eject stations will have
to be located 12 in (30 cm), 18 in (46 cm) and 24 in (61 cm)
downstream from the sensing head, otherwise the shift
registers will have to be lengthened or shortened.

When the information entered in a memory has been
shifted the maximum number of shifts, the output of the shift
register changes state (in this case from HIGH to LOW) for
the duration of the one clock cycle, i.e. the output goes
LOW for 1 1/2 in (3.8 cm) of the conveyor belt movement.

FIGURE 3.19   MEMORY CIRCUIT

109
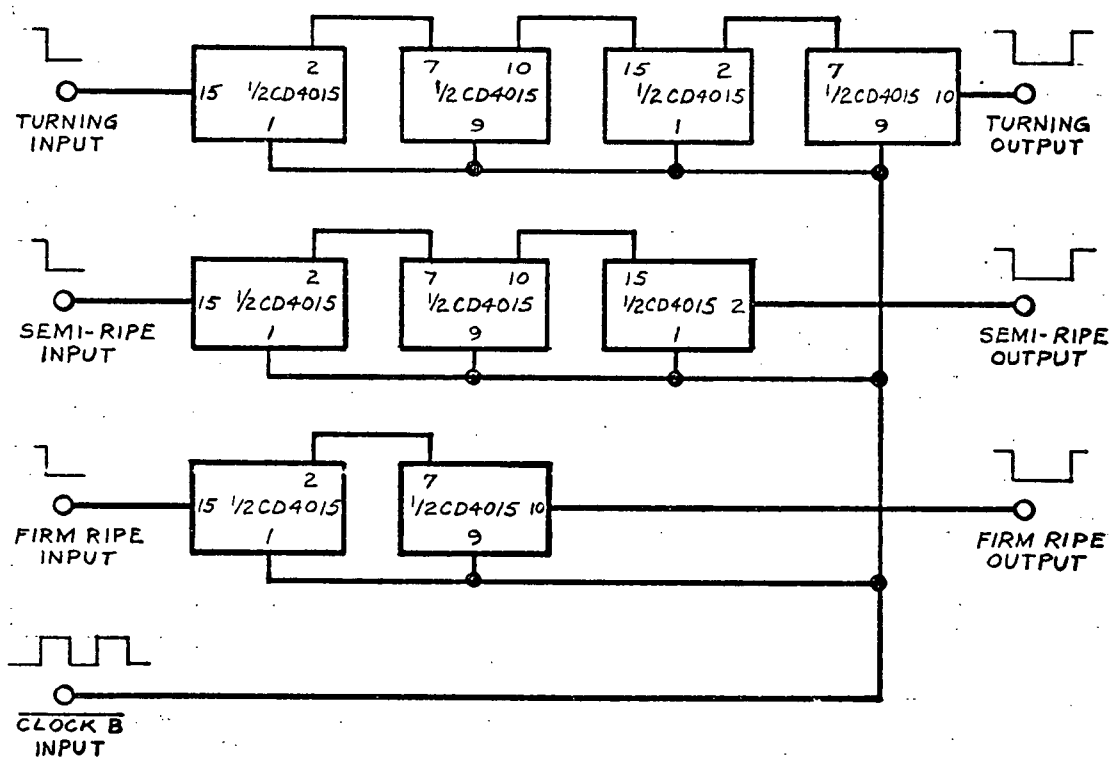
Opto-Isolators and Triacs (Box S, Figure 3.2)

If the LOW output signal from a memory is coupled to an electromechanical device, such as a pneumatic or hydraulic solenoid valve, the device will be activated for 1 1/2 in (3.8 cm) of belt movement. There is no advantage to coupling a shift register output to a timer which operates the electromechanical device, unless the device must be operated for less than 1 1/2 in (3.8 cm) of belt movement. A timer having a duration greater than the time required for 1 1/2 in (3.8 cm) of belt will interfere with normal operations. Two tomatoes of different colour can be spaced by as little as 1 1/2 in (3.8 cm), and if the first is ejected by a device operating over 2 in (5.1 cm) of belt, for example, the second tomato will probably also be ejected. For these reasons, no timers were used to operate the electromechanical eject devices.

Relays have been used in the past to act as an interface between low power devices such as transistors, and high power devices such as solenoids. However, relays have moving parts and have been replaced in many cases by semi-conductor devices like opto-isolators and triacs. The latter were used in the colour grader to act as the couplers between the CMOS memories and the solenoids. The optic couplers can be connected to CMOS devices through the use of a transistor, and the optic coupler can also drive a 110 volt AC triac. Common solenoids are operated by 110 volt AC sources.

The optic couplers provide complete isolation of

the CMOS devices from the 110 vAC line voltage present at the triacs. This is most desirable since noise common on the 110 vAC line must not feed back into the logic circuitry and disrupt normal operation.

A schematic of the opto-isolator and triac circuit is shown in Figure 3.20. A 2N3638 PNP transistor is used to drive the light emitting diode (LED) of the MOC1003 opto-isolator. When the LOW signal in a memory reaches the end of the shift register, the LED's are activated and the photo-transistors of the MOC1003's conduct current for the duration of the LOW signal. The phototransistors are coupled to the gates of the triacs. The triacs will conduct the 110 vAC line current as long as the gate is conducting. The 110 vAC load (the electromechanical eject mechanism) is in series with the triacs, and thus the load is active for the duration of the memory output LOW signal, equivalent to 1 1/2 in (3.8 cm) of conveyor belt travel.

Note that the phototransistors which drive the gates of the triacs operate on a separate power supply -- not the ± 15 volt IC supply. This ensures maximum noise isolation between the 110 vAC circuit and the low power IC circuitry. The only coupling that exists is between the LED and photo-transistor of the MOC1003, and the isolation resistance between the two is typically 10^{11} ohms.

The maximum current handling capability of the L2001L5 triacs is 1 ampere, and loads will have to be

FIGURE 3.20   OPTO-ISOLATORS AND TRIACS
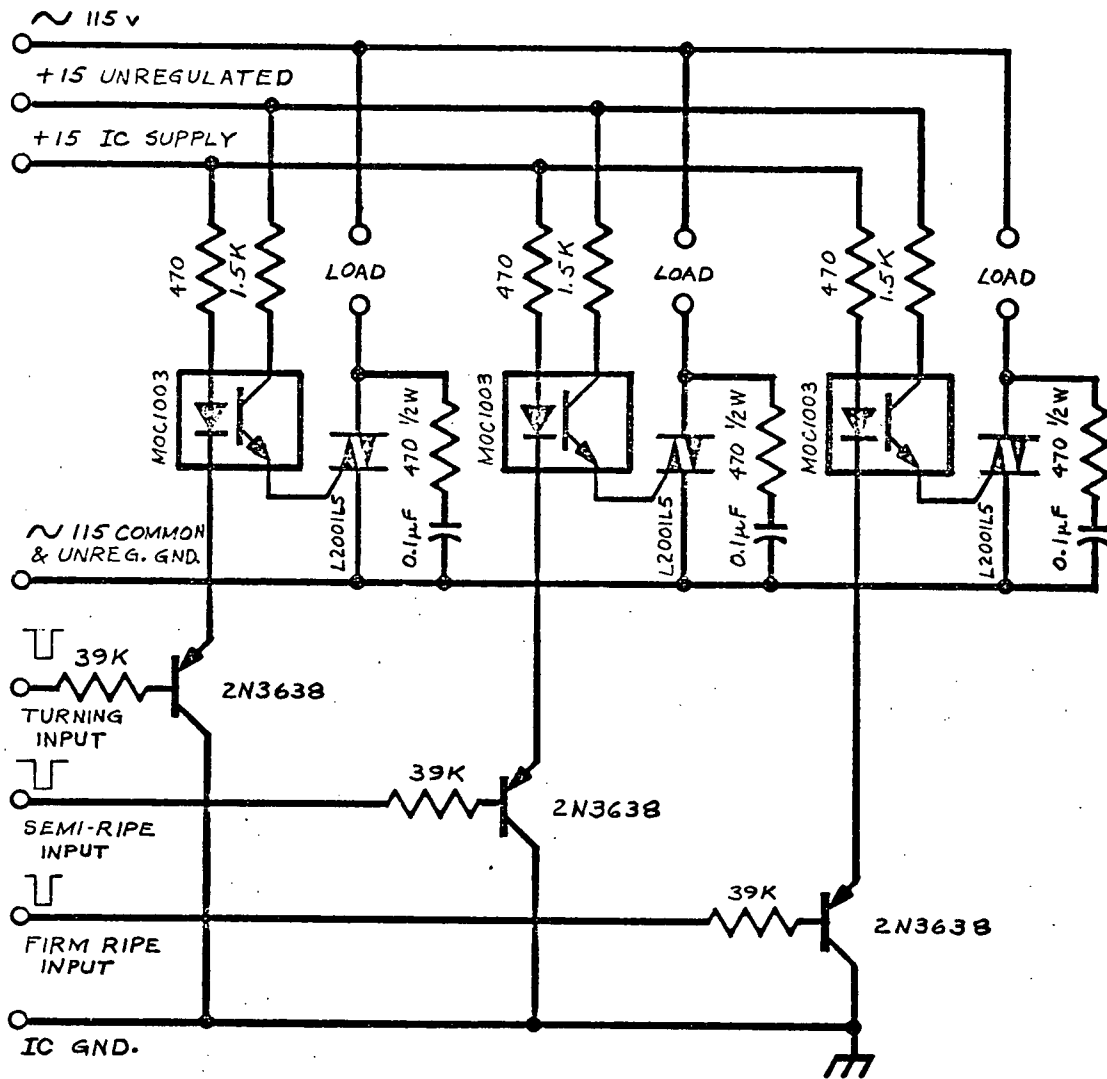
maintained below that level. The 470Ω resistor and 0.1µF capacitor across the triac dissipates stored energy in an inductive load when the triac is suddenly turned off.

Display Timers (Box T, Figure 3.2)

The display timer circuit does not contribute directly to the sorting function of the grader. Its function is to light one of three LED's on the front panel of the grader cabinet, thus identifying the colour category into which a tomato has been placed by the machine. A red LED was used to identify firm ripe tomatoes, an orange LED for semi-ripe and a green for turning tomatoes. The green tomatoes required no display, by elimination. The displays were used primarily in setting up the comparator (Box F, Figure 3.2) voltage settings (V_{SET}). For example, a tomato would be visually selected as a semi-ripe such that anything redder would be classified as firm ripe. The tomato was passed under the sensing head and the comparator voltage adjusted on the front panel until the orange LED stopped flashing after the tomato passed and the red LED started to flash instead. The comparator voltage was then returned to a point where the orange LED would flash. This method enabled rapid set up of the machine without waiting for the eject mechanism to be activated. The same method was used in setting the other colour category comparator voltages.

A schematic of the display timer circuit is shown in Figure 3.21. The circuit is basically the same as the data latch circuit described previously, and shown in Figure 3.16. The inputs to NAND gates, NAND 1, NAND 2 and NAND 3 are connected directly to the outputs of the decoding gates

115

FIGURE 3.21 DISPLAY TIMER CIRCUIT
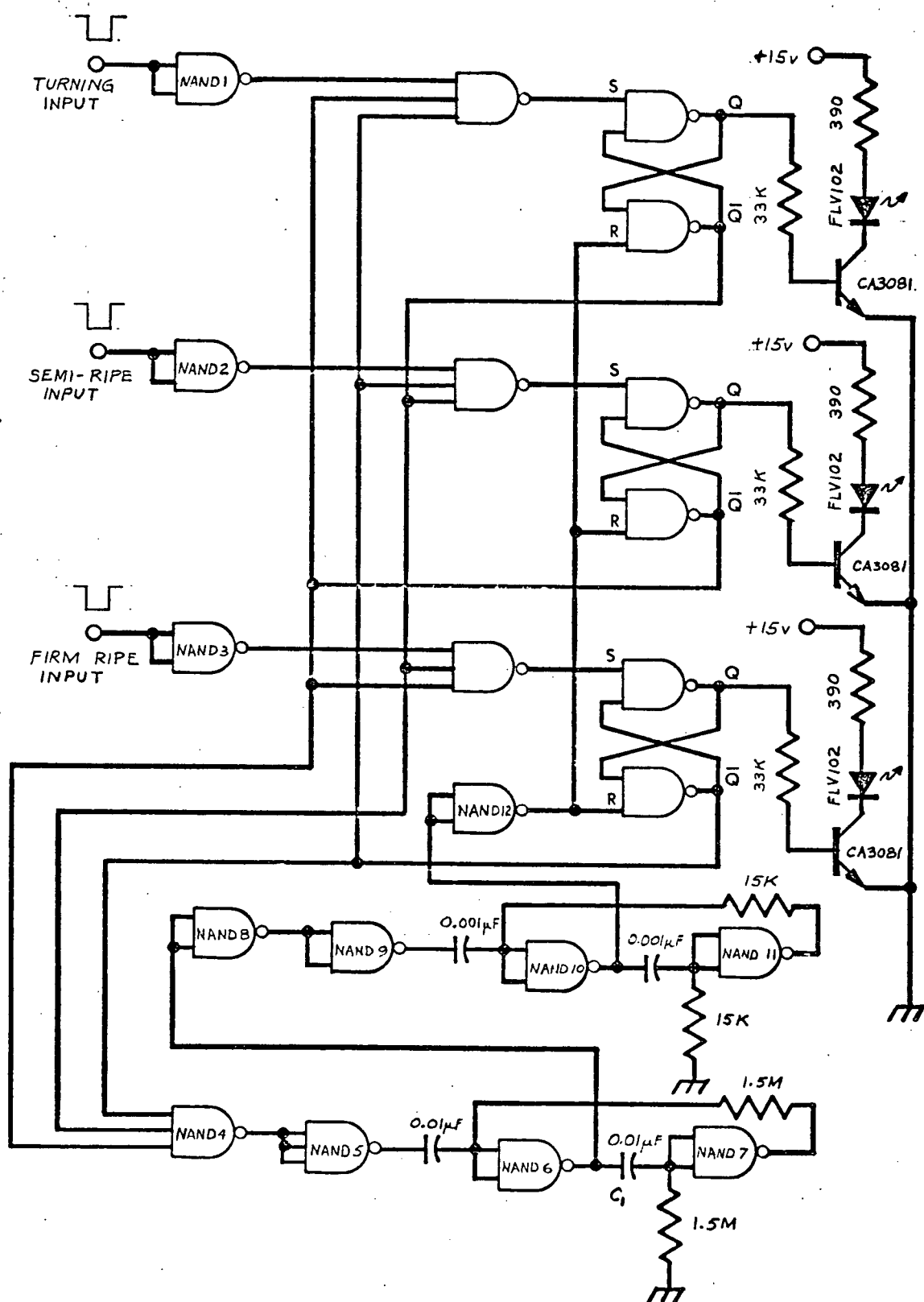
(Figure 3.13). The latch outputs are connected to transistor
buffers to drive the LED's. The CA3081 NPN transistor array
provides up to 7 such transistors. The 33 KΩ and 390 Ω
resistors are current limiting resistors.

The output Q (Figure 3.21) of a latch is normally
LOW, and $\bar{Q}$ is normally high. When one of the inputs goes LOW,
a LOW appears at the S(set) input to the latch and Q becomes
latched in a HIGH state, and $\bar{Q}$ in a LOW state. As long as Q
is HIGH, the LED at the latch output will light. The $\bar{Q}$ out-
put of a latch is fed back to the inputs of the other two
latches via the CD4023 three input NAND gates. As soon as one
$\bar{Q}$ output goes LOW, the other two latches are gated out.

The three $\bar{Q}$ outputs are connected to the inputs of
one 3 input NAND gate, NAND 4. When one of the $\bar{Q}$ outputs goes
LOW, the normally LOW output of NAND 4 goes HIGH. This HIGH
is inverted through the three input NAND gate, NAND 5, which
has all three inputs tied together. As the output of NAND 5
goes LOW, the monostable multivibrator comprised of NAND 6
and NAND 7 produces a HIGH state at the output of NAND 6 for
about 20 ms. As the output of NAND 6 returns LOW, the mono-
stable multivibrator consisting of NAND 10 and NAND 11 is
triggered to produce a HIGH RESET pulse of about 20 μs. The
pulse is inverted through NAND 12, which resets all of the
latch outputs. The two NAND gate inverters, NAND 8 and NAND 9
are used as pulse shapers, to speed up the transition from
HIGH to LOW of the output pulse at NAND 6, which is quite slow

due to capacitor C_1.

One of the three LED's will light for approximately 20 ms depending on which one of the three inputs first goes LOW.

POWER SUPPLIES

The design of a ± 15 volt regulated power supply based on the theoretical current consumption of the circuits described so far would require many long and unnecessary calculations. Instead, the system was tested using a test circuit board and experimental power supply and the current consumption was measured. Maximum current for the integrated circuits was around 100 ma. A ± 15 volt regulated power supply kit (RAE 1510 KIT) was available which was capable of delivering ± 500 ma. The power supply was more than adequate to drive the IC's. Voltage regulation was desirable in order to maintain stable operation of the linear integrated circuits.

A separate + 15 volt unregulated power supply, shown in Figure 3.22, was designed to drive the phototransistors in the opto-isolators (Figure 3.20). Maximum current per opto-isolator transistor is governed by the 1.5 KΩ resistor at the collector, and is 10 ma. A transformer, and rectifier diodes capable of handling 1 ampere were chosen thus allowing further expansion of the system. No voltage regulation was required for this power supply. The supply GROUND is connected to the 115 vAC COMMON lead. The separate power supply for the opto-isolators and triacs assures maximum isolation between the sensitive integrated circuits and the electrically noisy 115 volt AC lines.

119

FIGURE 3.22 POWER SUPPLY CIRCUIT FOR TRIACS
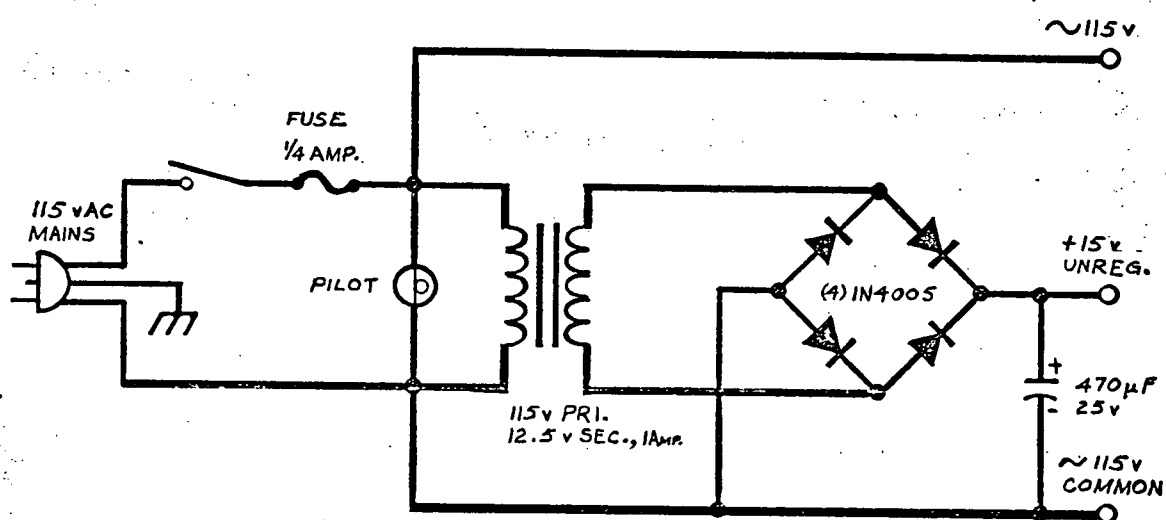
MECHANICAL HANDLING SYSTEM

As mentioned in the introduction, it was not the objective of the present research to design a new type of tomato handling system, but rather to use a typical flat conveyor belt to transfer the tomatoes to the sensing head and eject stations. The problem of singulating and centering of fruit on conveyor belts has been studied and developed to a reasonable degree by large manufacturing companies such as FMC Corporation in the United States. The perfection of an ejection system for the tomatoes from the conveyor belt after classification was not of prime concern either. Of importance was the design of a reasonable conveyor and eject system which could be used to test the electronic design, features of which could be employed in a large scale prototype.

The Conveyor System

The conveyor system consisted of a flat, matte-black 6 inch (15 cm) wide belt having a working length of about 6 feet (2.44 cm). The belt was stretched between two rollers, one of which was chain driven by a Zero Max E2M2 motor and variable speed gearbox (Zero-Max Industries, Inc.). Conveyor belt speed could be adjusted continuously from zero to more than 60 inches/sec (152 cm/sec).

The belt system and motor was mounted on a metal frame with a plywood top. The sensing head was mounted about 1/3 of the way from the feed end of the conveyor, across the belt, as shown in Figure 3.23a. The light copper disk and photodetector assembly mounted on the idler pulley at the feed end is shown in Figure 3.23b.

After passing underneath the sensing head, the belt was tilted slightly, to assist in the removal of tomatoes from the belt at the eject stations.

FIGURE 3.23 (a) SENSING HEAD, AND
(b) LIGHT CHOPPER ASSEMBLY

(a)
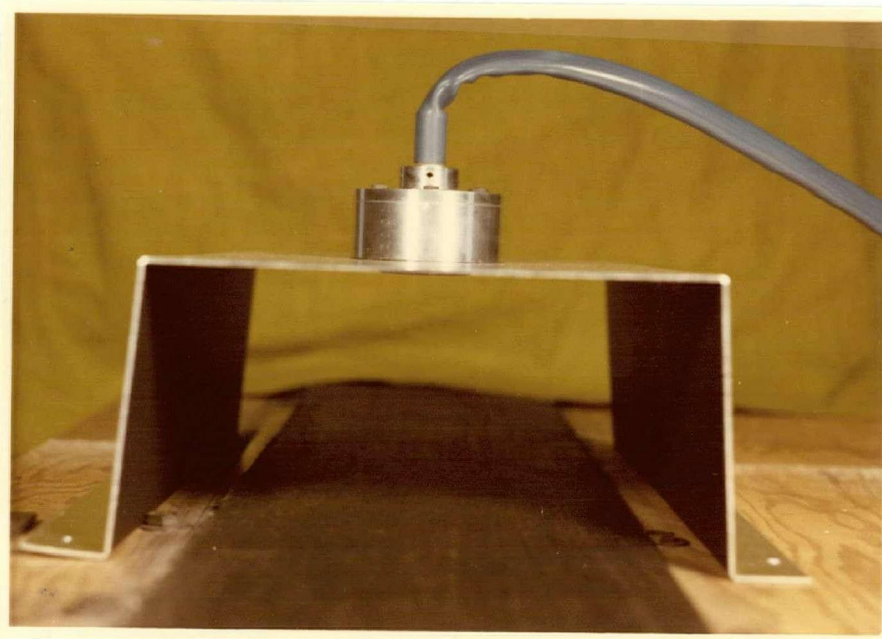
(b)
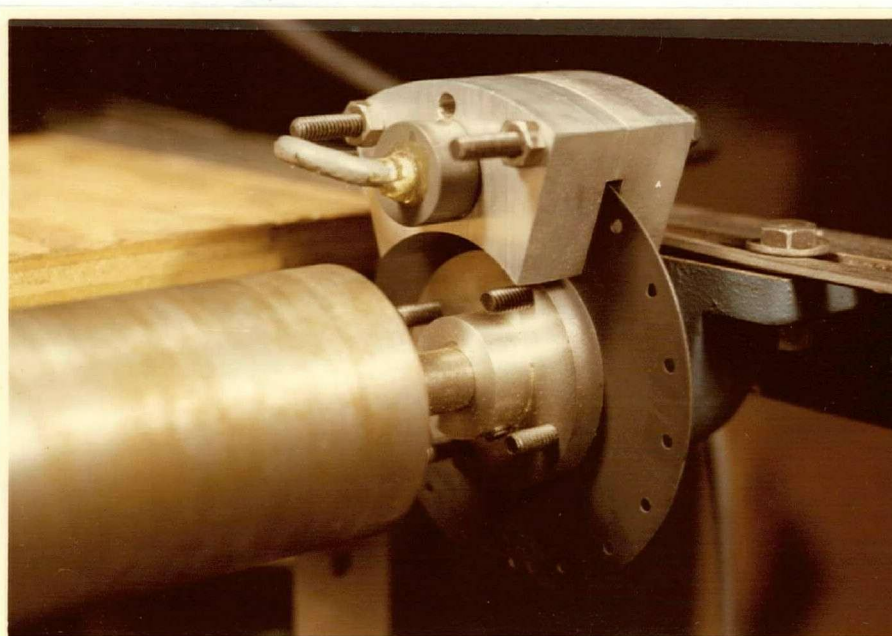
Eject System

Of the many possible ways of ejecting tomatoes the
method chosen to test the electronic system was pneumatic
ejection.

The desired operating speed of the system was in the
neighbourhood of 5 tomatoes per second. Any mechanical eject
system operating at that speed would subject the tomato to
large undesirable impact stresses.

The compressed air for the pneumatic eject system was
obtained from a 1 1/2 H.P. Jaccuzzi Compressor (Jaccuzzi Canada
Ltd.) having a 1 ft^3 (0.028 m^3) surge tank.

This main surge tank supplied a secondary surge tank
on which the eject solenoids were mounted. The secondary surge
tank, having a volume of 0.018 ft^3 (510 cm^3) was constructed of
1 1/2 in (3.8 cm) galvanized pipe. Since the solenoids are
operated for only 1 1/2 in (3.8 cm) of conveyor belt, then at
a 2 ft/sec (61 cm/sec) belt speed a solenoid would be active
for 62.5 ms. Using Devilbiss DGD101 (Devilbiss (Canada) Ltd.)
air booster nozzles a 15 psig (10^5 newtons/m^2 g) drop was
measured across the ASCO (Ascoelectric Limited) 8262C90 solenoid
valve at 100 psig (6.9 X 10^5 newtons/m^2 g) inlet pressure. For
a 62.5 ms duration, this represents a 0.005 ft^3 (142 cm^3)
depletion of the primary surge tank. The secondary surge tank
volume was more than three times this volume, hence three
solenoids could be operated simultaneously for 62.5 ms at a rate
determined by the time required to recharge the secondary surge
tank. The Devilbiss DGD101 nozzles are rated at a delivery of

11 ft^3 (0.31 m^3) of air/min at 80 psig (5.5 X 10^5 newtons/m^2 g).
A rough measurement confirmed about 12 ft^3/min (0.34 m^3/min) at
85 psig (5.9 X 10^5 newtons/m^2 g).

Since four colour categories were to be sorted, three
solenoid valves were used to eject three of the tomato cate-
gories transversely to the movement of the conveyor belt, and
the fourth category was allowed to drop-off the end of the con-
veyor. The solenoid valves were spaced 6 in (15 cm) apart
(4 CLOCK B cycles or 4 memory bits) and the first was located
12 in (30 cm) from the sensing head. Galvanized 1/4 in (0.6 cm)
pipe was used to connect the solenoid valves, secondary surge
tank and nozzles together. A photograph of the eject mechanism
is shown in Figure 3.24.

A receiving bin, consisting of three compartments, was
constructed to catch the tomatoes as they were ejected from the
belt by the pneumatic system. The tomatoes were forced to drop
about 8 in (20 cm) into the bin due to the test conveyor design
and compartments were heavily padded with polyurethane to
minimize mechanical damage to the tomatoes. [In a prototype,
the tomatoes would not need to drop to the receiving unit more
than a fraction of an inch]. A cloth pouch was also constructed
to both guide the tomatoes into the bin compartment and break
their fall. (Refer to Figure 3.24).

The tomatoes which rolled off the end of the conveyor
were allowed to drop into a packing box just below the level
of the belt.

FIGURE 3.24 PNEUMATIC EJECT MECHANISM
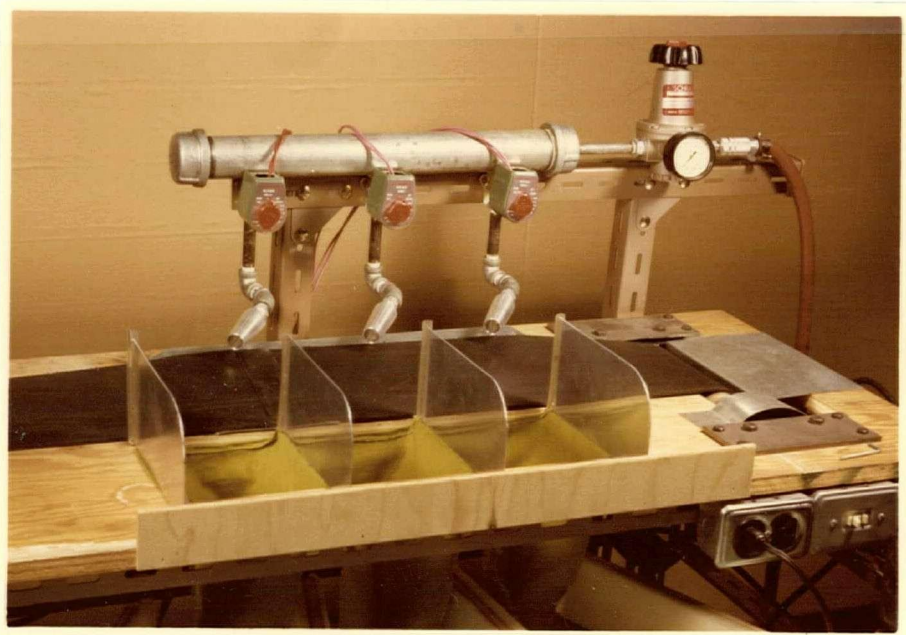
C H A P T E R   4

SYSTEM TESTING

MATERIALS AND METHODS

(I) Electronic System

The ability of the electronic colour grading system to separate tomatoes into different colour categories was tested by grading and regrading the same group of tomatoes, ranging in colour from green to firm ripe, at various comparator settings and observing the results. $V_{SET\ 1}$ (Figure 3.8) was set so that the green tomatoes would always drop off the end of the conveyor. $V_{SET\ 2}$ and $V_{SET\ 3}$ were adjusted on the front panel of the instrument. $V_{SET\ 2}$ and $V_{SET\ 3}$ determine the borders or cut-offs between turning and semi-ripe, and semi-ripe and firm ripe, respectively.

Field testing at the Western Greenhouse Co-operative Warehouse was also conducted, and the automatically graded produce was judged by federal government graders and members of the co-operative.

(II) Eject System

The pneumatic eject system was adjusted so that the tomatoes would be ejected transversely from the conveyor belt into their appropriate storage bins. The adjustment involved setting the air pressure regulator and adjusting the air nozzles to optimum angles with respect to the belt so that at a given conveyor speed the tomatoes would be ejected as desired. The maximum operating speed of the eject mechanism was also established.

RESULTS AND DISCUSSION

(I)   A voltage $V_{SET\ 1}$ = 0.77 volts, was found sufficient to

separate the green tomatoes from the turning group.

This cut-off voltage compares favourably with the

predicted mean voltage for the green tomatoes,

0.41 volt, as suggested in Table 3.2.

The effects of changing the comparator voltages,

$V_{SET\ 2}$ and $V_{SET\ 3}$ are shown in the photographs in

Figure 4.1.   If both $V_{SET\ 2}$ and $V_{SET\ 3}$ are relati-

vely high (Figure 4.1a) then all tomatoes can be

categorized into the turning and semi-ripe groups.

If both $V_{SET\ 2}$ and $V_{SET\ 3}$ are lowered (Figure 4.1b),

then most of the tomatoes can be categorized as firm

ripe.   A reasonable colour split was obtained with

$V_{SET\ 2}$ = 5.25 volts, and $V_{SET\ 3}$ = 8.25 volts, as

shown in Figure 4.1c. $V_{SET\ 2}$ falls between the

predicted turning and green voltages previously

shown in Table 3.2, but $V_{SET\ 3}$ is much lower than

the predicted mean of 11 volts for the semi-ripe.

[$V_{SET\ 3}$ would be expected to be greater than 11

volts, but less than 11.93 volts].   The difference

may be explained by the darker red tomatoes used

for the physical properties studies than those used

for the present tests.   The tomatoes used in the

physical properties studies were purposely chosen

to include extremes in both the green and firm ripe

FIGURE 4.1 COLOUR GROUPINGS AT VARIOUS
COMPARATOR VOLTAGE SETTINGS

$\dfrac{V_{SET2}}{6.00}$ $\dfrac{V_{SET3}}{9.75}$ (a)
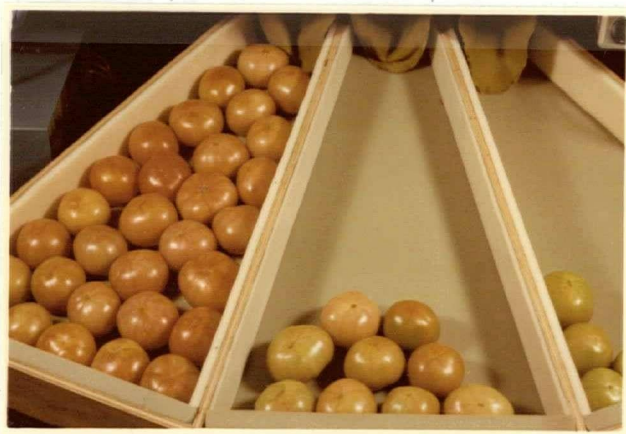
(b) $\dfrac{V_{SET2}}{3.75}$ $\dfrac{V_{SET3}}{6.75}$

$\dfrac{V_{SET2}}{5.25}$ $\dfrac{V_{SET3}}{8.25}$ (c)

categories.

The field test results at the co-operative were very promising. The graded tomatoes were judged acceptable by both the federal graders and the co-operative members.

(II) Preliminary tests involving the eject mechanism showed that a lateral angle of about 10° on the conveyor belt as it passed the eject nozzles, greatly improved the efficiency of the eject system. With the incline, the pneumatic system was only required to start the tomato rolling, after which gravity pulled the tomato off the belt.

The 100 psig(6.9×10^5 newtons/m^2 g) pneumatic system was found adequate at conveyor speeds up to 2.5 ft/sec (76 cm/sec). Ejection of the large tomatoes became difficult at higher speeds. Allowing 5 in (13 cm) of conveyor belt per tomato, i.e. a maximum of 3.5 in (8.9 cm) for the tomato plus 1.5 in (3.8 cm) separation between tomatoes, the corresponding grading rate is approximately 5 tomatoes/sec. This rate would be sufficient for an organization such as Western Greenhouse Co-operative at the peak harvest period, based on 1975 yield predictions (see Appendix B).

The solenoid valves were found to fail at operating frequencies above 10 cycles/sec. The

maximum grading rate attainable with this system
will be 10 tomatoes/sec, provided that the air
flow is sufficient to eject the tomatoes from the
belt. Grading rate is presently limited by the
air flow obtainable during the short period that
the solenoids are active.

SECTION II

SIZE AND COLOUR GRADER

C H A P T E R   5

PHYSICAL PROPERTIES OF TOMATOES AS

RELATED TO SIZE GRADING

INTRODUCTION

The most common criteria for size classification
of fruits and vegetables are dimension and weight. The
industry standard in B.C. for tomato size classification is
based on the measure of the maximum diameter of the fruit
(Appendix A). Usually, this maximum diameter is in a plane
perpendicular to the polar axis formed by the blossom and
calyx ends of the tomato.

The shape of the fruit is of utmost importance when
designing a machine to size grade according to a single
diameter measurement. Variations in shape will determine any
possible need for orientation of the fruit before measurement.
Dimensionless quantities, such as sphericity have been used
in physical properties analyses (25) to describe fruit shape.

Sphericity, a relative measure of spherical uni-
formity based on three diameters, was of less importance in
the design of the size grader than the absolute differences
between the diameters.

In the present investigation of physical properties
related to size grading, the difference between diameters was
studied to establish the need, if any, for fruit orientation
before the diameter is measured. The calculation of area
based on two diameter measurements, and the calculation of
volume based on three diameters will be discussed with regard
to the use of composite values as criteria for size evalua-
tion. Since the only known commercially available size

graders for tomatoes use weight as the size criterion, it
was also of interest to investigate the relationship between
the maximum diameter and the weight of the fruit.

MATERIALS AND METHODS

The ellipsoid was chosen as the approximation for the shape of a tomato, as suggested by Mohsenin (25), having a polar axis formed by the calyx and blossom ends of the tomato. The three diameters, DIA.1, DIA.2, and DIA.3 are the maximum (major) diameter measured at the equatorial plane; the minor diameter, perpendicular to DIA.1, measured at the equatorial plane; and the maximum polar diameter measured at a plane perpendicular to the equatorial plane. When DIA.1 is equal to DIA.2 and DIA.3 is less than DIA.1, the shape of the tomato approximates an oblate spheroid. When DIA.2 and DIA.3 are equal and DIA.1 is greater than DIA.2, the shape approximates a prolate spheroid.

The three diameters, DIA.1, DIA.2, and DIA.3, and the weight of each of 153 tomatoes were measured and recorded.

The samples ranged in size from DIA.1 = 1.43 in (3.63 cm) to 3.85 in (9.78 cm) (which covers the federal size category standard from small to extra large) and weights ranged from 0.92 oz (26.4 g) to 10.82 oz (309.1 g). The area of the equatorial plane was estimated using the approximation of an ellipse:

$$AREA = \frac{\pi}{4} (DIA.1 \times DIA.2).$$

The volume of the tomato was estimated using the approximation of an ellipsoid:

$$VOLUME = \frac{\pi}{6} (DIA.1 \times DIA.2 \times DIA.3).$$

Correlations among the measured diameters and weights, and calculated areas and volumes were obtained as well as linear regressions for the measured weight versus each of the three diameters, calculated area and volume. The correlations and linear regressions were used to justify the use of a single diameter, DIA.1, as a measure of the fruit size.

The data for the 153 tomatoes was grouped into the size categories, small, medium, large and extra large. The difference [DIA.1 - DIA.2] was calculated for each tomato in each of the four size categories as a measure of the circular uniformity at the equatorial plane. A difference of zero would imply that in the equatorial plane the tomato shape could be approximated by a circle; a difference greater than zero would suggest an ellipse as the approximation. The difference between DIA.1 and DIA.2 was used to evaluate the effect of tomato orientation on size measurement at the equatorial plane.

Each size category was treated separately, rather than pooling the data, since the shape of the fruit seemed to vary with size.

The mean differences of [DIA.1 - DIA.2] between size categories were compared and 95% confidence intervals were determined for the differences within each category.

RESULTS

The correlation matrix of DIA.1, DIA.2, DIA.3, weight, calculated area in the equatorial plane, and calculated volume is shown in Table 5.1, based on the 153 samples. Five linear regression equations of weight versus each of the three diameters, as well as area and volume are listed in descending order according to their correlation coefficients (r^2) in Table 5.1.

The differences of [DIA.1 - DIA.2] within a size category were found to follow a skewed distribution for all size categories. The distribution of $\sqrt{DIA.1 - DIA.2}$ was found to be more normal, hence the means and 95% confidence intervals were calculated on the square root basis, and the results transformed by squaring them. The means, and 95% confidence intervals for the difference of [DIA.1 - DIA.2] are listed in Table 5.2 for all four size categories.

There was no correlation between the difference [DIA.1 - DIA.2] and DIA.1 itself, for the small, medium and large categories. As the tomatoes increased in size, the difference between DIA.1 and DIA.2 remained relatively constant. The standard deviations of [DIA.1 - DIA.2] for the small, medium and large categories were small.

A correlation did exist between [DIA.1 - DIA.2] and DIA.1 for the extra large tomatoes, represented by a correlation coefficient of 0.7393. In this size category the larger the tomato, the more elliptical it is in the

TABLE 5.1   DIAMETER-WEIGHT CORRELATIONS AND
                           LINEAR REGRESSION EQUATIONS

	DIA. 1	DIA. 2	DIA. 3	WEIGHT	AREA	VOLUME
DIA. 1	1.0000					
DIA. 2	0.9762	1.0000				
DIA. 3	0.8544	0.8928	1.0000			
WEIGHT	0.9836	0.9798	0.8895	1.0000		
AREA	0.9940	0.9863	0.8575	0.9926	1.0000	
VOLUME	0.9822	0.9820	0.8992	0.9985	0.9920	1.0000

$$\text{WEIGHT } (\pm 0.150)\text{oz} = (0.599 \pm 0.003) \text{ VOLUME} - (0.015 \pm 0.024)$$
$$r^2 = 0.9971 \qquad [5\text{-}1]$$

$$\text{WEIGHT } (\pm 0.337)\text{oz} = (1.32 \pm 0.012) \text{ AREA} - (1.10 \pm 0.063)$$
$$r^2 = 0.9852 \qquad [5\text{-}2]$$

$$\text{WEIGHT } (\pm 0.499)\text{oz} = (4.15 \pm 0.062) \text{ DIA. 1} - (5.70 \pm 0.159)$$
$$r^2 = 0.9675 \qquad [5\text{-}3]$$

$$\text{WEIGHT } (\pm 0.553)\text{oz} = (4.89 \pm 0.081) \text{ DIA. 2} - (6.82 \pm 0.195)$$
$$r^2 = 0.9600 \qquad [5\text{-}4]$$

$$\text{WEIGHT } (\pm 1.26)\text{oz} = (6.56 \pm 0.274) \text{ DIA. 3} - (10.11 \pm 0.622)$$
$$r^2 = 0.7913 \qquad [5\text{-}5]$$

where AREA $= \dfrac{\pi}{4}$ (DIA. 1 X DIA. 2) inch^2

and VOLUME $= \dfrac{\pi}{6}$ (DIA. 1 X DIA. 2 X DIA. 3) inch^3

TABLE 5.2   MEAN DIFFERENCES BETWEEN DIA.1 AND
             DIA.2, AND 95% CONFIDENCE INTERVALS
             FOR FOUR SIZE CATEGORIES.

Size Category	Mean [DIA.1-DIA.2], inch (cm)	95% Confidence Interval [DIA.1-DIA.2], inch (cm)
Small	0.045 (0.114)	0.000 to 0.165 (0.111) (0.419)
Medium	0.073 (0.185)	0.015 to 0.175 (0.038) (0.445)
Large	0.096 (0.244)	0.011 to 0.263 (0.028) (0.668)
Extra large	0.271 (0.688)	0.016 to 0.834 (0.041) (2.118)

equatorial plane. As a result, the standard deviation of [DIA.1 - DIA.2] for the extra large category is greater than that of the other three categories. Because of the correlation this standard deviation does not represent the range of difference between DIA.1 and DIA.2 that one would expect for a single tomato in the extra large category.

A linear regression performed on [DIA.1 - DIA.2] versus DIA.1 for the extra large tomatoes, produced the equation:

$$[DIA.1 - DIA.2] \pm 0.149 = (0.659 \pm 0.299)$$
$$DIA.1 (1.86 \pm 0.091) \qquad [5-6]$$

where DIA.1 and DIA.2 are in inches, and

$$r^2 = 0.5466.$$

The 95% confidence interval for a tomato with a DIA.1 equal to 3.00 in (7.62 cm) would be:

0.00 in < [DIA.1 - DIA.2] < 0.411 in

or 0.00 cm < [DIA.1 - DIA.2] < 1.044 cm

whereas a tomato with a DIA.1 equal to 3.50 in (8.89 cm) would have a 95% confidence interval:

0.157 in < [DIA.1 - DIA.2] < 0.741 in

or 0.399 cm < [DIA.1 - DIA.2] < 1.882 cm

DISCUSSION

The correlation matrix shown in Table 5.1 indicates that the maximum diameter at the equatorial plane, DIA.1, may be used as an indication of the weight of the tomato. The minor diameter, perpendicular to DIA.1 at the equatorial plane is closely correlated to DIA.1, whereas DIA.3, the polar diameter is more independent of DIA.1. The best correlation between a single diameter measurement and weight is that of DIA.1 versus weight. The second largest correlation coefficient associated with weight is that of DIA.2, and the third largest is that of DIA.3.

The calculation of volume based on the assumption that the tomato is an ellipsoid, results in the largest correlation coefficient for weight. The calculation of area at the equatorial plane based on an ellipse results in the second largest correlation coefficient for weight.

A system of measurement which includes the determination of all three diameters, and the calculation of volume based on the three diameters would be ideal if the best correlation with weight was desired. A system of measurement which includes the determination of DIA.1 and DIA.2 only, and the calculation of area based on the two diameters, would be second best. A system which measures only the largest diameter, DIA.1, at the equatorial plane, would be third best as an estimate of the tomato's weight.

The regression equations and their associated r^2

values shown in Table 5.1 indicate that DIA.1, DIA.2, DIA.3,
area, and volume are linearly related to the tomato's
weight.

The third largest correlation coefficient, 0.9675,
was obtained for the weight versus DIA.1 regression equation.
A system which measures only DIA.1 could therefore reasonably
estimate the weight of a tomato.

As shown in Table 5.2, the mean differences of
[DIA.1 - DIA.2] increase with increasing size categories,
from small to extra large. The equatorial plane becomes less
circular as the tomato size increases. There was no correla-
tion between [DIA.1 - DIA.2] and DIA.1 within the small,
medium and large size categories. The 95% confidence inter-
vals for [DIA.1 - DIA.2] apply for the smallest tomato in a
size category as well as for the largest. For example, the
smallest large tomato has DIA.1 = 2.25 in (5.72 cm) and the
largest large tomato has DIA.1 = 3.00 in (7.62 cm), and the
95% confidence interval, 0.011 to 0.263 for [DIA.1 - DIA.2],
applies for both tomatoes.

The 95% confidence interval for the extra large
tomatoes shown in Table 5.2 does not apply since
[DIA.1 - DIA.2] increases with DIA.1 in this size category.
For any given DIA.1 in the extra large category, the 95%
confidence interval may be calculated using equation [5-6].

The shape of the tomato, especially in the equator-
ial plane will determine the need for orientation of the

tomato, before DIA.1 can be measured. If the tomato is
spherical, no orientation is required, since DIA.1 = DIA.2 =
DIA.3. If the tomato is an oblate spheroid, the tomato tends
to rest with the polar axis perpendicular to the plane on
which it rests, and no further orientation is required, since
DIA.1 = DIA.2. If the tomato is a prolate spheroid, no
orientation in the polar plane will be required, since DIA.2
= DIA.3, however, orientation of the DIA.1 axis will be
required. If the tomato is an ellipsoid, orientation of the
polar axis and equatorial plane will be required. The
ellipsoid tomatoes are generally the extra large tomatoes,
and DIA.3 is usually the smallest, making the tomato most
stable if resting on one of its poles. Orientation in the
equatorial plane will therefore be required.

The mean differences and 95% confidence intervals
of [DIA.1 - DIA.2] shown in Table 5.2 indicate the worst
measurement error that would be expected if the tomatoes
were not oriented in the equatorial plane, i.e. of DIA.2 was
measured instead of DIA.1, the error in the measure of DIA.1
would be [DIA.1 - DIA.2]. Only one orientation of the tomato
in the equatorial plane produces no error in the measure of
DIA.1, and only one orientation produces a maximum error
equal to [DIA.1 - DIA.2]. All other orientations in the
equatorial plane produce diameter measurements having errors
greater than zero but less than [DIA.1 - DIA.2].

It is concluded that orientation of the tomato for

the accurate determination of DIA.1 will be more important
for the larger tomatoes than the small ones, since the
measurement error due to lack of orientation increases with
tomato size.

C H A P T E R   6

SIZE DETERMINATION USING THE COLOUR GRADER

SCHMITT TRIGGER PULSE

INTRODUCTION

The Schmitt trigger pulse width of the colour grader is proportional to the length of time that the tomato spends under the fibre optic sensing head. If the tomato is centered on the conveyor belt with respect to the sensing head, and the conveyor belt is moving at a constant speed, the Schmitt trigger pulse width will be a function of a diameter of the tomato. If the tomato is not centered or the conveyor belt is travelling at a varying speed, an error in the diameter measurement will result.

In this chapter, the relationship between the Schmitt trigger pulse width and various tomato sizes will be studied at a fixed conveyor belt speed. Factors which affect the Schmitt trigger pulse, such as belt speed, and misalignment of the tomato with respect to the fibre optic sensing head will also be examined.

The "limit of detection" of the present sensing head design will be discussed. The limit of detection is the diameter of a tomato which is too small to be detected, and thus does not produce a Schmitt trigger pulse. The resolution of the instrument is the smallest difference between two diameters which can be discriminated.

MATERIALS AND METHODS

Size Standards

It was evident from the beginning of the study of tomato size versus Schmitt trigger pulse width that some tangible size standards, other than tomatoes, were required. Tomatoes have a finite shelf life which makes them undesirable for long term testing. The green tomatoes, with the longest shelf life at room temperature change colour as they ripen, making them unsuitable as standards.

Three white textured styrofoam spheres were chosen as size standards, one small, one medium, and one large. Their diameters were 2.0 in (5.1 cm), 2.5 in (6.4 cm) and 2.9 in (7.4 cm) respectively. A segment was cut from each sphere, so that the spheres could be placed on the conveyor belt with the flat side down, as well as approximating more realistically the shape of a tomato, where the flat side represented the calyx end. The three diameters, DIA.1, DIA.2 and DIA.3 of each styroball are listed in Table 6.1.

The divider output of the colour grader was measured for the three styroballs, and since their colours were all the same, the divider output voltage for each of the three was approximately 2 volts. This voltage rendered the styroballs as "turning" in colour, i.e. the styroballs reflected slightly more light in the red region than in the green region. The styroballs were therefore suitable as standards.

TABLE 6.1   DIA.1, DIA.2, and DIA.3 of
                   THREE STYROBALL SIZE STANDARDS

Styroball Size	DIAMETERS, inch (cm)		
	DIA.1	DIA.2	DIA.3
Small	2.00 (5.08)	2.00 (5.08)	1.63 (4.14)
Medium	2.48 (6.30)	2.48 (6.30)	2.01 (5.11)
Large	2.85 (7.24)	2.85 (7.24)	2.35 (5.97)

Pulse Width Measurement Technique

The flat side of each styroball was attached to the black conveyor belt for all tests, using double sided adhesive tape, and the Schmitt trigger pulse of the colour grader was measured using a Tektronics Frequency Counter, Model DC 503.

Measurement of Belt Speed

Since the frequency of CLOCK A (Figure 3.15) is directly proportional to the rate of belt movement, the measure of the CLOCK A frequency will give an accurate measure of belt speed. An approximate conversion scale of the CLOCK A frequency versus belt speed is shown in Table 6.2. A Tektronics Frequency Counter, Model DC 503 was used to measure the CLOCK A frequency. The CLOCK A frequency will be quoted as the measure of belt speed in subsequent tests.

Effect of Styroball Size on Schmitt Trigger Pulse Width at Four Conveyor Belt Speeds

A. The large styroball was centered and taped to the conveyor belt surface. The belt was set in motion, and the belt speed determined by measuring the CLOCK A frequency. The styroball remained attached to the conveyor allowing a Schmitt trigger pulse width measurement to be obtained every time the styroball passed under the sensing head, thus eliminating recentering of the styroball for each measurement.

TABLE 6.2   THE COLOUR GRADER *CLOCK A*
                 FREQUENCY VERSUS APPROXI-
                 MATE CONVEYOR BELT SPEED.

CLOCK A Frequency (Hz)	Conveyor Belt Speed, inch/sec (cm/sec)
20	10 (25)
40	20 (51)
60	30 (76)
80	40 (102)
100	50 (127)
120	60 (152)

B. Thirty Schmitt trigger pulse width measurements were

obtained for each of four belt speeds -- 30, 40,

50, and 60 Hz.

C. The procedure described in A and B was repeated for the

medium and small styroballs.

Effect of Off-Center Viewing of a Styroball on the Measured Diameter

Each of the three styroballs was centered and taped
to the conveyor belt, one at a time, to establish the effects
of off-center viewing of the styroball by the fibre optic
sensing head. The measurement error produced by such off-
center viewing will indicate the need (if any) for centering
tomatoes on the conveyor belt. A belt speed of 40 Hz was
chosen for the tests. The fibre optic sensing head was
deliberately off-set from the center of the belt by about
5/8 inch (1.6 cm). The sensing head was moved transversely
to the movement of the belt, in five 1/4 inch (0.64 cm)
intervals. Ten Schmitt trigger pulse width measurements were
obtained as the styroball passed under the sensing head, for
each 1/4 inch (0.64 cm) interval.

RESULTS AND DISCUSSION

Effect of Styroball Size on Schmitt Trigger Pulse
Width at Four Conveyor Belt Speeds

The means, standard deviations, and standard errors
of the Schmitt trigger pulse widths and their associated
styroball diameters, for four belt speeds are listed in
Table 6.3. The means of the Schmitt trigger pulse widths
versus styroball diameter are plotted for four belt speeds
in Figure 6.1.

Ideally, the relationship between pulse width and
diameter shown in Figure 6.1, is linear with all lines
passing through the origin. Practically, a reflectance
threshold must be exceeded before the Schmitt trigger circuit
responds. This threshold is a function of the field of view
at the sensing head and the reflectance difference between a
tomato and the conveyor belt. The threshold will be indepen-
dent of conveyor belt speed. A tomato, or styroball, must be
large enough to occupy sufficient area in the fibre optic
field of view before it is detectable above background. Based
on experience with the colour grader, the threshold relates
to a tomato diameter of about 1.5 inches (3.8 cm). The
dotted portions of the curves in Figure 6.1 are extrapolated
to a probable asymtote around 1.5 inches (3.8 cm). Above
2.5 inches (6.4 cm) the curves appear quite linear.

Resolution

The standard deviations of the Schmitt trigger
pulse widths for the three styroballs at four belt speeds

TABLE 6.3   MEANS, STANDARD DEVIATION, AND STANDARD ERRORS OF SCHMITT TRIGGER PULSE WIDTHS FOR THREE STYROBALLS AT FOUR CONVEYOR BELT SPEEDS.

Styroball	PULSE WIDTH (ms)		
Dia.,inch (cm)	Mean	S.D.	S.E.
Belt Speed: 30 Hz			
2.00 (5.08)	153.7	2.935	0.545
2.48 (6.30)	199.4	1.634	0.298
2.85 (7.24)	224.3	1.509	0.276
Belt Speed: 40 Hz			
2.00 (5.08)	117.1	0.888	0.165
2.48 (6.30)	150.4	1.180	0.215
2.85 (7.24)	169.9	1.093	0.200
Belt Speed: 50 Hz			
2.00 (5.08)	93.3	1.241	0.230
2.48 (6.30)	120.6	0.828	0.151
2.85 (7.24)	137.8	1.300	0.237
Belt Speed: 60 Hz			
2.00 (5.08)	79.0	0.883	0.164
2.48 (6.30)	102.7	1.037	0.189
2.85 (7.24)	118.2	1.210	0.221

FIGURE 6.1 MEAN SCHMITT TRIGGER PULSE WIDTH VS. STYROBALL DIAMETER AT FOUR CONVEYER BELT SPEEDS
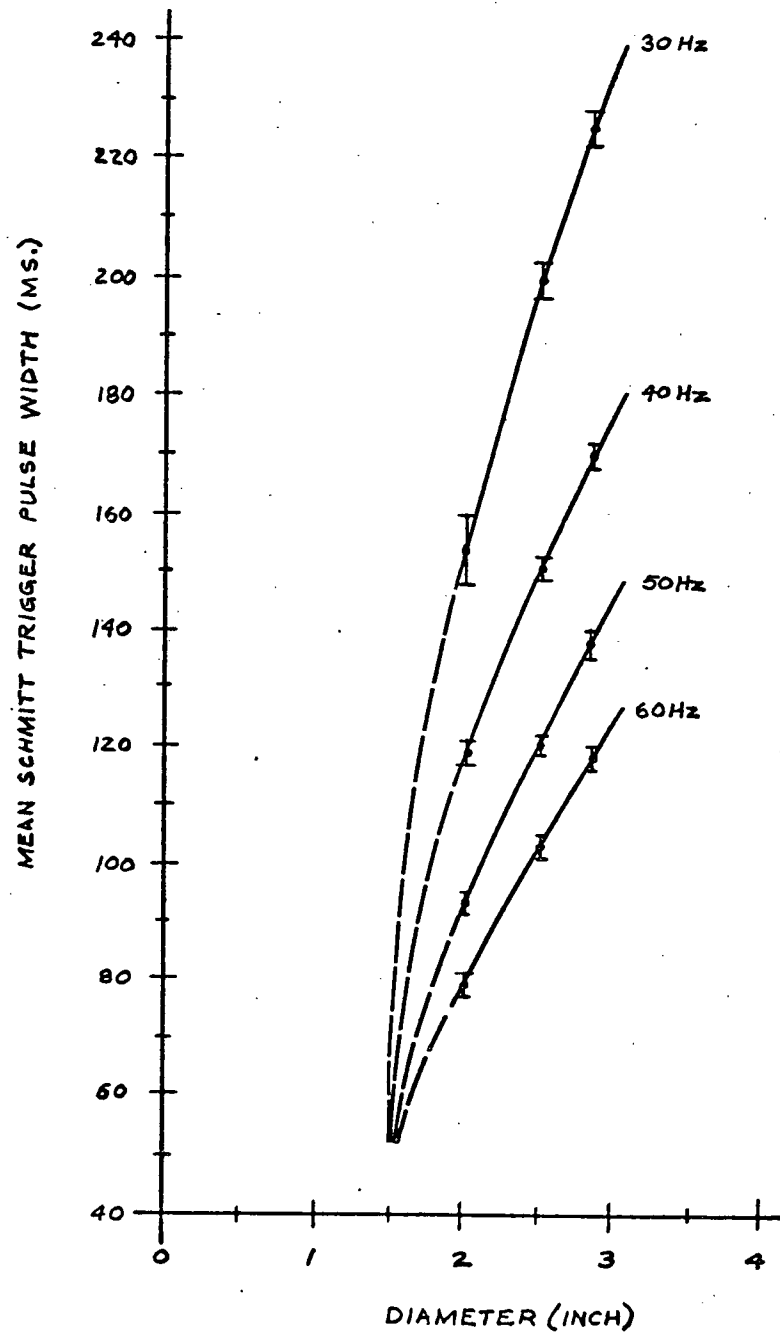
as listed in Table 6.3 give some indication of the resolu-
tion of the instrument if the Schmitt trigger pulse width
is used as a measure of diameter. The magnitudes of the
standard deviations are probably due to non-uniformity of
the conveyor belt speed, and lateral "squirming" of the
conveyor belt. The largest standard deviation listed in
Table 6.3 is 2.935 ms for the 2.00 inch (5.08 cm) styroball
at the 30 Hz belt speed. As a percentage of the mean, and
converted to inches, the standard deviation is 0.038 inch
(0.10 cm) and the 95% confidence interval for a given
diameter will be: the diameter ± 0.075 (0.19 cm). This
variation in size is probably negligible.

The worst case resolution is therefore slightly
greater than 1/16 inch (0.16 cm). Typically, however, the
standard deviation will be 0.023 inch (0.058 cm) (the mean
of the standard deviations expressed as a percent of the
diameters, in Table 6.3) and the 95% confidence interval
will be: the diameter ± 0.045 inch (0.11 cm). Therefore
95% of the diameters will be within 3/64 inch (0.12 cm) of
their true size.

The worst belt speed variation for the present
design would be approximately 4%. Better regulation would
increase the resolution.

Schmitt Trigger Pulse Width versus Conveyor Belt Speed for Three Styroball Sizes

For a given styroball diameter, the product of pulse width and conveyor belt speed (measured as the CLOCK A frequency) is constant. This is the result that one would expect, since a given styroball occupies a certain length of belt, and the number of CLOCK A cycles are the same measure of belt length. The products were approximately 4.7, 6.0 and 6.9 cycles, for the small, medium and large styroballs, respectively, calculated from the data in Table 6.3.

Effect of Off-Center Viewing of a Styroball on the Measured Diameter

The mean of the ten pulse widths obtained for each of the 1/4 inch (0.64 cm) intervals as the sensing head was moved across the conveyor belt was plotted against the distance the head was moved. The resulting curve was of parabolic shape, its maximum corresponding to the on-center view of the styroball. Deviations to the right or left of center caused a decrease in the measured pulse width.

Using the maximum pulse width obtained from the curve as the "true" measure of the styroball size, the error due to off-centering could be predicted. For example, the maximum pulse width for the small styroball was 126.5 ms, and at 1/4 inch (0.64 cm) from the maximum the pulse width was 122.5 ms. The measurement error in the diameter due to the 1/4 inch (0.64 cm) off-center viewing is thus:

$$\text{Error} = \frac{2.00 \text{ inch}}{126.5 \text{ ms}} \times (126.5 - 122.5) \text{ ms}$$

$$= 0.063 \text{ inch } (0.16 \text{ cm}).$$

Similarly, errors were calculated in 1/8 inch (0.32 cm) intervals from zero to 5/8 inch (1.6 cm) off-center. The error values are listed in Table 6.4.

The offset of the styroball from the center of the conveyor belt (or the center of the sensing head) does not seem to be too critical. A 1/4 inch (0.64 cm) offset results in a measurement error of about 0.025 inch (0.064 cm) for the 2.85 inch (7.24 cm) diameter styroball or a 0.9% measurement error, and a 0.063 inch (0.16 cm) error for the 2.00 inch (5.08 cm) diameter styroball, or a 3.2% error. A centering device on the feed end of the conveyor belt should be able to center tomatoes (especially smaller ones) within 1/4 inch (0.64 cm) of the belt center without much difficulty.

TABLE 6.4   APPROXIMATE DIAMETER MEASUREMENT ERROR
                   AT VARIOUS OFF-CENTER DISTANCES FOR
                   THREE STYROBALLS, RELATIVE TO THE ON-
                   CENTER MEASUREMENT.

Off-Center Distance inch (cm)	ERROR (inch)		
	Small Styroball	Medium Styroball	Large Styroball
0 (0)	0.000 (0.000)	0.000 (0.000)	0.000 (0.000)
1/8 (0.32)	0.016 (0.041)	0.016 (0.041)	0.008 (0.020)
1/4 (0.64)	0.063 (0.160)	0.039 (0.099)	0.025 (0.064)
3/8 (0.95)	0.103 (0.262)	0.078 (0.198)	0.059 (0.150)
1/2 (1.27)	0.174 (0.442)	0.132 (0.335)	0.110 (0.279)
5/8 (1.59)	0.245 (0.622)	0.202 (0.513)	0.170 (0.432)

SUMMARY

The colour grader Schmitt trigger pulse width for
the tests conducted using the styroball size standards, is
a function of the diameter of the styroball and the speed of
the conveyor belt. The product of the Schmitt trigger pulse
width and the belt speed (when measured as the frequency of
CLOCK A) for a given diameter is constant. The relationship
between the width of the Schmitt trigger pulse and the styro-
ball diameter is quite linear (for a constant belt speed)
down to about a 2 inch (5 cm) diameter, where the straight
line rolls off to a limit of about 1.5 inch (3.8 cm). Styro-
balls having diameters below this limit cannot be detected.

The measurement error resulting from a given off-
center placement of the styroball on the conveyor belt
increases as the styroball size decreases. The error in-
creases as the off-center distance increases for a given
styroball size. A 1/4 inch (0.64 cm) offset from the center
of the belt results in a measurement error of about 0.063
inch (0.16 cm) for the 2.00 inch (5.08 cm) diameter styro-
ball and as little as 0.025 inch (0.064 cm) for the 2.85
inch (7.24 cm) diameter styroball.

With a system capable of reasonable alignment of
tomatoes on the conveyor belt, it appears feasible to use
the Schmitt trigger pulse width as a measure of the tomato's
diameter, provided that the belt speed is relatively constant.
The resolution obtainable with the instrument will be

primarily a function of the regulation of conveyor belt speed. For the present design, the resolution was found to be about 3/64 inch (0.12 cm).

C H A P T E R   7

DESIGN   APPROACH

INTRODUCTION

A combined size and colour grader was designed by
incorporating the Schmitt trigger pulse with the colour
grader described in Section 1. A voltage proportional to the
Schmitt trigger pulse width was generated and processed in a
manner similar to the divider output voltage of the colour
grader. A number of comparators preset to the size category
limits were used to generate a digital signal which was
stored in a memory along with the colour category informa-
tion.

Since four colour categories and five size cate-
gories exist, twenty combinations of size and colour arise.
This would require a minimum of nineteen shift register
memories. It was decided that due to the low percentage of
green tomatoes and below small tomatoes generally encountered*
all sizes of green tomatoes (4 sizes) would be in one cate-
gory, and all colours of below small tomatoes (3 colours)
would be in another. This reduced the number of memories
required to thirteen, with the fourteenth category comprised
of those tomatoes which rolled off the end of the belt - all
tomatoes which were below small.

Not only can the Schmitt trigger pulse of the
colour grader be used in the size/colour grader, but other
timing pulses common to both graders can be drawn from the

---

* Personal communication with Western Greenhouse Co-op. members

colour grader.

The components to be used will match those of the colour grader, i.e. linear IC's will be used for analog signal processing, and CMOS IC's will be used for digital signal processing.

THEORY

It was decided that a linear relationship between diameter and Schmitt trigger pulse width would suffice as an approximation for the curves shown in Figure 6.1. Theoretically, neglecting the threshold effect, the straight lines would all pass through the origin, and the slopes of the lines would be a function of conveyor belt speed. Any one line may be represented by:

$$D = Kt \qquad\qquad [7\text{-}1]$$

where

D = diameter (volts)

K = constant

t = pulse width (sec)

or

$$D = \int Kdt \qquad\qquad [7\text{-}2]$$

An integrator circuit, which integrates a constant voltage (K) and is triggered to begin integrating at the start of the Schmitt trigger pulse, at t = 0, and to stop integrating at the end of the pulse would produce a final output voltage which could be used as a measure of the tomato's diameter.

For a fixed belt speed, a constant integrating voltage may be chosen. For the present test model it was decided that a range of operating belt speeds was desirable, and that the voltage to be integrated, E, would be directly

proportional to conveyor belt speed. A frequency to voltage
conversion was therefore necessary. Frequency to voltage
conversion may be achieved by generating a short pulse of
constant height and width and then integrating the pulses
over a fixed sampling time. Therefore,

$$E = \sum_{i=1}^{n} e_i \Delta t \qquad [7-3]$$

where

e_i = pulse height (volts)

Δt = pulse width (sec)

n = number of pulses

= f T = frequency X sampling time.

Since height e_i, and the width Δt, of the pulse are con-
stant then,

$$E = n e_i \Delta t \qquad [7-4]$$

or

$$E = f e_i \Delta t T \qquad [7-5]$$

Due to power supply limitations, the maximum
desired value of E is 10 v-sec. If the pulse height,
e_i = 15v, then,

$$f \Delta t T = 2/3 \qquad [7-6]$$

The conveyor belt speed was assumed not to exceed
5 ft/sec (152 cm/sec) or 120 Hz CLOCK A frequency, therefore
the maximum value of Δt is

$$\Delta t_{max} = \frac{1}{180 T} \qquad [7-7]$$

The sampling time, T, should be as long as possible so that many pulses are integrated. If T = 1 sec, then equation [7-7] becomes,

$$\Delta t = 5.56 \text{ ms} \qquad [7-8]$$

At a slow conveyor belt speed, of 10 inch/sec (25 cm/sec) or 20 Hz CLOCK A frequency, equation [7-5] becomes,

$$E = 20 \times 15 \times 5.56 \times 10^{-3} \times 1$$

$$E = 1.67 \text{ v-sec.}$$

Note that the 120 Hz and T = 1 sec, 120 pulses are integrated and at 20 Hz only 20 pulses are integrated. The sampling time may be increased up to a point, provided that E can be stored for the sampling period with negligible loss.

For a given belt speed, E remains constant. The integration of the constant produces a linear ramp voltage with respect to time. Substituting E for K in equation [7-2] and integrating from zero for the length of the Schmitt trigger pulse, produces:

$$D = A \int_{0}^{p} E dt \qquad [7-9]$$

or

$$D = A E p \qquad [7-10]$$

where

$$D = \text{voltage representing the diameter of the tomato}$$

$$E = \text{integrating voltage}$$

p = Schmitt trigger pulse width produced by the tomato

A = constant.

If the largest tomato to be encountered has a diameter of 4 inches (10 cm), then at 20 Hz belt speed, the pulse width is about p = 400 ms. The maximum value of D was chosen as 12.5v, therefore, solving for A in equation [7-10], we get,

A = 19. [7-11]

Note that for the same diameter, if the belt speed = 60 Hz, or 30 inches/sec (76 cm/sec),

E = 5.00

p = 133 ms

A = 19.

By converting the belt speed, i.e. CLOCK A frequency, to a voltage, and integrating the voltage for the length of the Schmitt trigger pulse, a voltage D proportion to the Schmitt trigger pulse is generated. The Schmitt trigger pulse is a function of tomato diameter, as shown in Chapter 6, therefore D is proportional to diameter.

ELECTRONIC SIZE AND COLOUR GRADER:

OVERVIEW

A size grader was designed using some of the signals from the colour grader (Section 1) to produce digital size category signals. The size category digital signals were combined with the colour category signals to produce one signal for each of the different size/colour category combinations.

A block diagram of the size grader and size/colour grader digital processor is shown in Figure 7.1. [The circled inputs in the diagram are signals obtained directly from the colour grader described in Section 1].

The pulse generator and timer circuit (A in Figure 7.1) produces a pulse of uniform height and width every cycle of the CLOCK A signal, which is the measure of conveyor belt speed. The circuit also produces an INTEGRATE and an UPDATE signal, which allows the generated pulses to be integrated and the result of the integration to be stored by the intergrator and storage circuit (B). The integration takes place over a fixed time period, about 1 sec, after which the stored signal is updated and the integration begins anew. Thus the belt speed is monitored and a voltage, E, which is a function of belt speed is obtained at the output of (B).

The $\overline{\text{SAMPLE}}$ input from the colour grader is the complement of the Schmitt trigger pulse (see Figure 3.12) and is the measure of the tomato diameter. The voltage, E, is
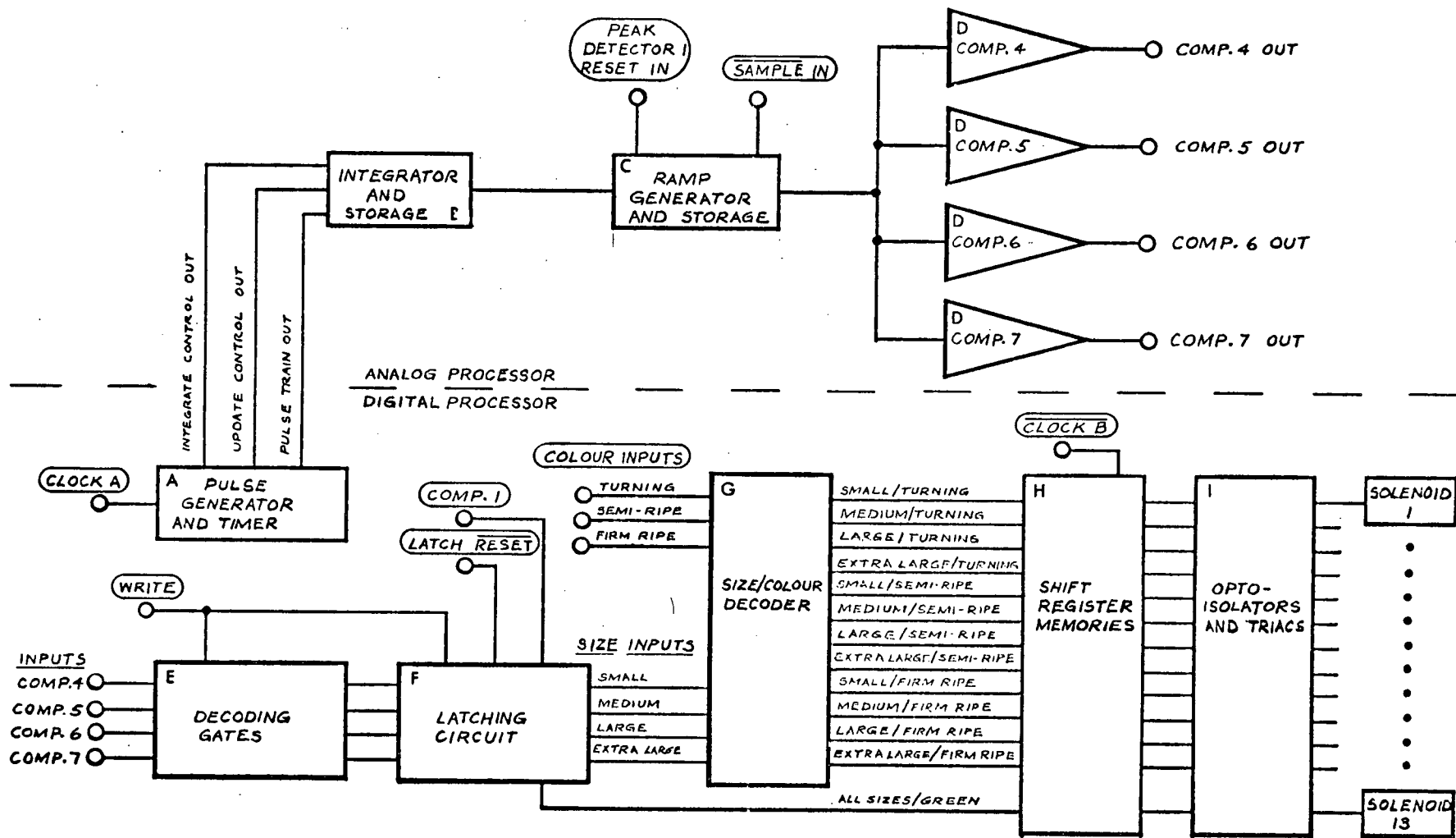
FIGURE 7.1   SIZE GRADER AND SIZE/COLOUR GRADER
DIGITAL PROCESSOR BLOCK DIAGRAM

170

integrated for the duration of the $\overline{\text{SAMPLE}}$ pulse, and the final voltage D is obtained which is a function of the tomato diameter. This integration takes place in the ramp generator and storage circuit (C).

The voltage, D, is then processed in the same way as the divider output signal of the colour grader. D is compared to four preset voltages corresponding to size category limits by the comparator circuits (D), and the outputs of the four comparators form a 4-bit digital signal ranging from 0000 to 1111 depending on the size category.

The digital signal is decoded (E) and stored temporarily in a latching circuit (F). The colour category information is then combined with the size category data (G) and a single size/colour signal is stored in a shift register memory (H). Thirteen shift register memories are used and one "drop-off" at the end of the conveyor belt, to store the information until the tomato gets to its eject station.

When a signal stored in a shift register appears at the shift register output, it is used to control a pneumatic solenoid to eject the tomato. As was the case for the colour grader, opto-isolators and triacs (I) were used to interface the low power digital IC's to the 115 volt AC solenoids.

Rather than build a long conveyor and purchase ten more solenoids and other hardware, it was decided that the ability of the system to both size and colour grade tomatoes

could be tested using the thirteen memory circuits together
with the three opto-isolator and triac circuits and the
three solenoids of the colour grader. The same conveyor
system could be used as well. Tomatoes could then be graded
for size and colour in groups of three, and the "drop-off"
group would contain all other size/colour categories. This
remaining group could be regraded, but the solenoids wired
to three other shift register memories. All permutations of
size and colour could be tested this way through the use of
only three solenoids.

A final prototype size and colour grader would
contain thirteen opto-isolators and triacs, and thirteen
solenoids mounted on a long conveyor system. It was believed
that construction of the final prototype was not necessary to
fulfill present objectives.

Pulse Generator and Timer Circuits (Box A, Figure 7.1)

A schematic of the pulse generator and timer circuits is shown in Figure 7.2.

A period sampling of about one second was chosen over which the belt speed would be monitored. The input to the pulse generator is CLOCK A, which varies from about 24 to 120 Hz. A sampling period of less than one second could result in an integration of less than 24 pulses, incurring large errors, since the integration error increases with decreasing number of pulses. (A belt speed of less than 1 ft/sec (30 cm/sec) would produce the same errors). Integration over several seconds would result in too much drift in the previously stored integration result.

A clock signal of 0.1 sec period was generated using NAND 1 and NAND 2 and timing components R_1 and C_1. The period of the clock signal is defined as:

$$T = 1.4 \, R_1 \, C_1 \qquad [7\text{-}12]$$

letting $C_1 = 0.1 \, \mu F$

and $T = 0.1$ sec

then $R_1 = 714$ KΩ $\qquad [7\text{-}13]$

R_1 was chosen as a 1 Meg Ω potentiometer to allow adjustment of the period. R_x is an input protection resistor, which maintains stability, and is generally twice R_1.

The sampling clock is gated via one of the NAND 1 inputs, #1* in Figure 7.2. The sampling clock must be

* # refers to circled points in the figure.

174

FIGURE 7.2   PULSE GENERATOR AND TIMER CIRCUITS
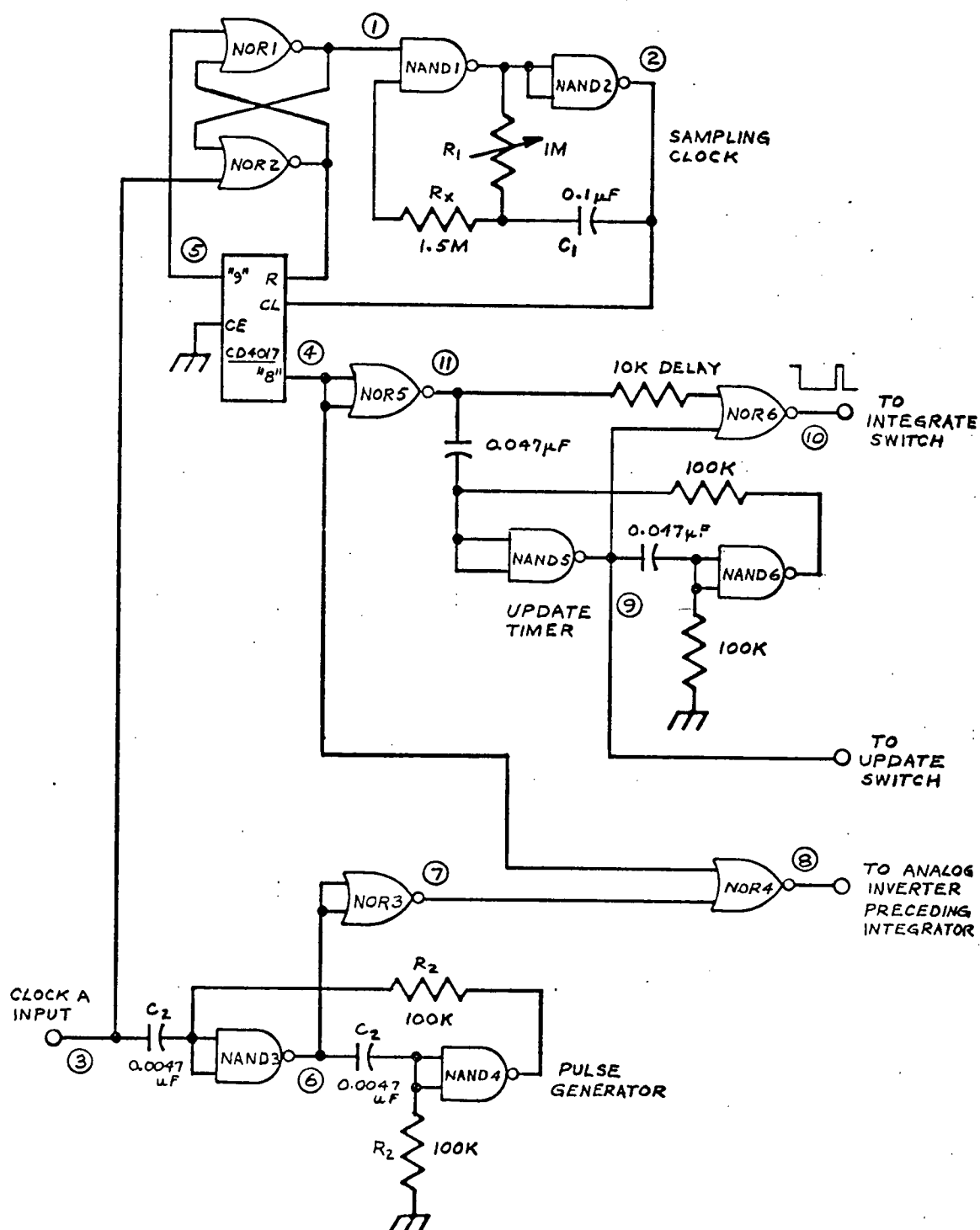
synchronized with the CLOCK A frequency so that the same number of pulses are always being integrated. The synchronization is ensured through the use of the R/S latch comprised of NOR 1 and NOR 2. The sampling clock operates only when #1 is HIGH.

The sampling clock output, #2, is fed into a CD4017 decade counter having ten decoded outputs. The reset input of the CD4017 is normally low, maintained by the presence of CLOCK A at input #3 of the latch. The "8" decoded output, #4, goes HIGH for 100 ms after 8 sampling clock pulses, or T = 800 ms. The "9" decoded output, #5, goes HIGH for 100 ms after 9 sampling clock pulses, or T = 900 ms. As soon as #5 goes HIGH, the latch output #1 goes low, thus stopping the sampling clock. At the same time, the CD4017 reset input goes HIGH, thus resetting the counter to zero. The sampling clock does not start again until the next positive going CLOCK A pulse appears at input #3. This assures synchronization of the two clock signals.

The pulse generator is a monostable multivibrator circuit* comprised of NAND 3 and NAND 4. Every time the CLOCK A signal goes LOW, a short positive going pulse of about $\Delta t = 658$ μs is produced at #6. This pulse is inverted through NOR 3 and appears at the input to NOR 4, #7. The output of NOR 4, #8, is the complement of #7 only when #4 is LOW. If #4 is HIGH, then #8 is always LOW. As previously

---

* The component selection of this circuit is described later.

mentioned, #4 is LOW for 800 ms thus allowing the pulses of the pulse generator to appear at #8 for 800 ms. The pulses at #8 are the pulses to be integrated.

Operation of the integrator and storage circuit (Box B, Figure 7.1) is controlled by output #4 and which triggers the UPDATE timer comprised of NAND 5 and NAND 6. The UPDATE timer output, #9, is normally LOW, therefore the #4 signal appears first inverted through NOR 5 and again through NOR 6 at #10. As soon as #4 goes HIGH, the inverted signal at #11 goes LOW, triggering the UPDATE time to produce a 66 ms pulse at #9. The 66 ms time period was arbitrarily chosen, and is not critical. The pulse allows the output of the integrator to be transferred to the storage circuit, thus updating the storage information. The output of NOR 6, #10, has not changed during the 66 ms period, since the former "1", "0" conditions at inputs #11 and #9 have reversed to "0", "1", resulting in the integrator pulse at #10 still being LOW. Only after the storage circuit has been updated, i.e. after the 66 ms has elapsed, does #10 go HIGH, thus resetting the integrator to zero. The integrator remains reset for 34 ms. The sampling clock is then stopped by a HIGH appearing at #5, and is then restarted by the CLOCK A signal appearing at #3. Integration of the 658 μs pulses starts again for a period of 800 ms.

Integrator and Storage Circuit (Box B, Figure 7.1)

The integrator and storage circuit is shown in Figure 7.3. The equation governing the output of the integrator, comprised of the 741 Op. Amp. and R_3, C_3, is:

$$E = -\frac{1}{R_3 C_3} \int e_i \, dt \qquad [7\text{-}14]$$

where e_i = input voltage

                E = output voltage

or referring to equation [7-5];

$$E = -\frac{1}{R_3 C_3} [f \, e_i \, \Delta t \, T]. \qquad [7\text{-}15]$$

In order to maintain small resistance and capacitance values, R_3 was chosen as $1M\Omega$ and C_3 as $0.1 \, \mu F$. Now equation [7-15] becomes:

$$E = -10 \, [f \, e_i \, \Delta t \, T]. \qquad [7\text{-}16]$$

In order to stay within the operating voltage range, f, e_i, Δt, or T must now be divided by 10. It was found advantageous to divide Δt by 10. Therefore equation [7-7] becomes:

$$\Delta t_{max} = \frac{1}{1800T} \qquad [7\text{-}17]$$

and since $T = 800$ ms (integration time), [7-17] becomes

$$\Delta t_{max} = 694 \, \mu s. \qquad [7\text{-}18]$$

For this reason, R_2 and C_2 were chosen in the pulse generator circuit to produce a pulse close to 694 μs, which turned out

FIGURE 7.3 INTEGRATOR AND STORAGE CIRCUIT
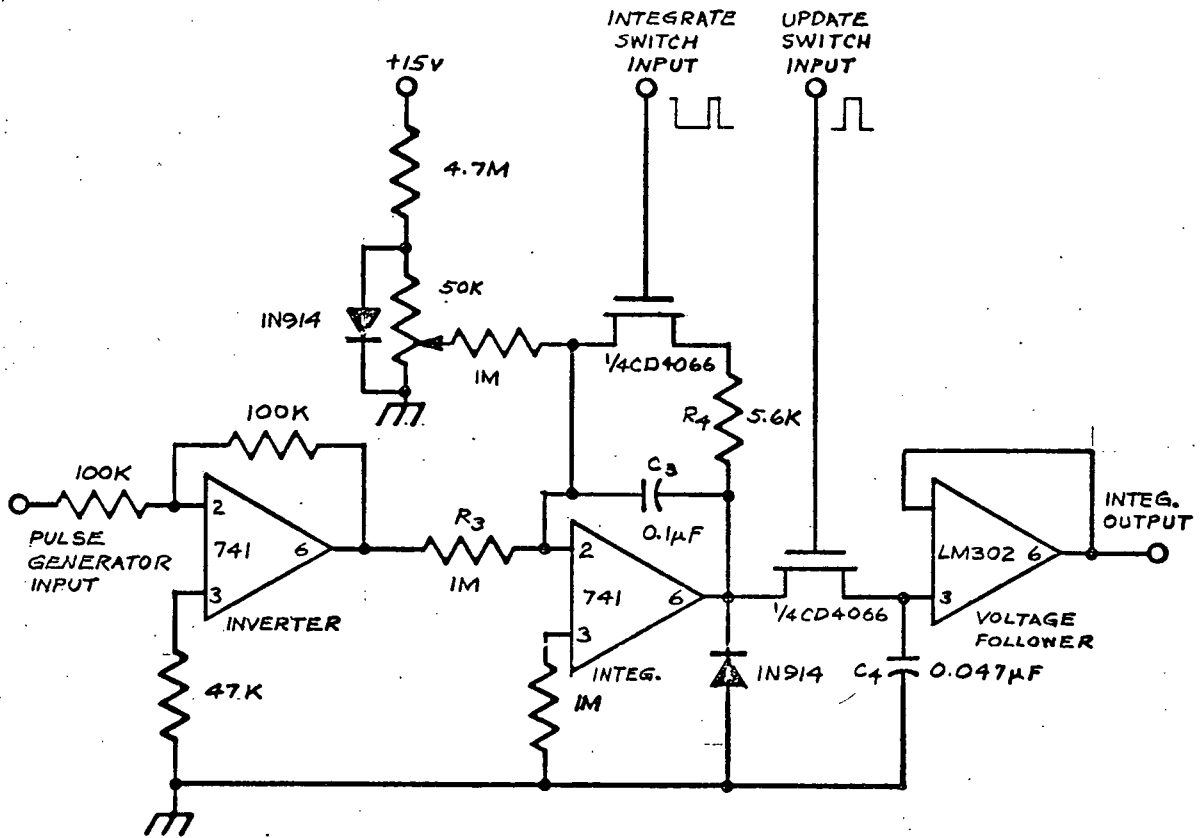
to be $\Delta t = 658$ μs, when standard capacitors and resistors were used.   (Refer to Figure 7.2).

Resetting of the integrator to zero is accomplished through the use of a CD4066 bilateral switch across C_3. Since the bilateral switch operates on a +15 volt supply, it was undesirable for the integrator output to go negative, as suggested by equation [7-16]. The positive input pulses to the integrator were first inverted using a unity gain 741 amplifier, thus making e_i negative, and E positive.

A standard offset circuit was used to adjust the integrator for zero drift. The IN914 at the integrator output was used to ensure that no negative voltage would appear across either of the two bilateral switches. R_4 is a current protection resistor.

The second bilateral switch controls the UPDATE information to the high impedence input of the LM302 voltage follower. The integrator output is connected to the input of the LM302 for the last 66 ms of integration time, thus allowing C_4 to charge to the new integrator output voltage. When the bilateral switch is reopened after the 66 ms duration, the capacitor discharges through the 10^{12} Ω input of the LM302 and the 10^{12} Ω "off" resistance of the CD4066. Very little charge is lost over the 800 ms integration period which follows initial storage. The LM302 output remains relatively constant for a given conveyor belt speed.

The output of the LM302 was measured for several

conveyor belt speeds, and the theoretical values were calculated using equation [7-16] by letting

$$e_i = 15 \text{ volts}$$

$$\Delta t = 658 \text{ } \mu s$$

$$\text{and } T = 800 \text{ ms.}$$

The theoretical and experimental values are listed in Table 7.1.

TABLE 7.1   THEORETICAL AND MEASURED INTEGRATOR
                   OUTPUT VOLTAGES AT VARIOUS CONVEYOR
                   BELT SPEEDS.

CLOCK A Freq. (Hz)	Theoretical E (volts)	Measured E (volts)
30	2.4	2.3
40	3.2	3.1
50	3.9	4.0
60	4.7	4.8
70	5.5	5.5
120	9.5	9.2

Ramp Generator and Storage Circuit (Box C, Figure 7.1)

A schematic of the ramp generator and storage circuit is shown in Figure 7.4. The ramp generator is an integrator as suggested by equation [7-9]:

$$D = A \int_0^P Edt \qquad [7-9]$$

The equation for the integrator is:

$$D = - \frac{1}{R_5 C_5} \int e_i \, dt \qquad [7-19]$$

Therefore in [7-9], $A = \frac{1}{R_5 C_5}$

and $E = - e_i$.

From [7-11] $\qquad A = 19$

Therefore $\qquad R_5 C_5 = 0.05 \qquad [7-20]$

Letting $R_5 = 1$ MΩ

then $C_5 = 0.05$ μF

A suitable value for $C_5 = 0.047$ μF.

As in the case for the integrator (Figure 7.3), the input was first inverted with a unit gain 741 Op Amp, in order to maintain a positive ramp generator output, and to prevent a negative voltage from appearing across the CD4066 bilateral switch. The IN914 also acts as a protection against negative voltages at the ramp generator output.

FIGURE 7.4 RAMP GENERATOR AND STORAGE CIRCUIT
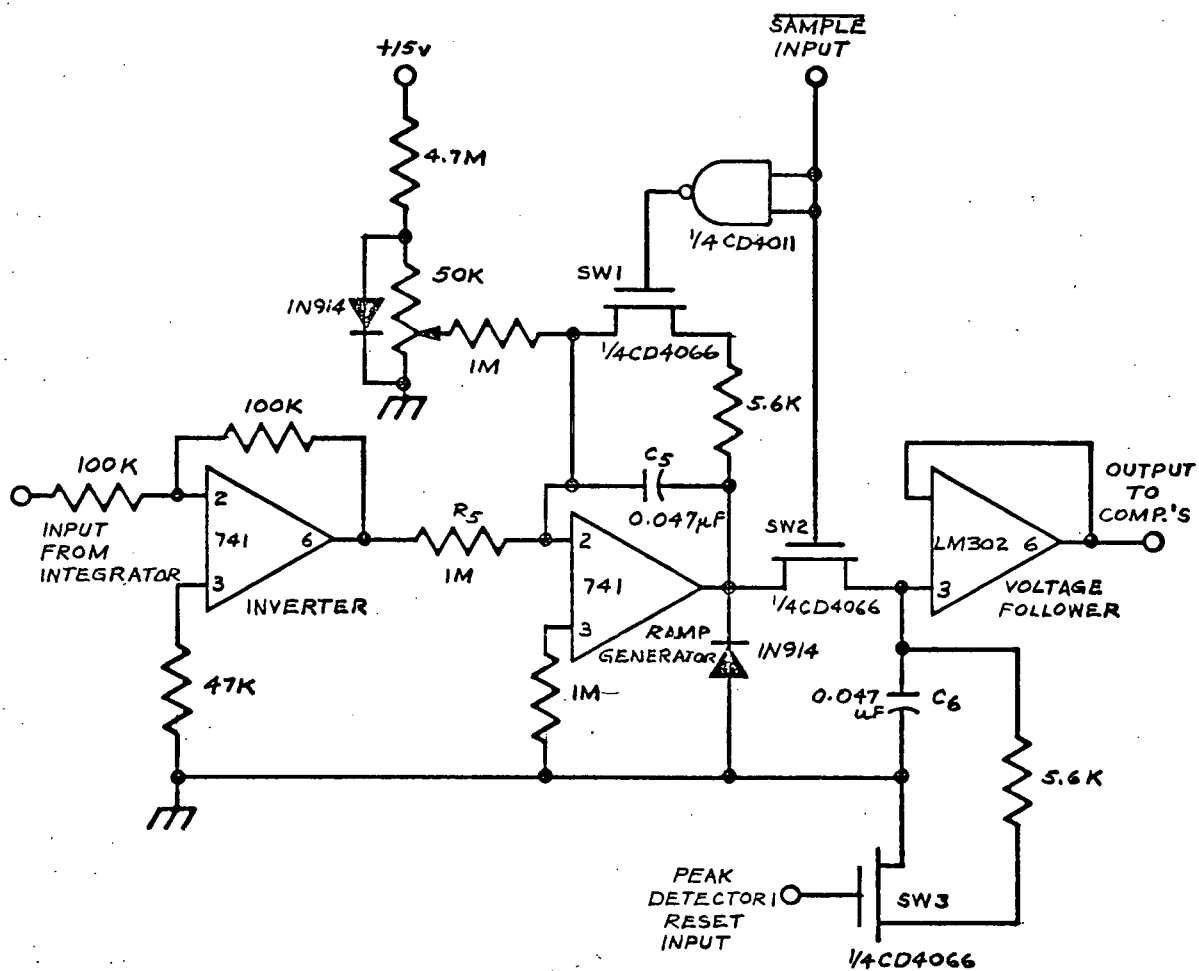
The $\overline{\text{SAMPLE}}$ signal from the colour sorter (Figure 3.12) is the measure of the tomato diameter. It controls the two bilateral switches, SW1 and SW2. While a tomato is under the sensing head, the $\overline{\text{SAMPLE}}$ is HIGH, and therefore SW1 is open (due to the NAND gate inverter) and SW2 is closed. The ramp generator integrates the incoming voltage, E, for the duration of the $\overline{\text{SAMPLE}}$ pulse, and at the same time charges C_6 to the ramp generator output voltage. When the $\overline{\text{SAMPLE}}$ signal goes LOW, SW1 discharges capacitor C_5, thus resetting the ramp generator. At the same time the ramp generator is separated from C_6 as SW2 is opened, leaving C_6 charged. The bilateral switch, SW3, is controlled by the PEAK DETECTOR 1 RESET pulse from the colour grader, and is therefore LOW for the duration of the $\overline{\text{SAMPLE}}$ signal plus the 210 µs WRITE signal from the colour grader. The 210 µs allows the stored voltage to be compared in the comparator circuits after which C_6 is discharged to ground until the next tomato arrives under the sensing head.

Comparator 4, 5, 6, and 7 (Box D, Figure 7.1)

The size grader comparator circuit is similar to the colour grader comparator circuit, except that an extra comparator has been added to include five categories instead of only four. The schematic diagram of the comparator circuit is shown in Figure 7.5. The comparators have been numbered from 4 to 7 to distinguish them from the three comparator circuits of the colour grader.

The function of COMP. 4 is analagous to COMP. 1 of the colour grader, in that COMP. 4 has $V_{SET\ 4}$ internally adjusted for the smallest tomato size to be considered, in this case 1.5 inches (3.8 cm). When a tomato less than 1.5 inches (3.8 cm) diameter passes under the sensing head, the output of COMP. 4 remains HIGH, as normal, thus inhibiting information from entering any of the memories. Tomatoes of greater size produce a LOW output at COMP. 4, and data may be entered into the memories according to the conditions at the outputs of COMP. 5, COMP. 6, and COMP. 7. The size categories and the output states of the four comparators are listed in Table 7.2. The potentiometers for $V_{SET\ 5}$, $V_{SET\ 6}$, and $V_{SET\ 7}$ are mounted on the front panel of the size and colour grader to allow ready access and adjustment.

As in the colour sorter, input protection diodes and an output clamping diode are used to keep the comparator's output compatible with the CMOS devices.

186

FIGURE 7.5 COMPARATOR CIRCUIT
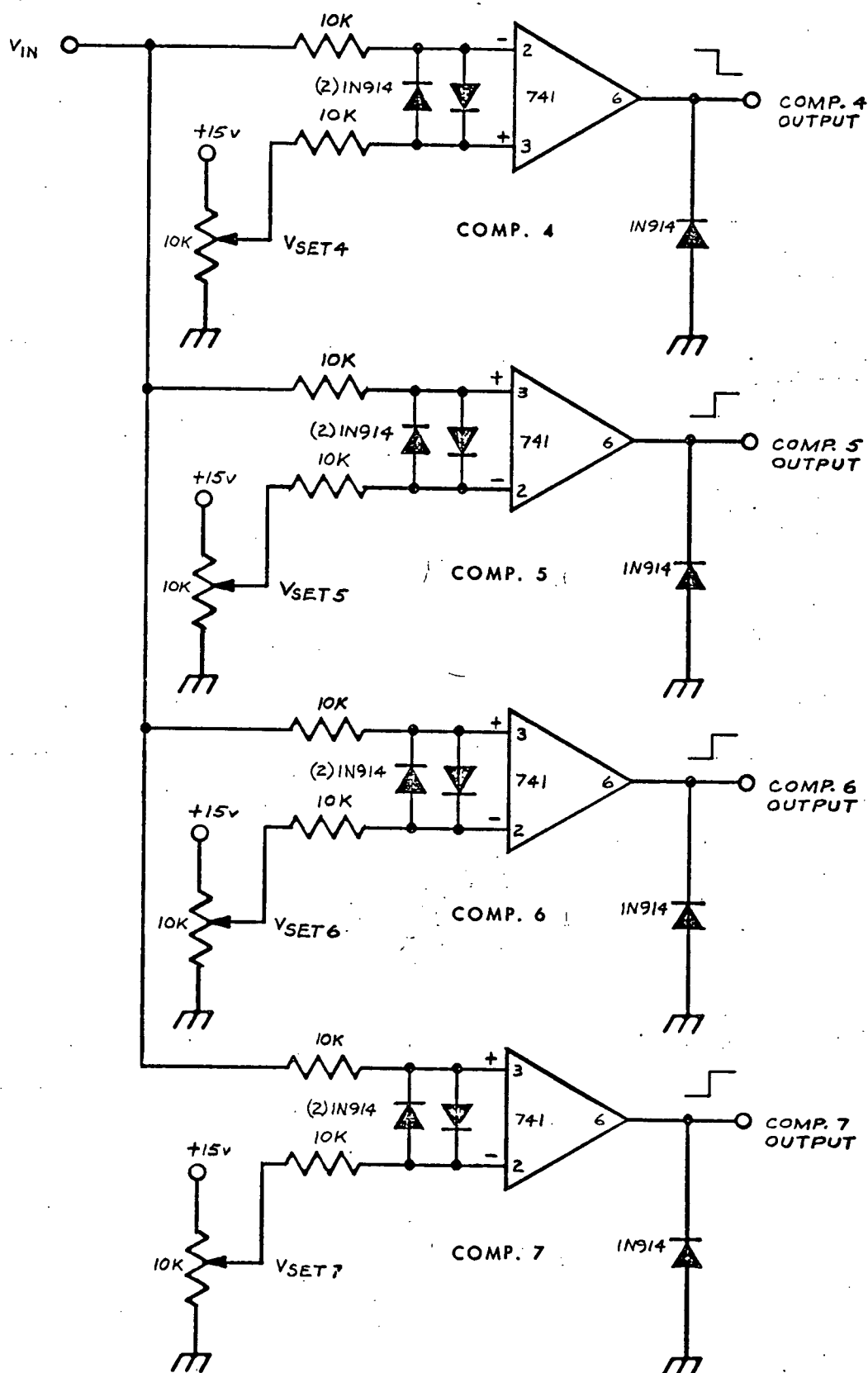
TABLE 7.2   OUTPUT STATES OF COMP. 4, COMP. 5,
                   COMP. 6, and COMP. 7 FOR FIVE SIZE
                   CATEGORIES.

Size Category	COMP. 4	COMP. 5	COMP. 6	COMP. 7
CULL	1	0	0	0
SMALL	0	0	0	0
MEDIUM	0	1	0	0
LARGE	0	1	1	0
EXTRA LARGE	0	1	1	1

Since all green tomatoes were to be ejected at
one location, the output of COMP. 1 of the colour grader
alone in combination with the WRITE pulse acted as the input
information for the GREEN shift register memory. It was
decided that all tomatoes less than 1.5 inches (3.8 cm)
diameter, represented by no change in the output of COMP. 4
would roll off the end of the conveyor belt in the
size/colour grader design. This leaves COMP. 2, COMP. 3,
COMP. 5, COMP. 6, and COMP. 7 to produce output states for
the twelve remaining colour categories, as shown in
Table 7.3.

TABLE 7.3   OUTPUT STATES OF COMPARATORS 2,3,5,6,7
             FOR TWELVE SIZE/COLOUR CATEGORIES.

CATEGORY		OUTPUT STATES				
Colour	Size	COMP.2	COMP.3	COMP.5	COMP.6	COMP.7
Turning	Small	0	0	0	0	0
Turning	Medium	0	0	1	0	0
Turning	Large	0	0	1	1	0
Turning	Extra Large	0	0	1	1	1
Semi Ripe	Small	1	0	0	0	0
Semi Ripe	Medium	1	0	1	0	0
Semi Ripe	Large	1	0	1	1	0
Semi Ripe	Extra Large	1	0	1	1	1
Firm Ripe	Small	1	1	0	0	0
Firm Ripe	Medium	1	1	1	0	0
Firm Ripe	Large	1	1	1	1	0
Firm Ripe	Extra Large	1	1	1	1	1

Decoding Gates (Box E, Figure 7.1)

A schematic of the decoding gates is shown in Figure 7.6. The function and design of the decoding gates is similar to that of the colour grader decoding gates in that a single output is LOW for the duration of the WRITE pulse for a specific combination of comparator outputs. The main difference between the colour grader and size grader decoding gates is that the latter uses 3-input NOR gates, NOR 1, NOR 2, NOR 3, and NOR 4, instead of the two input gates. The 3-input NOR gate IC, a CD4025, contains 3 gates and in order to minimize package count, the inverter NOR 5 is a 3-input gate, and NOR 6 acts as a 2-input gate, with two of the inputs tied together.

The WRITE input pulse is obtained from the colour grader, inverted through NOR 5 and gated through NOR 6 whenever the output of COMP. 4 is LOW. This enables the outputs of NOR 1, NOR 2, NOR 3 and NOR 4 to be transferred to the outputs of NAND 1, NAND 2, NAND 3, and NAND 4.

FIGURE 7.6 DECODING GATES
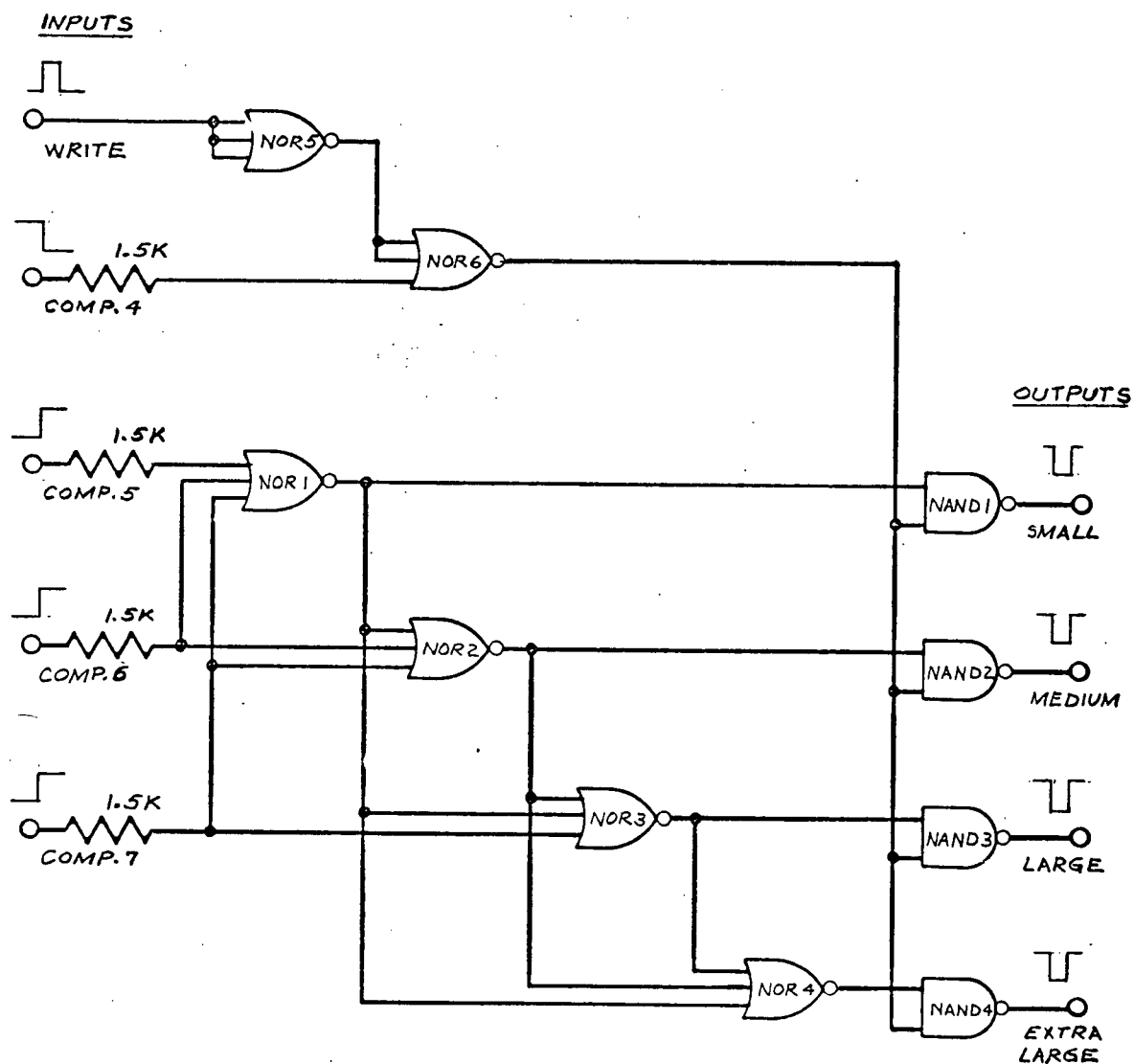
Latching Circuit (Box F, Figure 7.1)

A schematic of the latching circuit is shown in Figure 7.7. The design and function of this latching circuit is similar to the colour grader latching circuit. The main differences are that the new circuit uses 4-input NAND gates instead of 3-input NAND gates, and the latches which were comprised of 2-input NAND gates have been replaced by a single IC, a CD4044 which contains 4 such latches.

The output of COMP. 1 and the WRITE input, both from the colour grader are fed into NAND 1. If the output of COMP. 1 is HIGH and a WRITE signal appears, the output of NAND 1 goes LOW (indicating a green tomato). The LOW signal sets the output of the latch comprised of 2-input NAND gates, NAND 2, and NAND 3, to a HIGH state. The latch output is fed directly into the green category shift register memory. The latch is reset, as are the CD4044 latches by the LATCH RESET pulse obtained from the colour grader.

FIGURE 7.7 LATCHING CIRCUIT
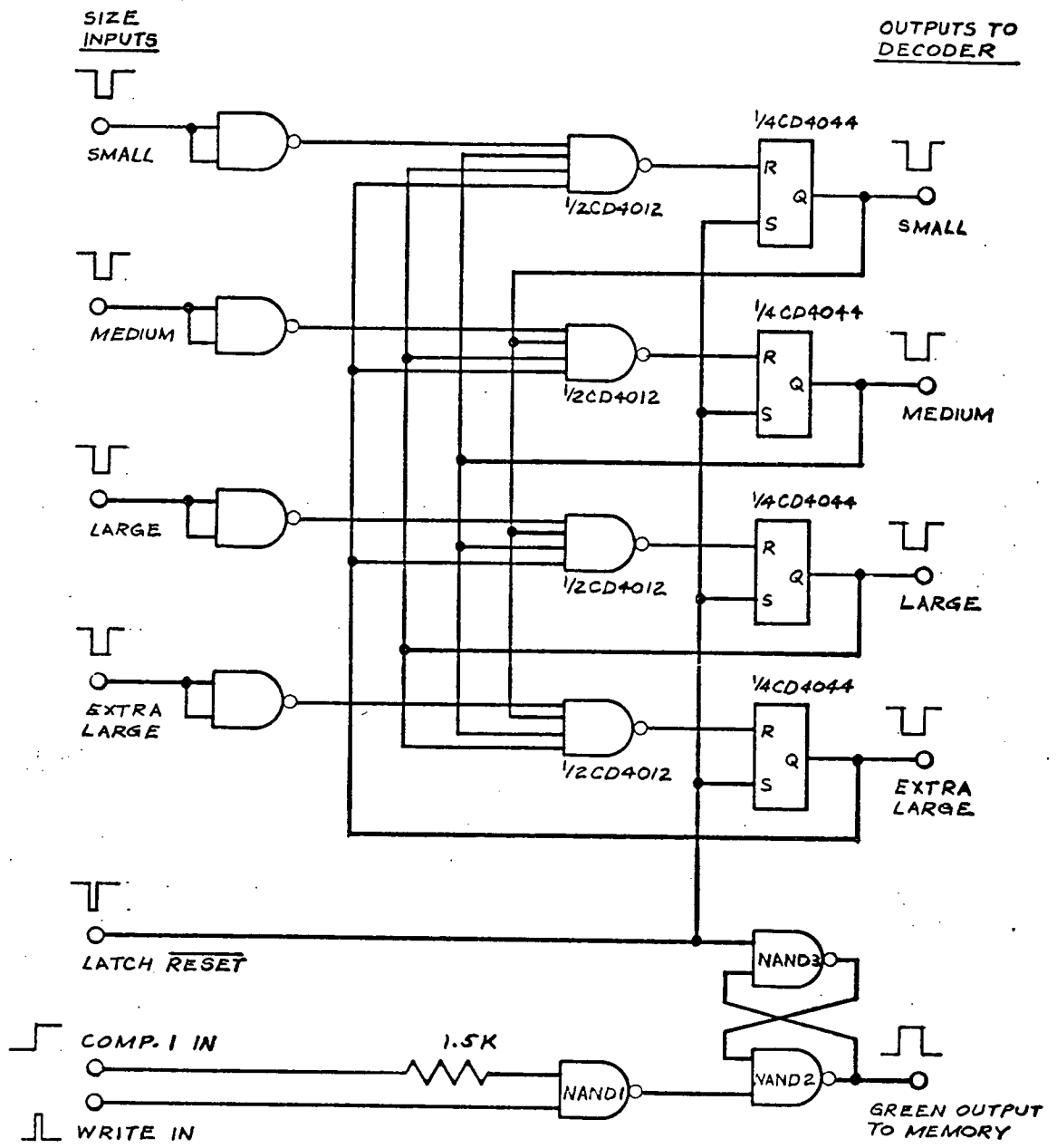
Size/Colour Decoder (Box G, Figure 7.1)

The size/colour decoder circuit is a series of gates used to decode the colour grader and size grader comparator outputs into a single output corresponding to a particular size/colour category, as described in Table 7.3. The schematic of the size/colour decoder is shown in Figure 7.8.

Both size and colour category input signals are LOW signals. For any single tomato, only one size and one colour signal will be present at the decoder inputs. Consequently, only one of the outputs of the twelve NOR gates will go HIGH.

The inputs to the 2-input NOR gates are connected to the outputs of the size grader latching circuits, Figure 7.7, and the colour grader latching circuit, Figure 3.16. The twelve outputs are connected directly to the inputs of the shift register memories.

FIGURE 7.8 SIZE/COLOUR DECODER CIRCUIT
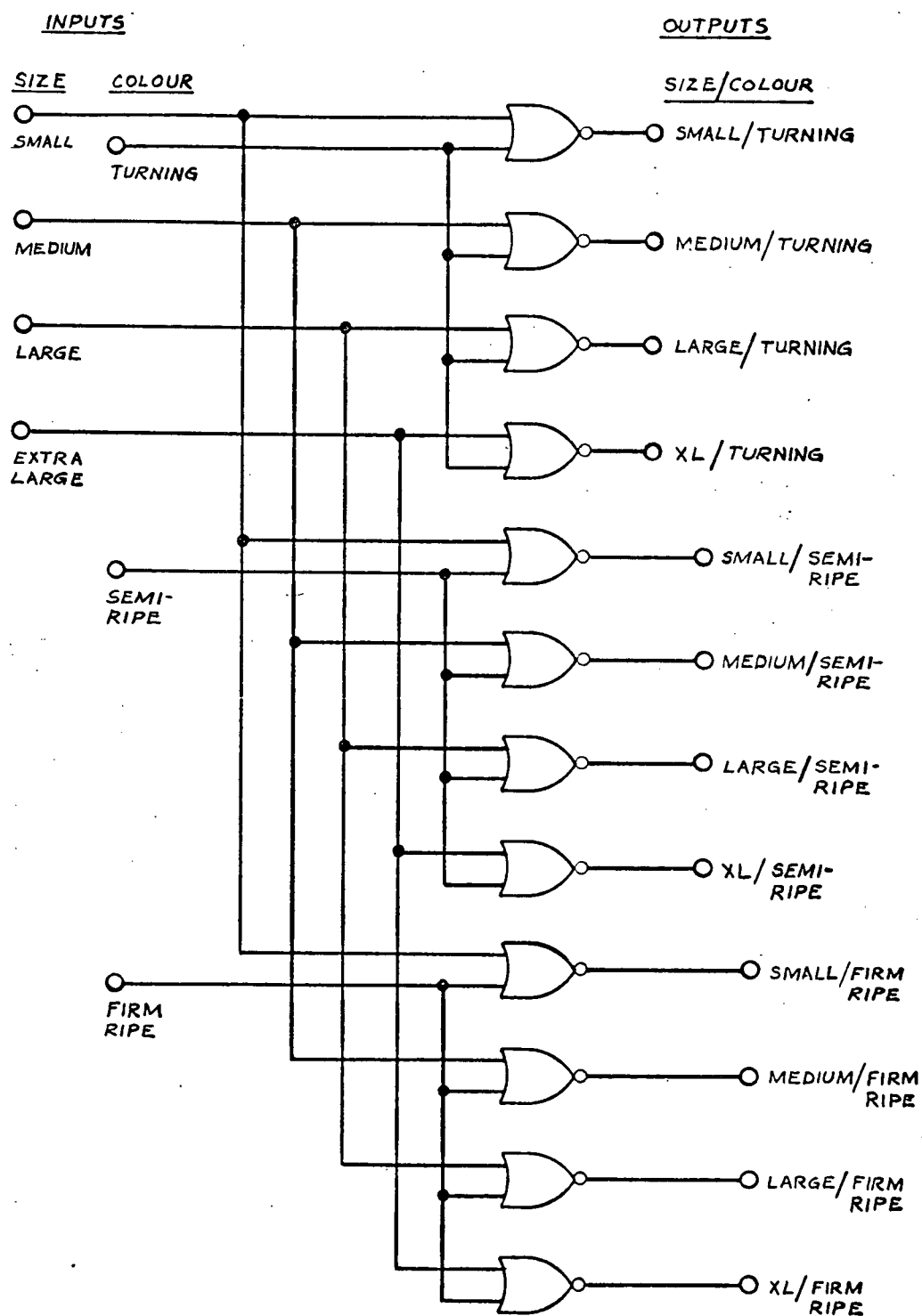
Memory Circuit (Box H, Figure 7.1)

The design of the size/colour memory circuit is similar to that of the colour grader memory circuit in that each size/colour category shift register is of a length (no. of bits) corresponding to a lineal distance downstream from the sensing head where the eject station for that size/colour category is located. The function of each shift register is the same as for the colour grader -- to store category information for a tomato as the tomato travels downstream from the sensing head, until it reaches its eject station, at which time the stored signal triggers an electromechanical device to eject the tomato from the conveyor belt.

The main difference between the colour grader memory and the size/colour memory is in the type of shift register used. The shift registers used in the colour grader were of the dual 4-bit type (CD4015) having a maximum 8 bit storage capability per IC.

When the colour grader was being designed, programmable shift registers were not available. However, during the design of the size/colour grader the MC14557 became commercially available. The MC14557 can be programmed for a length from 1 to 64 bits, depending on the conditions at the six programmable inputs. These new shift registers were incorporated into the size/colour grader because of their versatility.

The six programmable inputs which control the shift register length, were connected to six miniature SPST rocker switches. The rocker switch assembly consisted of a bank of seven switches which could be plugged into a standard 14 pin IC socket, making it ideal for the present design. The schematic for one of the thirteen shift register circuits used in the size/colour memory circuit is shown in Figure 7.9. Six 1 MΩ "pull up" resistors are used at the programmable inputs, L1, L2, L4, L8, L16, and L32, to keep these inputs normally HIGH unless a rocker switch is closed, making the input LOW.

The relationship between the length of the shift register and the condition of the programmable inputs is shown in Table 7.4.

Note that the DATA input is a positive going pulse instead of the negative going pulse used in the CD4015 of the colour grader. The outputs of the shift registers must be LOW in order to activate the opto-isolators. The CD4015 has only a Q output, thus the input to the memory must be of the same state as the desired output -- LOW. The MC14557 has two outputs, a Q and a $\overline{Q}$. This allows a choice of either a normally HIGH or normally LOW output. Since the size/colour decoder outputs go HIGH when a tomato is categorized, the HIGH may be stored in the MC14557 and the $\overline{Q}$ output used to feed a LOW signal to the opto-isolator circuit.

FIGURE 7.9 ONE OF 13 SHIFT REGISTER CIRCUITS USED
IN THE SIZE/COLOUR MEMORY CIRCUIT
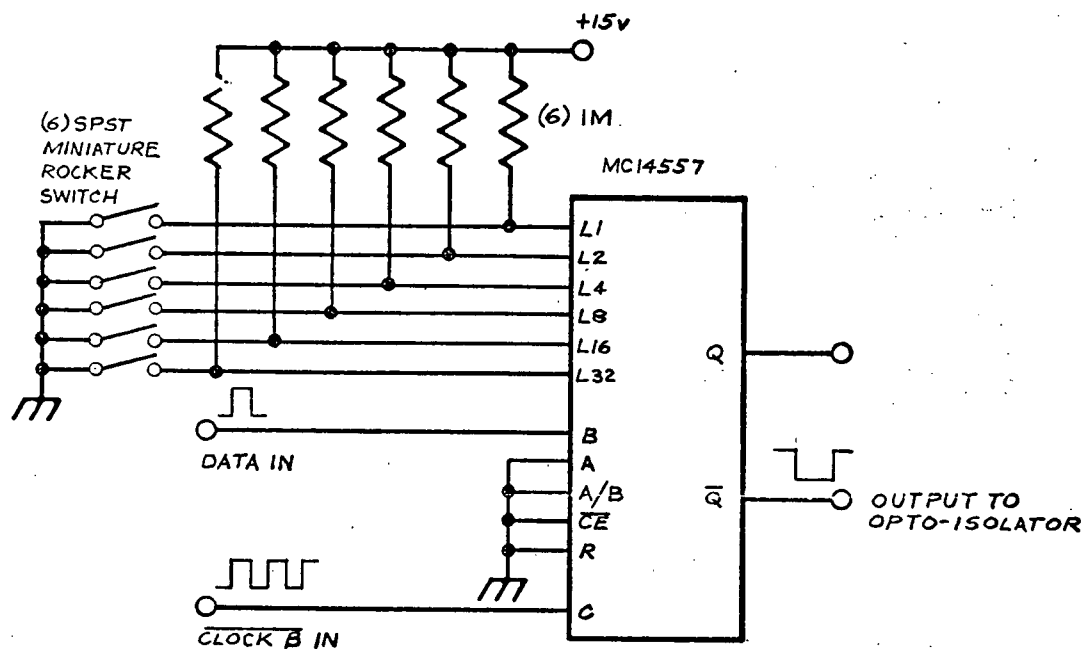
TABLE 7.4   SHIFT REGISTER LENGTH AND INPUT
CONDITIONS AT THE SIX PROGRAMMABLE
INPUTS.

INPUT						SHIFT REGISTER LENGTH	
L32	L16	L8	L4	L2	L1		
0	0	0	0	0	0	1	Bit
0	0	0	0	0	1	2	Bits
0	0	0	0	1	0	3	Bits
0	0	0	0	1	1	4	Bits
0	0	0	1	0	0	5	Bits
.	.	.	.	.	.		.
.	.	.	.	.	.		.
.	.	.	.	.	.		.
1	0	0	0	0	0	33	Bits
1	0	0	0	0	1	34	Bits
.	.	.	.	.	.		.
.	.	.	.	.	.		.
.	.	.	.	.	.		.
1	1	1	1	1	0	63	Bits
1	1	1	1	1	1	64	Bits

The $\overline{\text{CLOCK B}}$ signal is used to advance the shift registers, as was the case in the colour grader. The $\overline{\text{CLOCK B}}$ signal is obtained from the colour grader data latch timer circuit, Figure 3.17.

The schematic of the complete memory circuit is shown in Figure 7.10. For simplicity only the CLOCK, DATA and $\overline{\text{Q}}$ outputs are shown for each shift register. All other pins of each MC14557 are connected as shown in Figure 7.9. With a 64 bit storage capacity and 1.5 inches (3.8 cm) of conveyor belt movement per $\overline{\text{CLOCK B}}$ cycle, the maximum distance downstream from the sensing head that a eject station can be located is 8 feet (244 cm). With 6 inches (15 cm) between eject stations, it is possible to accommodate the 13 stations required. If greater spacing between eject locations is desired, any number of MC14557 shift registers may be cascaded to obtain the shift length required, where the output of the first is connected to the DATA input of the second and so on. Two shift registers in series can store data up to 16 feet (488 cm) downstream from the sensing head.

The DATA inputs of the first 12 shift registers are connected to the outputs of the size/colour decoder circuit. The thirteenth shift register stores the data for all sizes of green tomatoes, and its DATA input is connected directly to output of the latch comprised of NAND 2 and NAND 3, Figure 7.7. All $\overline{\text{Q}}$ to the output of the registers are connected to the opto-isolator circuit.

FIGURE 7.10 SIZE/COLOUR MEMORY CIRCUIT
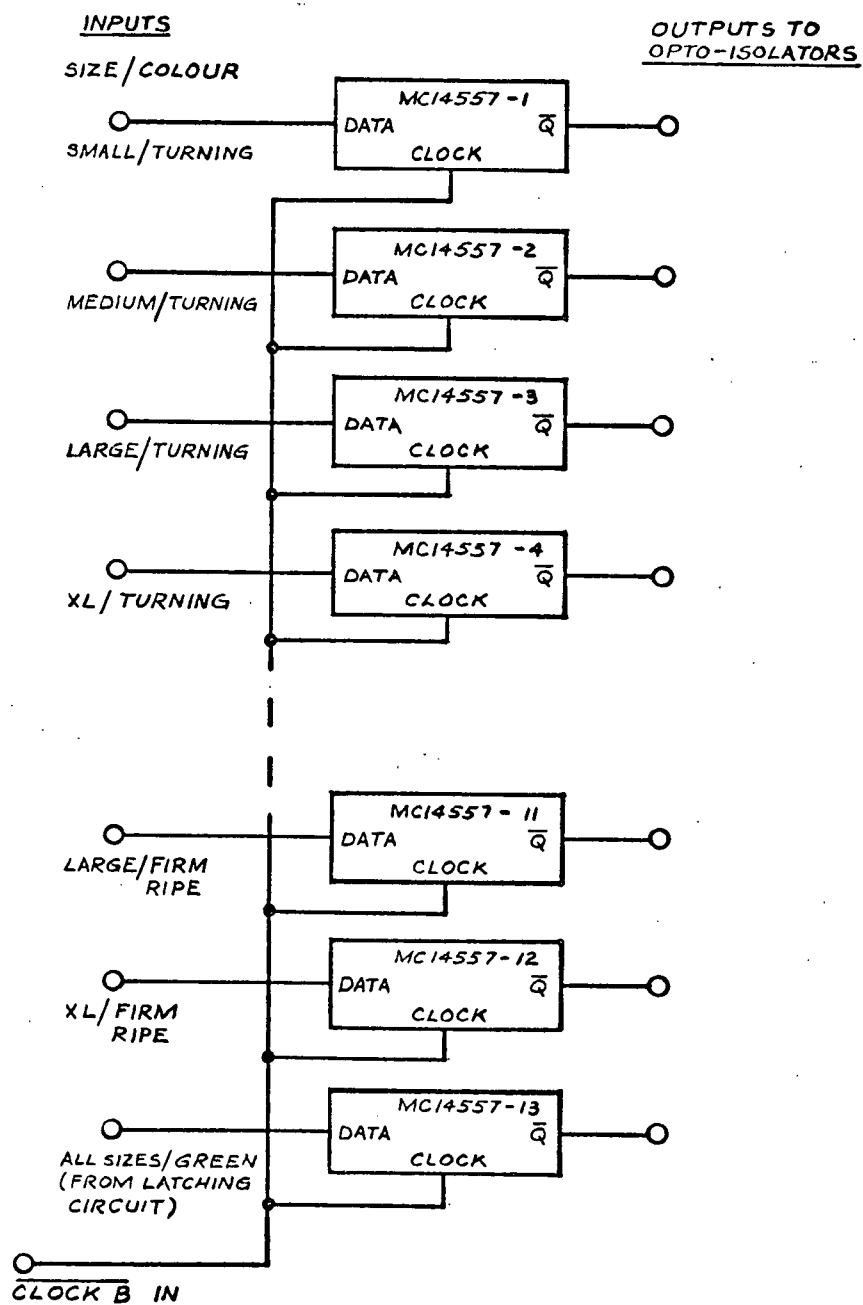
Opto-Isolator and Triac Circuit (Box 1, Figure 7.1)

The opto-isolator and triac circuit used to test the size/colour grader was the same one used in the colour grader. The size/colour categories were therefore tested three at a time. The proposed opto-isolator and triac circuit for the final size/colour prototype would consist of 13 rather than the 3 units comprised of the opto-isolator and triac shown in Figure 3.20.

Of prime concern in the design of the 13 unit circuit is the current drain in each unit from each of the two power supplies -- the +15 volt IC supply, and the +15 volt unregulated supply. The maximum current drain per unit (Figure 3.20) is 32 ma through a 470Ω resistor. The IC supply must be able to supply 416 ma for the 13 units, plus the current demanded by the other circuitry. In each unit, the maximum current requirement from the +15v unregulated supply is 10 ma, due to the 1.5 KΩ resistor in the phototransistor circuit. The unregulated supply must be capable of supplying a minimum of 130 ma. The triac power supply shown in Figure 3.22, would be adequate.

The solenoids used in the colour grader consumed 16.7 watts each, and if the same solenoids were employed, the 115v AC power consumption for the entire size/colour grader unit would be about 230 watts maximum.

MECHANICAL HANDLING SYSTEM

The size/colour grader mechanical handling system was identical to that used in the colour grader. The same solenoids, pneumatic supply and conveyor were used. Recommended improvements will be discussed in a later section.

C H A P T E R   8

SYSTEM TESTING

INTRODUCTION

Testing of the size/colour grader was concentrated around the size category section of the grader, since colour grading tests had been conducted earlier, as outlined in Chapter 4. Limits were set for size and colour categories by adjusting the V_{SET} controls of the comparators. The ability of the grader to classify tomatoes accurately was evaluated by examining the number of tomatoes which were misclassified in a given size category. Both oversize and undersize tomatoes were included in the misclassified category in all except the extra large group, where no over-size classification exists. Misclassifications due to mechanical problems associated with the eject mechanisms were not included. Testing of small tomatoes was virtually impossible, since with the present conveyor belt system, the relatively spherical small tomatoes would not stay on the flat belt. Consequently, tests were conducted on only the extra large, large, and medium size categories.

The effect of tomato colour on the size measured by the grader was investigated to establish whether tomatoes of different colour but equal size would be size graded differently.

The colour categories tested were firm ripe, semi-ripe and turning. The number of green tomatoes available at the time of testing was too small to be included in any of the tests.

MATERIALS AND METHODS

The tomatoes used in testing the size/colour grader varied in size from medium to extra large, and in colour from turning to firm ripe. Singulation and feeding of tomatoes onto the conveyor belt was carried out manually. The tomatoes were usually placed calyx end down, since this orientation was generally the most stable. No particular effort was made to place tomatoes exactly in line with the center of the sensing head, however, the tomatoes were not deliberatly offset either. Orientation in the equatorial plane was generally neglected, except where the differences between DIA. 1 and DIA. 2 were considered unusually large, in which case the tomatoes were oriented with DIA. 1 roughly parallel to the conveyor belt center line.

Tests were conducted at 20 inches/sec (51 cm/sec) belt speed, or 40 Hz CLOCK A frequency. The colour comparator settings, $V_{SET\ 1}$, $V_{SET\ 2}$, and $V_{SET\ 3}$ were chosen so that a relatively uniform numerical split of the samples in the three colour categories, firm ripe, semi-ripe and turning would result. The green/turning split was at $V_{SET\ 1}$ = 1 volt; the turning/semi-ripe split was at $V_{SET\ 2}$ = 4.8 volts; the semi-ripe/firm ripe split was at $V_{SET\ 3}$ = 9.3 volts.

Size classification as outlined in Appendix A, was based on the following DIA. 1 ranges:

3.000 in (7.62 cm) < extra large

2.250 in (5.72 cm) < large $\leq$ 3.000 in (7.62 cm)

1.875 in (4.76 cm) < medium $\leq$ 2.250 in (5.72 cm)

The size comparator settings were made using $V_{SET\ 4}$, $V_{SET\ 5}$, $V_{SET\ 6}$, and $V_{SET\ 7}$. The procedure for adjustment was as follows:

a) A tomato with DIA. 1 = 3.00 in (7.62 cm) was chosen as a size standard.

b) $V_{SET\ 7}$ was adjusted so that the standard tomato was consistently classified in the large category.

c) $V_{SET\ 7}$ was decreased until the standard tomato was consistently classified in the extra large category.

d) $V_{SET\ 7}$ was increased just enough so that the standard tomato was again consistently classified as large.

Steps a) through d) were repeated using different standard tomatoes for each of the V_{SET} adjustments remaining. A 2.250 inch (5.72 cm) tomato was used to adjust $V_{SET\ 6}$, and a 1.875 inch (4.76 cm) tomato was used to adjust $V_{SET\ 5}$.

Since small tomatoes were not included in the tests, $V_{SET\ 4}$ was adjusted arbitrarily, below $V_{SET\ 5}$.

Once the comparator voltages were set, the tomatoes, 193 in all, were graded by the size/colour grader three size/colour categories at a time. The opto-isolator circuit inputs, Figure 3.20, were connected to three outputs

of the size/colour memory, Figure 7.10, and all tomatoes placed sequentially on the conveyor belt. Only those tomatoes which belonged to the three size/colour categories under test were ejected by the pneumatic system; all other size/colour categories were collected at the end of the conveyor. The sorted tomatoes were separated from the remainder. The three opto-isolator inputs were then connected to three other size/colour category outputs of the memory, and the above testing procedure continued by regrading those tomatoes which were collected at the end of the conveyor until all of the size/colour categories had been tested (except, of course, the small and green categories).

An attempt was made to establish whether the colour of a tomato affects the measurement of its size. An analysis of variance on three colour categories which had been machine graded into the same size category was carried out. The three colour category means in each size category were compared using an F-test.

The nine machine graded size/colour categories were grouped into three three size categories -- extra large, large, and medium.

Each size category now contained a mixture of firm ripe, semi-ripe, and turning tomatoes. In each of the size categories, the number (or percentage) of misclassified tomatoes was recorded. Misclassified tomatoes were all tomatoes which fell outside the size category boundaries

stated previously. For example, a misclassified tomato in the large category would be any tomato having a DIA. 1 greater than 3.000 inches (7.62 cm) or having a DIA. 1 less than or equal to 2.250 inches (5.72 cm). The extra large category has no upper limit, and thus no tomatoes can be classified as oversize in this group. The standard deviation of the misclassified tomatoes around a given size category cut-off limit was used as the measure of the machine's ability to accurately size grade tomatoes.

RESULTS AND DISCUSSION

A. Theoretical Size Category Limits versus
    Experimental Limits

The voltage generated by the integrator circuit (Figure 7.3) for a belt speed of 40 Hz or 20 in/sec (51 cm/sec), is E = 3.1 volts (Table 7.1). Integration of E for the Schmitt trigger pulse width produces the voltage D which is the measure of tomato diameter. The pulse width may be predicted for any diameter at a given belt speed, and a theoretical value of D calculated.

Recall that,

$$D = A E p \qquad\qquad [7\text{-}10]$$

where $A = \dfrac{1}{R_5 C_5}$ (Figure 7.4)

$p = $ Schmitt trigger pulse width for a given diameter, in seconds.

Substituting R_5 = 1 MΩ, C_5 = 0.047, and E = 3.1 at 20 in/sec (51 cm/sec) belt speed, into [7-10] yields

$$D = 3.30 d \qquad\qquad [8\text{-}1]$$

where d = 20p = diameter in inches.

Using [8-1], the theoretical voltages for various diameters, including the critical cut-offs separating size categories were calculated and are listed in Table 8.1. The experimental values of D, i.e. $V_{SET\ 5}$, $V_{SET\ 6}$, and $V_{SET\ 7}$ are listed in Table 8.1.

The experimental values of D were consistently less than the theoretical values, suggesting that the

TABLE 8.1 THEORETICAL AND EXPERIMENTAL VALUES
OF D, FOR VARIOUS DIAMETERS.

Diameter, inch (cm)	D (volts)	
	Theoretical	Experimental
1.500 (3.810)	4.95	-
1.875 (4.763)	6.18	4.65 ($V_{SET\ 5}$)
2.250 (5.715)	7.42	6.30 ($V_{SET\ 6}$)
3.000 (7.620)	9.89	9.30 ($V_{SET\ 7}$)
3.500 (8.890)	11.54	-

tomatoes appeared smaller to the grader than their actual size. The difference between the theoretical and experimental values appears to be inversely proportional to size, suggesting that the larger the tomato, the more closely the machine-measured diameter approaches the true diameter. Recalling that the theoretical curve of D versus diameter is a straight line passing through the origin [8-1], the increasing difference between the theoretical and experimental values of D as the diameter decreases, as shown in Table 8.1, suggests that the actual relationship is curvilinear. The relationship of D versus diameter is probably the same as the relationship between Schmitt trigger pulse width and styroball diameter, shown in Figure 6.1. The voltage adjustments of $V_{SET\ 4}$, $V_{SET\ 5}$, $V_{SET\ 6}$ and $V_{SET\ 7}$ should be carried out as outlined previously, as opposed to setting the cut-off voltages to the theoretical values.

B. Effect of Tomato Colour on Size Measurement

The mean diameters (DIA. 1) of tomatoes in each of the three colour categories were compared for each of the three size categories, using the analysis of variance. The values of F in each size category are listed in Table 8.2. The F values indicate that, in the large and medium size categories, the mean diameters of the three colour categories are not equal. In the large and medium categories, the mean diameters of the three colour categories consistently increased as the redness of the tomato increased. The

TABLE 8.2   VALUES OF F RESULTING FROM A COMPARISON OF
             MEAN DIAMETERS OF THREE COLOUR CATEGORIES
             IN A GIVEN SIZE CATEGORY.

Size Category	F
Extra large	1.6†
Large	2.9*
Medium	5.8**

**   Significant at 1% level

*   Significant at 5% level

†   Not significant at 5% level.

difference between the mean of the medium/turning category and the medium/firm ripe category was 0.14 inch (0.36 cm). Although statistically significant, the difference is only 7% of the mean diameter in the medium category, which is probably insignificant, practically. The increasing mean size with increasing redness of the tomato may be explained by the fact that the phototransistor pre-amplifier circuits are most sensitive to the red wavelengths. The "green" amplifier output voltage is in most cases less than the "red" amplifier voltage, so the more red in a tomato of a given size, the sooner will it be detected by the grader, and the longer will it be seen by the sensing head.

The assumption which must be made in the use of analysis of variance is that the populations whose means are being compared are normally distributed. At a given harvest date, the size distribution of all tomatoes collected from a grower are probably normally distributed about some mean size. When tomatoes are sub-divided into size categories, each category is no longer normally distributed. For this reason, the F values listed in Table 8.2 should be considered with this fact in mind.

C. Size Grading Ability of the Size/Colour Grader

The ability of the size/colour grader to size and colour grade tomatoes is pictorially represented by the photographs in Figures 8.1, 8.2 and 8.3. Figure 8.1 a, b, and c, shows machine graded extra large/firm ripe,

FIGURE 8.1   MACHINE GRADED FIRM RIPE TOMATOES
(a) EXTRA LARGE
(b) LARGE
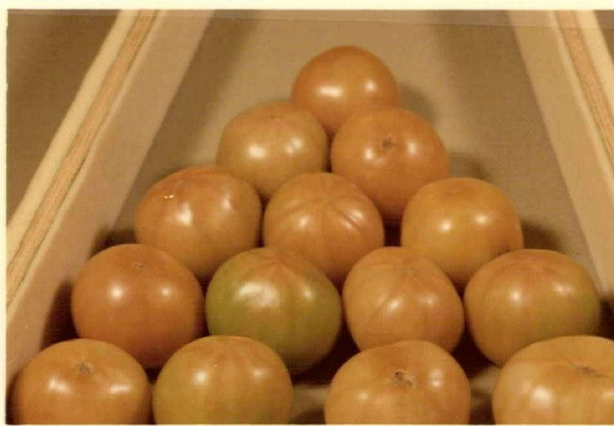(c) MEDIUM

(a)

(b)

(c)

216

FIGURE 8.2 MACHINE GRADED SEMI-RIPE TOMATOES
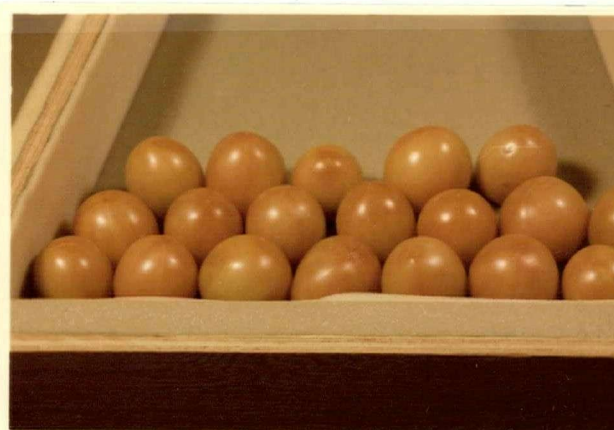(a) EXTRA LARGE
(b) LARGE
(c) MEDIUM

(a)

(b)

(c)

FIGURE 8.3 MACHINE GRADED TURNING TOMATOES.
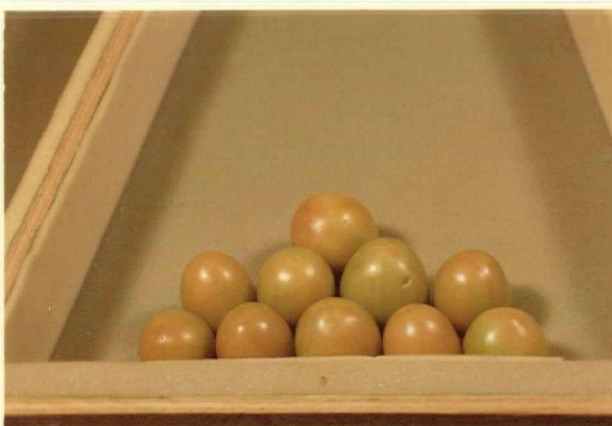(a) EXTRA LARGE
(b) LARGE
(c) MEDIUM

large/firm ripe, and medium/firm ripe tomatoes, respectively.
Figure 8.2 a, b, and c shows machine graded extra
large/semi-ripe, large/semi-ripe, and medium/semi-ripe
tomatoes, respectively. Figure 8.3 a, b, and c shows machine
graded extra large/turning, large/turning and medium/turning
tomatoes, respectively. Each size/colour category contains
tomatoes which fall within the specified boundaries for
size, and some tomatoes which fall outside these limits --
the misclassified tomatoes.

The percentage of misclassified tomatoes in a
given size category, alone, does not realistically represent
the size grading accuracy of the size/colour grader. The
deviation of the misclassified tomatoes from their cut-off
limits, however, does show the degree of overlap between
size categories.

Since only one size cut-off is used for all
colours of tomatoes, it is reasonable to pool all of the
misclassified tomatoes around a size cut-off, regardless of
colour. At each cut-off, i.e. at 1.875 in (4.76 cm),
2.250 in (5.72 cm), and 3.000 in (7.62 cm), it may be
assumed that a normal distribution of misclassified tomatoes
exists. To illustrate, at the 3.00 in (7.62 cm) cut-off,
there will be some tomatoes which are misclassified, being
oversize for the large category, and some tomatoes which
are misclassified, being undersize for the extra large
category. The assumption made here, is that the oversize

and undersize tomatoes when grouped will be normally distributed about a mean which is close to the 3.000 in (7.62 cm) cut-off. A similar distribution is expected at each of the other two cut-off limits. Confidence intervals may be calculated for each of the distributions, and a statement made on the magnitude of the size measurement error.

The means and standard deviations of the misclassified tomatoes around the 2.250 in (4.76 cm) cut-off and 3.000 in (7.62 cm) cut-off are listed in Table 8.3. The data for the 1.875 in (4.76 cm) cut-off is not included, since only half of the normal distribution (the undersize half for the medium category) was available.

The 95% confidence interval for each misclassified group was calculated and the results are also listed in Table 8.3. Assuming a standard deviation of 0.082 in (0.208 cm) at 1.875 in (4.76 cm) cut-off, the 95% confidence interval has a lower limit of 1.714 in (4.35 cm). All of the medium undersize tomatoes were greater than 1.714 in (4.35 cm) in diameter. This may suggest a smaller standard deviation at that cut-off or a mean less than 1.875 in (4.76 cm) for that group.

An F-test at the 95% confidence level yielded a value of F = 1.295 (for 8 and 6 degrees of freedom in the numerator and denominator, respectively) for the two normal distributions of Table 8.3. The variances were therefore

TABLE 8.3   MEANS, STANDARD DEVIATIONS AND 95%
             CONFIDENCE INTERVALS FOR MISCLASSIFIED
             TOMATOES AROUND THE 2.250 INCH (5.715 CM)
             AND 3.000 INCH (7.620 CM) CUT-OFFS.

Cut-off, inch (cm)	Mean inch (cm)	Standard Deviation,inch (cm)	95% Confidence Interval, inch (cm)
2.250 (5.715)	2.204 (5.598)	0.092 (0.234)	mean ± 0.180 (0.457)
3.000 (7.620)	3.021 (7.673)	0.082 (0.208)	mean ± 0.161 (0.409)

assumed equal. It is proposed that the variance at the
three cut-off limits are equal. Consequently, it is
possible to apply one standard deviation to each cut-off.
The standard deviation selected for this purpose was the
mean of the standard deviations listed in Table 8.3,
namely, $\bar{s}$ = 0.087 in (0.22 cm).

The percentages of oversize and undersize tomatoes
in each size category, as graded by the machine, were
recorded and are listed in Table 8.4. Combining the data
in Table 8.4 and $\bar{s}$ yields the following prediction:

If tomatoes are graded with V_{SET} adjustment set
as outlined, then,

a) 6.5% of the medium tomatoes will be oversize; 68% of
these will be within 0.087 in (0.22 cm) of
2.250 in (5.72 cm) or < 2.337 in (5.936 cm) in
diameter.

b) 9.7% of the medium tomatoes will be undersize; 68% of
these will be within 0.087 in (0.22 cm) of
1.875 in (4.76 cm) or > 1.788 in (4.54 cm) in
diameter.

c) 5.9% of the large tomatoes will be oversize; 68% of
these will be within 0.087 in (0.22 cm) of
3.000 in (7.62 cm) or < 3.087 in (7.84 cm) in
diameter,

d) and so on.

It is difficult to assess the acceptability of

TABLE 8.4   PERCENTAGE OF OVERSIZE AND UNDERSIZE
TOMATOES FOR EACH SIZE CATEGORY AS
GRADED BY THE SIZE/COLOUR GRADER.

Size Category	Percent Oversize	Percent Undersize	Total No. of Tomatoes in each size category
Medium	6.5	9.7	62
Large	5.9	7.4	68
Extra Large	-	4.8	63

the size graded categories above since tolerances for size ranges are not given in the standards. From a practical standpoint, the few machine graded tomatoes which are oversize and undersize are believed to deviate insignificantly from their size category boundaries.

It is not necessary that equal percentages of tomatoes are graded oversize and undersize around a given size category cut-off limit. The limit may be adjusted to required specifications, such that only a given percentage of tomatoes will fall either to the high or low side of the boundary. The 9.7% of undersize tomatoes in the medium category can be decreased if the 1.875 in (4.76 cm) limit is increased slightly. The decrease in the undersize percentage will be at the expense of a greater proportion of small tomatoes being oversize. The limits should be adjusted for an optimum oversize/undersize ratio.

SUMMARY

Experimentally obtained values for the size category cut-off limits, $V_{SET\ 5}$, $V_{SET\ 6}$, and $V_{SET\ 7}$, deviated somewhat from the theoretical values obtained from a linear relationship passing through the origin. The deviation from the straight line is due to the fact that the Schmitt trigger pulse width versus diameter relationship is not linear. Setting of the cut-off limits should be carried out using tomatoes as standards, rather than adjusting the V_{SET} controls to their theoretical voltage values.

The effect of tomato colour on the measurement of diameter has not clearly been established. It appears that the redder the tomato, the larger will its machine-measured diameter be. The correlation, if any, between colour and size measurement is probably insignificant since the overall percentage of misclassified tomatoes, and their deviations from their size category boundaries are small.

The greatest percentage of misclassified tomatoes was in the medium category, where 9.7% were graded undersize. The smallest percentage of misclassified tomatoes was in the extra large category, where 4.8% were graded undersize. A standard deviation of 0.087 in (0.22 cm) was applied to all misclassified tomatoes, and thus 68% of these will be within 0.087 in (0.22 cm) of the size category cut-off limit. The deviation of the misclassified tomatoes from the size category boundaries was considered practically insignificant.

FINAL SUMMARY

A summary of the major findings of the investigations reported here are listed in point form below.

1. Physical Properties of Tomatoes as Related to Colour Grading.

    - The wavelength ratio which is associated with a maximum reflectance ratio difference between the greenest and reddest tomatoes, is not necessarily the ideal wavelength ratio for the best statistical separation of tomatoes into more than two colour categories.

    - The wavelength ratio, 600 nm/660 nm maximizes Students' t between firm ripe, semi-ripe, turning and green colour categories.

    - Ratios other than 600 nm/660 nm may be used, but at the expense of optimum separation between categories.

2. Physical Properties of Tomatoes as Related to Size Grading.

    - The maximum diameter of a tomato, in the equatorial plane, correlates well with the weight of the tomato.

    - The smaller the tomato, the smaller the difference between the major and minor diameters, in the equatorial plane.

- Orientation of tomatoes on a conveyor belt before
    making a diameter measurement is more critical
    for larger than smaller tomatoes.
- The difference between the major and minor diameters
    in the equatorial plane is correlated with the
    major diameter in only the extra large size
    category.

3. Colour Grader Design.
- Photodetector amplifier design can only be carried
    out if the characteristics of the light source,
    optic filters and photodetectors are known.
- Detection of the presence of a tomato can be carried
    out using the algebraic sum of the two photo-
    detector signals as the trigger.
- Reasonable colour separation is accomplished by
    continuously calculating the ratio of voltages
    from two phototransistors sensing reflected
    light and comparing the peak voltage to preset
    values.
- Combination of the stored peak voltage and the use
    of the sum of the two photodetector voltages as
    the sensing trigger, overcomes difficulties
    associated with synchronization of separate
    sensing and triggering systems.
- Without background monitoring, small degress of drift
    in the reflectance of the conveyor belt can

detrimentally affect both sensing of the tomato
and triggering of the signal processors.

- Conveyor belt background monitoring may be accom-
plished through the use of a circuit which
follows the low frequency drift of the background,
but not the high frequency of the sorting
operation.

- Storage of category information in a dynamic memory
synchronized with the movement of the conveyor,
guarantees that at the ejection time, the eject
mechanism and tomato are in juxtaposition,
regardless of conveyor belt speed.

4.   Size Grader Design.
- Diameter measurement of a tomato can be accomplished
through the conversion of the colour grader
Schmitt trigger pulse into a voltage, and com-
paring the voltage to preset values.

- Since the Schmitt trigger pulse width is a function
of conveyor belt speed, a compensating circuit
must be provided which maintains a constant
voltage for a given tomato diameter, regardless
of belt speed.

- Category information can be processed in the same
manner as in the colour grader.

5. Test Results.

- Colour grading can be satisfactorily accomplished with
the present design for all tomatoes except those
less than or equal to about 1 1/2 in (4 cm) in
diameter, since detection becomes difficult.

- The grading rate of 5 tomatoes/sec, for both colour
and size/colour are limited by the capacity of
the pneumatic eject mechanism employed in the
tests.

- The electronic sorting operations using the present
design should be capable of grading at speeds up
to 20 tomatoes/second.

- The resolution of the size grader, based on styroball
measurements, appears to be 0.045 in (0.11 cm) at
the 95% confidence level.

- The effects of off-center sensing of the tomato on
the diameter measurement, based on styroball
studies, are practically insignificant at off-set
distances up to 1/4 in (0.64 cm) for diameters
above 2 in (5 cm).

- Size/colour grading, based on tests conducted on 9
categories of tomatoes, with the present design,
should yield no more than 10% oversized and 10%
undersized tomatoes in any category.

- Of the 10% undersize or oversize tomatoes, 68% will
be within 0.087 in (0.22 cm) of the category
boundary, for all categories.

RECOMMENDATIONS

Recommendations with respect to the future application of the present design in the manufacture of a complete size/colour grader for tomatoes, as well as further testing procedures to be carried out on a modified version of the present design, are listed in point form below.

1. Electronic and Optical System Design.

  - In the present design, there may be a few redundancies which are necessary due to the modular design of the system which was carried out over a long period. These redundancies should be eliminated in the final design.

  - The phototransistor amplifiers should be redesigned for use with 600 nm and 660 nm optic filters, and testing conducted using the optimum 600 nm/660 nm wavelength ratio.

  - The width of the fibre optic sensing head could be increased, to increase the amount of incident light and reflected light, thus increasing the signal to noise ratio of the phototransistor amplifiers.

  - Background belt reflectance should be maintained at a minimum with respect to all tomatoes so that tomatoes smaller than 1 1/2 in (4 cm) may be sensed.

- If a tomato is large enough (> 2.5 in (6.4 cm)
  diameter) to occupy two bits of storage area
  in the shift register, it may be possible to
  enter two consecutive "eject" signals into the
  memory. Consequently the eject solenoid would
  be activated for 3 in (7.6 cm) of conveyor
  belt, as opposed to only 1.5 in (3.8 cm). This
  would probably increase sorting speed consider-
  ably.

2. Mechanical Handling System.

- The electronic system described should be tested with
  a different conveying system, preferably a unit
  which automatically feeds, centers and orients
  the tomato, in order to minimize misclassification.
  A single Vee belt may suffice and should be tested
  before more complicated systems are considered.

- It may be necessary to increase the relative storage
  capacity of the secondary surge tank or the
  orifice size of the solenoids to increase the
  flow of air across the tomato at ejection time,
  or, if necessary, operate two solenoids in
  parallel. The latter proposal would be con-
  siderably more expensive.

- The drop from the conveyor belt to the storage bins or
  cross conveyors should be maintained at a minimum,
  in order to minimize mechanical damage to the
  tomato.

CITED REFERENCES

1. Allshouse, G.W. and K.Q. Stephenson. 1969. Development of a handling and sorting system for certain fruits and vegetables. Trans. ASAE 12(3) 290-291, 294.

2. Birth, G.S., K.H. Norris and J.N. Yeatman. 1957. Non-destructive measurement of internal colour of tomatoes by spectral transmission. Food Technol. 11(11): 552-557.

3. Birth, G.S. and K.H. Norris. 1958. An instrument using light transmittance for non-destructive measurement of fruit maturity. Food Technol. 12(11): 592-595.

4. Bittner, D.R. and K.H. Norris. 1968. Optical properties of selected fruits vs. maturity. Trans. ASAE 11(4) 534-536.

5. Bittner, D.R. and K.Q. Stephenson. 1968. Reflectance and transmittance properties of tomatoes vs. maturity ASAE Paper No. 68-329.

6. Brantley, S.A. Jr., D.D. Hamann and J.K. Whitfield. 1975. A multiple belt, adjustable vee size grader for sweet potatoes and cucumbers. Trans. ASAE 18(2): 350-354, 362.

7. Buckley, D.J. 1975. Application of photoelectric image sensing arrays in dimension and area measurement of agricultural products. Presented at 1975 Annual Meeting of the Canadian Society of Agricultural Engineering, June 22-26, Brandon University, Manitoba.

8. Bulley, N.R., L.M. Staley and H.K. Mehra. 1973. Electronic colour sorting of strawberries. Can. Agric. Eng. 15(2): 103-105.

9. Burkhardt, T.H. and R.F. Mrozek. 1974. An orienting and conveying device for sorting dried prunes. Trans. ASAE 17(6): 1173-1175.

10. Colosie, S.S. 1973. An electronic apple redness meter. J. Food Sci. 38(6): 965-967.

11. Goddard, W.B., M. O'Brien, C. Lorenzen and D.W. Williams. 1975. Development of criteria for mechanization of grading processing tomatoes. Trans. ASAE 18(1): 190-193.

12. Goodman, H.C. and D.D. Hamann, 1971. A machine to field size sweet potatoes. Trans. ASAE 14(1): 3-6.

13. Greenwood, C.S. and D.W. Chamberlin. 1973. Apparatus for sorting fruit according to colour. U.S. Patent No. 3,770,111, patented November 6, 1973.

14. Heron, J.R. and G.L. Zachariah. 1974. Automatic sorting of processing tomatoes. Trans. ASAE 17(5): 987-992.

15. Hood, C.E., B.K. Webb and L.O. Drew. 1968. Correlations of certain physical properties of tomatoes. ASAE Paper No. 68-120.

16. Irving, D.W. and C.S. Greenwood. 1973. Circuitry for sorting fruit according to colour. U.S. Patent No. 3,750,883, patented August 7, 1973.

17. Keitel, D., H. Weinhold and R. Scharlemer. 1973. Method of and device for photometrically sorting lumpy minerals. U.S. Patent No. 3,762,546, patented October 2, 1973.

18. Krivoshiev, G.P., D.C. Kolev, C.Y. Tanev, D.K. Erinkov, G.S. Petrov, A.T. Vassilev and P.S. Vatev. 1973. Method and apparatus for sorting tomatoes by colour. U.S. Patent No. 3,781,554, patented December 25, 1973.

19. Manfre, B.L. 1968. The mechanical harvesting of tomatoes -- for profit. Trans. ASAE 11(3): 356-359.

20. Matson, G.D. and N.N. Mohsenin. 1973. Mechanical orientation and packing of apple fruit. Trans. ASAE 16(6): 1190-1193.

21. McClure, W.F., R.P. Rohrbach, L.J. Kushman and W.E. Ballinger. 1973. The Berrymatic: An automatic fruit sorting machine. ASAE Paper No. 73-6525.

22. McClure, W.F. and P. Rohrbach. 1973. Blueberry sorter. U.S. Patent No. 3,773,172, patented November 20, 1973.

23. McClure, W.F., R.P. Rohrbach, L.J. Kushman and W.E. Ballinger. 1975. Design of a high speed fiber optic blueberry sorter. Trans ASAE 18(3): 487-490.

24. Mehra, H.K., N.R. Bulley and L.M. Staley. 1972. Some
     physical and rheological properties of strawberries.
     Can. Agric. Eng. 14(2): 85-88.

25. Mohsenin, N.N. (ed.) 1970. Physical Properties of Plant
     and Animal Materials. Volume I. Published by
     Gordon & Breach, Science Publishers Inc., 150 Fifth
     Avenue, New York, N.Y. 10011.

26. O'Brien, M. and S.C. Sarkar. 1973. Computerized grading
     of tomatoes by optical transmission characteristics.
     ASAE Paper No. PC-73-09.

27. O'Brien, M. and S.C. Sarkar. 1974. System for optical
     transmission characteristics for computerized
     grading tomatoes. Trans. ASAE 17(2): 193-194.

28. Palmer, J. 1961. Electronic sorting of potatoes and
     clods by their reflectance. J. Agric. Eng. Res.
     6: 104-111.

29. Powers, J.B., J.T. Gunn and F.C. Jacob. 1953. Electronic
     colour sorting of fruits and vegetables. Agric.
     Eng. 34: 149-154, 158.

30. Rohrbach, R.P., W.F. McClure, L.J. Kushman and W.E.
     Ballinger. 1973. Developments in automatic light
     transmission difference soring of blueberries. ASAE
     Paper No. 73-6528.

31. Sarkar, S.C. and M. O'Brien. 1975. Measurement of power
     spectra for optoelectronic sorting of tomatoes.
     Trans. ASAE 18(1): 177-180, 184.

32. Stephenson. K.Q., R.K. Bryler and M.A. Wittman. 1973.
     Vibrational response properties as sorting criteria
     for tomatoes. Trans. ASAE 16(2): 258-260.

33. Stephenson, K.Q. 1974. Colour sorting system for
     tomatoes. Trans ASAE 17(6): 1185-1186.

34. Traub, L.G., P.L. Wright and H.L. Steele. 1971. Machine
     harvesting tomatoes. Amer. Veg. Grower., Sept.
     18-20, 47, 49.

35. Wood, R.A. 1973. Apparatus for sorting products.
     U.S. Patent No. 3,776,381, patented December 4, 1973.

36. Worthington, J.T., D.R. Massie and K.H. Norris. 1973.
      Light transmission technique for predicting ripening
      time for intact green tomatoes. ASAE Paper No.73-6526.

37. Yeatman, J.N. and K.H. Norris. 1965. Evaluating internal
      quality of apples with new automatic fruit sorter.
      Food Technol. 19(3): 123-125.

GLOSSARY OF TERMS

band pass filter
- with reference to optical filters, an interference filter having a half bandwidth greater than 5% of the central wavelength.

category information
- a digital signal, either HIGH or LOW, or combination of signals, generated when a tomato is categorized electronically, which refers specifically to a colour or size/colour category.

central wavelength
- with reference to optical filters, the wavelength at the midpoint of the half bandwidth.

CMOS
- Complementary Symmetry Metal Oxide Semiconductor.

dB, decibel
- may be expressed as 20 $\log V_o/V_i$. where
  V_o = output voltage
  V_i = input voltage.

division
- with reference to analog signals, the algebraic operation conducted on two voltages.

- with respect to digital signals, the integral division of a frequency.

gain
- ratio of output voltage to input voltage.

gain ratio
- ratio of the gain of one amplifier to the gain of another amplifier.

half bandwidth
- with reference to optical filters, the width of a band measured at half peak transmission.

inverter

- with reference to analog signals, a device whose input and output voltages are different by algebraic sign only.

- with reference to digital signals, a device whose output is the complement of its input i.e. if the input is LOW, the output is HIGH, and vice versa.

memory

- a digital storage area comprised of one or more shift registers.

NAND gate

- a digital device whose output is LOW only when all of its inputs are HIGH.

narrow band pass filter

- with reference to optical filters, an interference filter having a half bandwidth between 1% and 5% of central wavelength.

NOR gate

- a digital device whose output is HIGH only when all of its inputs are LOW.

octave

- doubling of a frequency.

Op Amp, operational amplifier

- a high-gain dc amplifier that has a differential input and a single ended output.

open loop gain

- the gain of an Op Amp when no negative feedback is used.

optic filter

- an interference filter capable of transmitting a wavelength band of the visible spectrum, and blocking others.

peak wavelength

- with reference to optical filters, wavelength at maximum transmission.

percent (%) bandwidth

- the half bandwidth expressed as a percentile of central wavelength; i.e. 0.1% filter at 440 nm has a half bandwidth of 0.44 nm.

phototransistor

- solid state device similar to an ordinary transistor except that light incident on the pn junction controls the response of this device; offers built-in gain and greater sensitivity than photodiodes.

reflectance ratio

- ratio of reflected energies at two wavelengths when the incident energies at the two wavelengths are equal.

singulate

- to arrange in single file.

TTL

- Transistor-Transistor Logic integrated circuit.

very narrow band pass filter

- with reference to optical filters, an interference filter having a half bandwidth between 0.1% and 1% of central wavelength.

wavelength ratio

- ratio of two wavelengths; reflected energy at one of these wavelengths divided by the reflected energy at the other wavelength produces the reflectance ratio.

APPENDIX A

Federal* and Industry**Grading Standards for Greenhouse Tomatoes

I. Federal and Industry Colour Grades and Standards***

Canada No.1 Grade

71.(1)(d) are, in any individual package, one of the following
states of development: "mature", "turning", "semi-
ripe" or "firm ripe".

73.(1)(a) "mature" means,

(i) except for field tomatoes grown in British
Columbia and Manitoba, that the tomato shows a
definite tinge of pink at the blossom end, and
in the case of field tomatoes grown in British
Columbia and Manitoba, that the tomato is fully
developed, well filled out, gives a feeling of
springiness when pressure is applied, is bright
waxy in appearance, has seeds that are well
developed and seed cavities of a jelly-like
consistency, and

(ii) not more than 25% of the field tomatoes by

(ii) CONTINUED

count are turning in the case of tomatoes grown

in British Columbia and Manitoba, and not more

than 10% of the field tomatoes by count are

turning in the case of tomatoes grown other

than in British Columbia and Manitoba;

(b)   "turning" means

(i)   that the field tomato shows from a tinge to

25 percent pink or red colour, and

(ii) not more than 10% of the field tomatoes by

count are mature or semi-ripe;

(c)   "semi-ripe" means

(i)   that the field tomato shows from 25 percent

to 75 percent pink or red colour, and

(ii) not more than 10 percent of the field tomatoes

by count are turning or firm ripe;   and

(d)   "firm ripe" means

(i)   that the field tomato shows from 75 percent

to 100 percent pink or red colour, and

(ii) not more than 10 percent of the field tomatoes

by count are semi-ripe.

II. Federal Size Standards

Canada No.1 Grade

76.(1)(g) have a minimum diameter of 1 1/2 inches;

(h) have, when in a package, with the exception of one specimen, a maximum variation in diameter of 1 inch in the case of tomatoes with a minimum diameter of 2 inches, and a maximum variation in diameter of 1/2 inch in all other cases;

78. Notwithstanding anything in these Regulations, in the grading of greenhouse tomatoes not more than

(a) 5 percent of the greenhouse tomatoes by count may be below the minimum size;

(b) 10 percent of the packages, when the greenhouse tomatoes are in packages, may contain greenhouse tomatoes that exceed the permitted size variation;

III. Industry Size Grades in British Columbia

(1) Greenhouse tomatoes are grouped into five size categories:

(a) "cull", all tomatoes having a minimum diameter less than 1 1/2 inches,

(b) "small", all tomatoes having maximum diameters between 1 1/2 inches and 1 7/8 inches,

III. CONTINUED

(c) "medium", all tomatoes having maximum diameters between 1 7/8 inches and 2 1/4 inches,

(d) "large", all tomatoes having maximum diameters between 2 1/4 inches and 3 inches,

(e) "extra large", all tomatoes having maximum diameters greater than 3 inches.

(2) Federal Standards apply to general tolerances.

APPENDIX B

GRADING RATE AT PEAK OF GROWING SEASON FOR B.C. LOWER MAINLAND BASED ON 1975 YIELD PREDICTIONS, MEAN WEIGHT OF TOMATOES IN EACH SIZE CATEGORY, AND APPROXIMATE DISTRIBUTION OF SIZE CATEGORIES*

Size Category	Mean Tomato Weight (lbs)	No. of Tomatoes per 20 lb box
Small	0.107	187
Medium	0.163	123
Large	0.346	58
Extra large	0.495	40

Maximum B.C. 1975 yield in one week = 20,000 boxes at 20 lbs ea.

Maximum Lower Mainland 1975 yield in one week = 70% X 20,000 = 14,000 boxes

Size Distribution	% of Total	No. of Boxes/week
Small	4	560
Medium	23	3220
Large	54	7560
Extra large	11	1540
No.2 Grade	8	1120 (hand sorted)

Total without No.2's = 1,000,860 tomatoes/week
=======================

Based on a 6 day work week, at 8 hours/day

Grading rate = 5.8 tomatoes/sec

Based on a 7 day work week, at 8 hours/day

Grading rate = 5.0 tomatoes/sec

* Courtesy of Western Greenhouse Co-operative, Burnaby, B.C.